Controls on Temporal Variation in Ecosystem-Atmosphere Carbon Dioxide Exchange in Lakes and Reservoirs

by

Malgorzata Golub

A dissertation submitted in partial fulfillment of

the requirements for the degree of

Doctor of Philosophy

(Freshwater and Marine Sciences)

at the

UNIVERSITY OF WISCONSIN-MADISON

2016

Date of final oral examination: November 1, 2016

The dissertation is approved by the following members of the Final Oral Committee:

Ankur R. Desai, Professor, Atmospheric and Oceanic Sciences

Emily H. Stanley, Professor, Center for Limnology

Galen McKinley, Professor, Atmospheric and Oceanic Sciences

Christina Remucal, Assistant Professor, Civil and Environmental Engineering

Paul Hanson, Professor, Distinguished Research Professor, Center for Limnology

ABSTRACT

Inland waters are significant conduits of carbon dioxide (CO_2) to atmosphere, offsetting over 60% of net uptake of carbon into the terrestrial biosphere. However, these estimates are highly uncertain, rely heavily on point-in-time indirect measurements, and did not capture highly dynamic CO_2 fluxes at the air-water interface. Therefore, temporal CO_2 flux variability and governing processes remain understudied, making predicting future flux responses to environmental changes extremely difficult and uncertain.

To address these knowledge gaps, I combined the analysis of CO_2 fluxes and their drivers at the short time scale (hourly-seasonal) using eddy covariance observations together with longer time scale drivers (seasonal-decadal) using synthesis of long-term lake chemistry observations and application of the traditional boundary layer techniques.

I evaluated uncertainties attributed to pCO_2 estimation using carbonate equilibria, the most commonly used method of estimating CO_2 flux from freshwater systems and assessing the role of aquatic ecosystems in regional and global carbon balances. The results showed that systematic errors dominate random errors in pCO_2 calculations, and given all sources of error, the historical observations of carbon system parameters were unlikely to provide robust estimates of mean or temporal trends in pCO_2.

I also explored ice feedbacks on interannual pCO_2 variability in seven lakes in northern Wisconsin. Although declining ice cover significantly increased water temperature, these increases do not correspond to temperature-mediated pCO_2 increases. Ice duration and length of thermal stratification were poor indicators of springtime and fall pCO_2. I showed that even extreme warming events remained undetected when pCO_2 was estimated from pH-based carbonate

equilibria. The results imply that detecting pCO_2 variability and change in response to climate warming is rather unlikely.

The synthesis of eddy covariance observations from globally distributed lakes and reservoirs showed higher variability of temporal patterns of CO_2 flux and a lack of relationship with latitudinal gradients of precipitation and temperature relative to other terrestrial components of global carbon balances. All representative lakes showed surprisingly coherent CO_2 flux oscillations in diurnal and sub-monthly time scales. The up-scaled CO_2 flux were 40% lower than current global CO_2 fluxes.

ACKNOWLEDGEMENTS

This work would not have been possible without the help, support, and collaboration of many people. First, I would like to thank my advisor, Ankur R Desai, for being immensely patient with me, his moral support, quick responses to questions, showing a human face of academia, and financial support. I would also thank Emily H Stanley for providing financial support. I would also thank to my committee for reading this document and for their helpful comments and contributions.

Special thanks for Jonathan Thom for his support in the field and maintaining flux towers. Thanks to the lab members and Freshwater and Marine Sciences graduate students for being great to work with, having great memories from Madison, and helping me to stay sane.

I am also extremely grateful for my mom, Jedrek, Adam, Marysia, Blazej, Patrycja, and many friends from various stages of my life for their moral and financial support, and endless encouragement.

I would like to acknowledge the following funding sources for their support of this research and my education: National Science Foundation LTER Program for North Temperature Lakes LTER (NSF DEB-1440297, NTL LTER) and NSF DEB-0845166, University of Wisconsin Anna Grant Birge Memorial Award For Graduate Research, UW-Madison Conference Presentation Grants, UW-Madison John Jefferson Davis Travel Award, Global Lake Ecological Observatory Network.

CONTENTS

1 Background 1

1.1 Lake and reservoirs as significant components of a global carbon budget 1

1.2 Air-water carbon flux: theory and measurements 2

1.3 Drivers of carbon flux between lakes and atmosphere 5

1.4 Water chemistry 6

1.5 Biology 7

1.6 Seasonal and long-term drivers 8

1.7 Overview of dissertation research 11

2 Large uncertainty in estimating pCO_2 from carbonate equilibria in lakes 14

2.1 Introduction 15

2.2 Material and methods 18

2.3 Results 27

2.4 Discussion 31

2.5 Conclusions 44

2.6 Tables 46

2.7 Figures 50

2.8 Appendix I 53

3 Limited role of ice duration and thermal stratification on interannual variability CO_2 efflux from seasonally ice-covered lakes 56

3.1 Introduction 57

3.2 Material and methods 59

3.3 Results 62

3.4 Discussion 65

3.5 Conclusions 69

3.6 Tables 71

3.7 Figures 74

4 Multi-temporal patterns and environmental drivers of CO_2 fluxes in lakes and reservoirs 79

4.1 Introduction 80
4.2 Material and methods 84
4.3 Results 87
4.4 Discussion 92
4.5 Conclusions 104
4.6 Tables 106
4.7 Figures 108
4.8 Appendix II 120

5 Conclusions 123

5.1 Why temporal variability matters? 123
5.2 Key findings for estimating CO_2 in lakes and reservoirs 124
5.3 Implications for understanding the roles of lakes in regional and global carbon cycles 126
5.4 Future work 127

6 References 129

CHAPTER 1

BACKGROUND

1.1 *Lakes and reservoirs as significant components of a global carbon budget*

Inland waters are significant conduits of carbon dioxide (CO_2) to atmosphere [*Cole et al.*, 2007; *Aufdenkampe et al.*, 2011], and while previously under-appreciated [*Battin et al.*, 2009], are now included in global carbon balances [*Ciais et al.*, 2013]. Outgassing of carbon dioxide (CO_2) from inland waters has been estimated at 1 PgC yr^{-1}, comparable in magnitude to cumulative anthropogenic carbon release due to net land use change, offsetting over 60% of net uptake of carbon into the terrestrial biosphere or 40% of ocean uptake for 2002-2011 [*Ciais et al.*, 2013].

Of the 1 PgC flux, lakes and reservoirs are estimated to emit from 0.32 to 0.64 PgC yr^{-1} [*Cole et al.*, 2007; *Tranvik et al.*, 2009; *Aufdenkampe et al.*, 2011; *Raymond et al.*, 2013]. Lakes are subsidized with terrestrially-derived inorganic and organic carbon [*McCallister and del Giorgio*, 2012; *McDonald et al.*, 2013; *Finlay et al.*, 2015; *Weyhenmeyer et al.*, 2015], which is further recycled in lakes. The eventual fate of carbon in lakes includes three pathways: export, sedimentation, and exchange of C with atmosphere [*Cole et al.*, 2007], and the balance between C evasion and sedimentation determines whether lakes are net sources or net sinks of carbon to the atmosphere [*Hanson et al.*, 2004]. Although lake C flux has been shown to be very dynamic [*Jonsson et al.*, 2008a; *Atilla et al.*, 2011; *Bennington et al.*, 2012; *Karlsson et al.*, 2013], the temporal variability of lake – atmosphere CO_2 exchange is rarely resolved in regional and global carbon balances, which to date rely heavily on extrapolation from limited sets of infrequent observations. The overarching goal of this dissertation is to address the lack of consideration of temporal variability of lake-atmosphere exchanges of carbon from hours to decades.

1.2 *Air-water carbon flux: theory and measurements*

A key to understanding CO_2 flux at the lake-atmosphere interface is the near – surface turbulence in the air boundary layer. It can be generated either mechanically due to surface friction when wind flows over lake's surface (i.e., shear-induced turbulence, u_*) or due to surface heating and buoyancy (i.e., buoyancy-generated turbulence, w_*, Figure 1) [*MacIntyre et al.*, 2010]. What is unique for aquatic systems is that the surface itself is highly dynamic and has an additional, waterside boundary layer affecting the air-water interface from below [*Wanninkhof et al.*, 2009]. Waterside shear (u_{aq*}) and convection w_{aq*} also contribute to near-surface turbulence. Moreover, two diffusive sublayers develop above and below water surface, where a constant slow gas diffusion occurs [*Wanninkhof et al.*, 2009].

Wind forcing has a dominant effect on turbulence, hence, gas transfer velocity is often parameterized as a function of wind speed [*Wanninkhof*, 1992; *Cole and Caraco*, 1998; *Wanninkhof et al.*, 2009]. However, in low wind conditions or water convective mixing associated with heat losses, the buoyancy-generated turbulence can modulate the rate of gas exchange [*Eugster*, 2003; *MacIntyre et al.*, 2010; *Polsenaere et al.*, 2013]. In small lakes, buoyancy is a dominant forcing over the exchange rates [*Read et al.*, 2012], and although buoyancy is a significant component of k, the w_{aq*} term is rarely included in the estimates of carbon emissions from the lakes [*MacIntyre et al.*, 2010; *Read et al.*, 2012]. The extent to which atmospheric and

waterside boundary layer processes control gas exchange at air-water interface is a topic of hot debate. However, the presence of significant waterside forcing on CO_2 flux implies gas exchange even without significant kinetic forcing from atmosphere [*Aubinet et al.*, 2012].

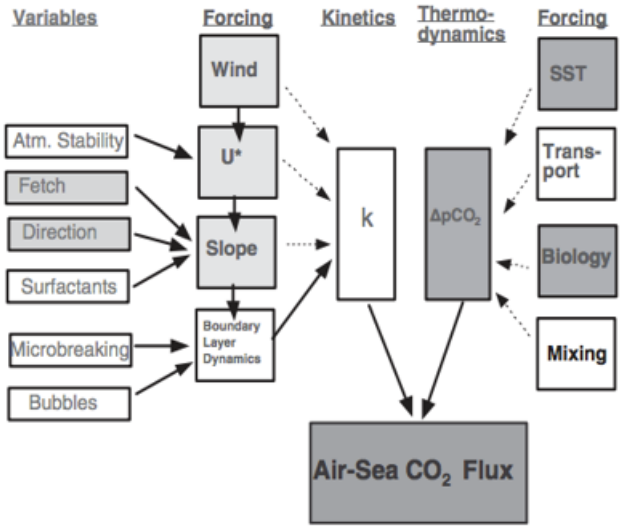

Figure 1. Simplified diagram of complex interactions between physical and biogeochemical processes contolling CO_2 fluxes at air-sea interface (after Wanninkhof et al., 2009)

To estimate lake-air carbon flux, one can use indirect or direct methods. Indirect methods include floating chambers, tracer gas, mass balance, boundary layer mass balance [*Cole and Caraco*, 1998; *Algesten et al.*, 2005; *Torgersen and Branco*, 2007; *Jonsson et al.*, 2008b; *Stets et al.*, 2009; *Cole et al.*, 2010]. The most commonly used method is the boundary layer (BL) technique where the flux depends on the amount of turbulent kinetic energy (TKE) exchange between the lake – air interface, and the concentration gradient between the lake surface and the air. In this approach, the flux is computed as:

$$\boldsymbol{Fc = k \times K_0 \times (pCO_{2\,(aq)} - pCO_{2\,(air)})} \quad (1)$$

where k is the gas transfer velocity, K_0 is the solubility of CO_2 in the water, $pCO_{2\,(air)}$ is the partial pressure of CO_2 in air, and $pCO_{2\,(aq)}$ is the partial pressure of CO_2 in water [*Cole and Caraco*, 1998]. In hardwater lakes, fluxes are chemical enhanced and require the addition of the α coefficient [*Wanninkhof and Knox*, 1996]. While the differential pCO_2 in air and in water is

relatively straightforward to measure, the measurement of physical exchange is challenging [*Cole et al.*, 2010; *Galfalk et al.*, 2013], and remains a key uncertainty in constraining lake C flux in shorter timescales.

The eddy covariance (EC) technique, in contrast to indirect methods, directly measures air-water exchange of CO_2, H_2O, energy, and momentum. It does not disturb the water - air interface and captures all sources of turbulent gas exchange across a lake flux footprint (i.e., lake fetch). Neglecting mean advection, column CO_2 storage, and vertical flux divergence, which are all good assumptions for a flat surface like a lake [*Lee*, 1998], EC flux is given as:

$$\boldsymbol{Fc} = \boldsymbol{\rho}\,\overline{\boldsymbol{c'w'}} \tag{2}$$

where $\boldsymbol{\rho}$ is the density of the dry air, $\boldsymbol{c'}$ and $\boldsymbol{w'}$ are the instantaneous deviations from the time-averaged values of the mixing ratio of gas concentration in the air (c') and vertical wind speed components, respectively [*Aubinet et al.*, 2012]. The bar above the product of fluctuations denotes ensemble or time averaging. These terms can be measured by high frequency (>10 Hz) observations of atmospheric CO_2 and vertical wind velocity over the water surface. If simultaneous water CO_2 concentration is measured, it is also possible to infer *k* by re-arranging equation 1 [*MacIntyre et al.*, 2010; *Heiskanen et al.*, 2014], providing a secondary estimate of lake flux. Simultaneous measurements of CO_2 using eddy covariance (EC) combined with indirect methods (chamber or models of surface renewal and boundary layer) showed good agreement between flux estimates [*Eugster*, 2003; *Vesala et al.*, 2006], flux underestimation [*Jonsson et al.*, 2008; *Podgrajsek et al.*, 2014; *Xiao et al.*, 2014] or overestimation [*Eugster*, 2003; *Guérin et al.*, 2007] when using indirect methods, and variable periods of agreement and disagreement [*Podgrajsek et*

al., 2014]. The largest discrepancies were found between EC and floating chamber measurements [*Eugster*, 2003].

Although measurements of CO_2 concentration in water are relatively easy, the paucity of direct CO_2 measurements over chemically diverse ecosystems is a major problem in deriving robust estimates of CO_2 flux from inland waters [*Raymond et al.*, 2013], and hence, the fluxes are poorly constrained [*Ciais et al.*, 2013]. All global estimates of CO_2 emissions to the atmosphere rely on estimating pCO_2 from carbonate equilibria from temperature, pH, and alkalinity (ALK)/ dissolved inorganic carbon (DIC), however, the quality of these estimates is questioned [*Wallin et al.*, 2014; *Abril et al.*, 2015]. Consequently, the uncertainty in global C emissions from lakes and reservoirs (0.32 Pg C yr^{-1}) ranges from 0.06 to 0.84 Pg C yr^{-1} [*Raymond et al.*, 2013], hindering the ability to detect long-term CO_2 change. The predictions on potential CO_2 responses to global changes are unreliable [*Phillips et al.*, 2015; *Hasler et al.*, 2016].

1.3 *Drivers of carbon flux between lakes and atmosphere*

In addition to constraining the air-water CO_2 flux, to predict its temporal variation, it is essential to understand the controls over gas exchange coefficient, *k*, and lake – air CO_2 difference, ΔpCO_2 (Fig. 1). First, the factors controlling *k*, called kinetic forcing, will be described. Further, the factors that affect ΔpCO_2, called, called thermodynamic forcing, are described.

Gas transfer

Gas transfer velocity, *k*, is primarily governed by the shear- and buoyancy-induced turbulence at water surface (Fig. 1). During unstable boundary layer conditions, the wind primarily affects the turbulence [*Stull*, 1988]. Wind and wind-generated wave fields, scale with the lake fetch, and significantly enhance gas exchange rates [*Wanninkhof et al.*, 2009; *Vachon and Prairie*, 2013; *Heiskanen et al.*, 2014]. Rainfall also has a large effect on *k* [*Cole and Caraco*, 1998; *Guérin et*

al., 2007], with rain intensity and drop size having the largest effect [*Wanninkhof et al.*, 2009]. For low winds and neutral stability, which are frequent over the lake water bodies [*Wanninkhof and Knox*, 1996; *Cole and Caraco*, 1998], buoyancy-induced turbulence controls *k* [*Aubinet et al.*, 2012]. Buoyancy-enhanced turbulent flux is strongly associated with the diurnal and seasonal lake surface heating cycles, creating local free convection during the night and in the fall [*Eugster*, 2003; *Jonsson et al.*, 2008b; *Mammarella et al.*, 2015; *Podgrajsek et al.*, 2015]. Conversely, heat gain and water column stratification have opposite effects on *k* and generally suppress turbulence [*Eugster*, 2003; *Jonsson et al.*, 2008b; *MacIntyre et al.*, 2010]. Even though convection and water column stability seem to be important for describing the flux rates, very few studies to date have investigated their interactions with *k* [*MacIntyre et al.*, 2010; *Heiskanen et al.*, 2014; *Mammarella et al.*, 2015] and their contribution to fluxes often remains unclear [*Podgrajsek et al.*, 2015].

1.4 *Water chemistry*

Water chemistry is an important aspect of CO_2 flux to be considered in aquatic ecosystems. The carbon dioxide in aquatic ecosystems is partitioned between dissolved CO_2^* (i.e., combined concentrations of carbonic acid H_2CO_3 and dissolved $CO_{2\,(aq)}$), and bicarbonate (HCO_3^-) and carbonate (CO_3^{2-}) ions. These three forms are referred to as DIC and are represented by the series of equilibria:

$$CO^*_{2(aq)} + H_2O \leftrightarrow H^+_{(aq)} + HCO_3^- \leftrightarrow H^+_{(aq)} + CO_3^{2-}$$

The relative proportion of these forms are sensitive to pH; hence, any changes in pH shift the proportion of CO_2 in the total DIC pool. Because most freshwaters have pHs between 5 and 8 [*Schlesinger and Bernhardt*, 2013], bicarbonate ions dominate over other carbonate species. The alkaline (HCO_3^-) and (CO_3^{2-}) ions are two major compounds of alkalinity [*Stumm and Morgan*,

1996] which provide acid buffering and resistance against pH changes. Lakes high in landscape position, for example, receive relatively low alkalinity loading; hence, tend to be poorly-buffered, have low pH, and high CO_2 concentrations [*Kratz et al.*, 1997; *Webster et al.*, 2000; *Hanson et al.*, 2006]. In contrast, in high pH lakes, the carbonate system favors (HCO_3^-) and (CO_3^{2-}), which has important ramifications for lake metabolic balance and C flux. When primary producers remove CO_2 during the photosynthesis, pH increases and shifts thermodynamic equilibria towards bicarbonate and carbonate ions; hence, the diurnal amplitude of CO_2 is dampened compared to O_2, leading to underestimation of gross primary production [*Hanson et al.*, 2003]. Moreover, gas transfer velocity in these lakes can be chemically enhanced up to 8% in low wind conditions [*Wanninkhof and Knox*, 1996]. Consequently, the magnitude of C flux at the lake – atmosphere interface can quickly change without a necessary driving force from the atmosphere [*Eugster*, 2003; *Aubinet et al.*, 2012].

1.5 *Biology*

It is important to recognize that lake CO_2 flux is an integrative measure of the net ecosystem exchange of CO_2 between the ecosystems and the atmosphere (i.e., NEE). It results from two fluxes of opposite signs: CO_2 uptake by photosynthesis (i.e., gross primary production, GPP) and CO_2 production from respiration (i.e., ecosystem respiration, ER), with negative NEE indicating CO_2 removal from atmosphere [*Aubinet et al.*, 2012]. Because lakes are subsidized with terrestrial organic and inorganic carbon, ER generally exceeds GPP, which results in net heterotrophy and net emission of CO_2 to atmosphere [*del Giorgio et al.*, 1997; *Cole et al.*, 2007]. GPP and ER rates are often estimated from dissolved oxygen (DO) observations [*Staehr et al.*, 2012; *Solomon et al.*, 2013]. In these lakes, GPP is tightly connected to total phosphorus (TP) while ER is controlled by dissolved organic carbon (DOC) concentration [*del Giorgio et al.*, 1997; *Hanson et al.*, 2003;

Perga et al., 2016], and ecosystem level CO_2 responses vary immensely depending on nutrient and color content. Additionally, anaerobic processes produce and consume CO_2 independent of biotic interactions [*Torgersen and Branco*, 2007; *Dubois et al.*, 2009; *Holgerson*, 2015]. Other controls over metabolic balance include temperature, photosynthetically active radiation (PAR), chlorophyll *a*, water column thermal stratification and stability [*Hanson et al.*, 2003; *Coloso et al.*, 2011; *Yvon-Durocher et al.*, 2012].

1.6 *Seasonal and long-term drivers*

CO_2 flux regulation is time dependent [*Hanson et al.*, 2006; *Finlay et al.*, 2015; *Perga et al.*, 2016]. Moreover, the same driver may affect different physical, chemical and biological processes at different temporal time scales [*Hanson et al.*, 2006; *Finlay et al.*, 2015; *Perga et al.*, 2016]. Thus, the importance of different drivers and their contribution to CO_2 flux change over time [*Sturtevant et al.*, 2015; *Perga et al.*, 2016]. The strength and even sign of ecosystem-scale CO_2 feedbacks also may significantly vary depending on nutrient, color, connectivity with landscape, waterbody morphometry [*Blenckner*, 2005; *Webster et al.*, 2008]. While our knowledge of controls of CO_2 flux comes mostly from space-for-time studies, often based on point-in-time-measurements, less is known about the importance of meteorological drivers of temporal variability of CO_2 and their contribution to fluxes as a function of time.

In seasonally ice-covered lakes, the timing of ice melt exerts the largest single control on seasonal thermal and energy regimes of northern lakes, as well as on annual CO_2 flux [*Rouse et al.*, 2003; *Karlsson et al.*, 2013]. The transition from ice-covered to open-water is accompanied with large pulses of CO_2 accumulated under the ice [*Anderson et al.*, 1999; *Riera et al.*, 1999; *Striegl et al.*, 2001; *Baehr and DeGrandpre*, 2002; *Huotari et al.*, 2009; *López Bellido et al.*, 2009;

Demarty et al., 2011]. Similar pulses are observed during the fall mixing, which tend to be higher than springtime emission due to prolonged thermal stratification (CO_2 accumulates in the hypolimnion) and longer mixis events [*Riera et al.*, 1999; *López Bellido et al.*, 2009; *Huotari et al.*, 2011]. While physical processes associated with ice phenology, convective mixing, and stratification exert control over diurnal to annual amplitude of lake CO_2 and flux [*Baehr and DeGrandpre*, 2002; *Eugster*, 2003; *Hanson et al.*, 2006; *Åberg et al.*, 2010; *Atilla et al.*, 2011; *Ducharme-Riel et al.*, 2015], inflow of nutrients and dissolved organic carbon controls CO_2 flux at regional time scales [*Denfeld et al.*, 2015]. Although carbon emissions from the "dormant" season can "switch" the annual net balance from a C sink to a source [*Karlsson et al.*, 2013], they are rarely included in annual carbon budgets [*Riera et al.*, 1999]. A major difficulty is that ice cover within a few weeks before/after ice off is too thin to allow safe sampling, hence this period is under-sampled [*Hanson et al.*, 2006]. Potential emissions can be estimated based on accumulated CO_2 inventories under the ice [*Striegl et al.*, 2001; *López Bellido et al.*, 2009]. However, these inventories may lead to erroneously high rates of evasion owing CO_2 reduction by under-ice algal blooms after the last sampling but before ice-off [*Baehr and DeGrandpre*, 2002] or may show no CO_2 accumulation with ice duration at all [*Denfeld et al.*, 2015]. Moreover, the linkages between ice dynamics and the timing and strength of springtime and fall CO_2 emissions are largely unexplored because of lack of multi-year time series.

The increase in CO_2 and other greenhouse gases in the atmosphere is causing climate warming at unprecedented rates [*Risbey et al.*, 2014]. The upward trends in air temperature and frequency of extreme precipitation events have already been observed across the U.S. [*Meehl et al.*, 2009; *Kucharik et al.*, 2010; *Villarini et al.*, 2013]. Many researchers have shown significant 20th century trends in physical and biological lake processes in response to climatic change,

including greater rates of water temperature warming over air temperature, decreases in ice cover, prolonged growing season, and greater resistance to water column mixing [*Magnuson*, 2000; *Winder and Schindler*, 2004; *Austin and Colman*, 2007; *Schneider and Hook*, 2010; *Weyhenmeyer et al.*, 2011; *O'Reilly et al.*, 2015]. However, there is less research on how these influence lake-atmosphere CO_2 flux [*Phillips et al.*, 2015; *Hasler et al.*, 2016]. In fact, the lack of time series to study temporal magnitudes and dynamics of CO_2 is one of the major obstacle to predicting responses to rising CO_2 in the atmosphere [*Hasler et al.*, 2016]. Hypothesized temperature-mediated effects include increased metabolic rates, promoting hypolimnetic and anoxic conditions in thermally stratified lakes, decrease gas solubility, and increase pCO_2 in the water [*Williamson et al.*, 2008; *Takahashi et al.*, 2009; *Tranvik et al.*, 2009; *Yvon-Durocher et al.*, 2010; *Demars et al.*, 2016]. However, in a globally distributed lake dataset, lake pCO_2 was found to be temperature-independent [*Sobek et al.*, 2005] or provide spurious relationships with temperature [*Alin and Johnson*, 2007].

It is proposed that climate-driven changes, such as changes in hydrology in the watersheds and altered delivery rates of terrigenous carbon, will be primary pathways of changes to lakes [*Williamson et al.*, 2008; *Tranvik et al.*, 2009; *Weyhenmeyer et al.*, 2015]. Annual CO_2 evasion rates in boreal lakes closely follow annual precipitation patterns [*Rantakari and Kortelainen*, 2005; *Roehm et al.*, 2009], hence the pCO_2-DOC relationship is proposed to be a useful metric of altered precipitation patterns and changes in the export of DOC to lakes [*Sobek et al.*, 2005]. More long-term empirical evidence supports the hypothesis that delivery of solutes (carbon and nutrients) to lakes is a primary control over dissolved inorganic carbon at the decadal scale [*Hanson et al.*, 2006; *Maberly et al.*, 2013; *Perga et al.*, 2016]. However, this relationship might be obscured by water browning, disturbance history, biotic and abiotic interactions [*Blenckner*, 2005; *Evans et al.*,

2006; *Monteith et al.*, 2007]. Development of mechanistic models to separate these effects is urgently needed [*Hasler et al.*, 2016].

Inland waters, in addition to climate change, are persistently subjected to human pressures, such as eutrophication, hydromorphological alterations, land use change, toxic substances inputs, invasive species expansion, or water infrastructure expansion [*Carpenter et al.*, 2011; *Lehner et al.*, 2011], all of which threaten the important ecosystem services inland waters provide [*Bennett et al.*, 2009; *Allan et al.*, 2015]. All these pressures likely exert synergistic and antagonistic effect on lakes [*Christensen et al.*, 2006; *Tranvik et al.*, 2009], significantly contributing to the complexity of climate – lake C interactions. Therefore, there is an urgent need to advance our understanding on key drivers and processed driving C flux in a variety of systems in time and in space.

1.7 *Overview of dissertation research*

The major theme of this dissertation is multi-temporal controls of air-water CO_2 exchange in lakes and reservoirs at scales ranging from half-hourly to interannual. Atmospheric exchange of CO_2 is a flux critical for balancing lake carbon budgets, assessing the role of lake ecosystems in a lake-rich region, and constraining fluxes in regional and global carbon balances. My dissertation focuses on both the short time scale (hourly-seasonal) using eddy covariance observations and the long time scale (seasonal-decadal) using synthesis of long-term lake chemistry observations and application of the traditional boundary layer technique. To improve process–level understanding of the variability of air-water CO_2 flux and advance prediction of CO_2 evasion variability from ecosystems facing global change, I address the following questions:

- What are the uncertainties attributed to pCO_2 calculations from carbonate equilibria using two CO_2-related parameters?
- Which environmental controls govern multi-temporal variability of CO_2 flux in lakes and reservoirs? How do ecosystem characteristics modulate responses to micrometeorological drivers?
- What is the role of ice cover duration in interannual variability of CO_2 flux from seasonally ice-covered lakes?

The dissertation is divided into three chapters that address these questions. In Chapter 2, I examine the uncertainty associated with estimating pCO_2, a proxy of CO_2 flux, from carbonate equilibria. This is currently the most commonly used approach of calculating pCO_2 but quantitative studies on uncertainties propagating through equilibria remain scarce. I conducted an error analysis of historical observations at North Temperate Lake Long Term Ecological Research (NTL LTER) site to quantify random errors in pH, DIC, and ALK measurements to examine how these uncertainties propagate onto uncertainties in pCO_2 estimated from three carbonate equilibria in four lake groups across a broad gradient of water chemical composition. Although this study primarily focused on random error analysis, the uncertainties in direct and estimated pCO_2 observations were compared to determine if other than random pCO_2 errors contributed to uncertainty in pCO_2 calculations. To date, there is no comprehensive evaluation of random errors effects on pCO_2 estimation.

In Chapter 3, I investigate the effects of interannual variability of lake ice on water temperature, thermal structure, and CO_2 efflux from seven NTL lakes in Northern Wisconsin. Because ice provides a “winter switch” for lake physical and geochemical processes, the interannual variability of ice provided an excellent tool to test relationships among climate, ice,

and lake ecosystem responses independent of long-term trends. The historical observations of long-term data from NTL-LTER sites were used to model lake thermal structure and CO_2 flux at annual basis and derive metrics to correlate with ice dynamics. The role of interannual variability in annual CO_2 efflux and implications for predicted further ice cover loss was investigated.

In Chapter 4, I ask: What are the multi-temporal patterns of CO_2 flux in globally distributed lakes and reservoirs? What governs those patterns? Are ecosystem-specific characteristics modulating ecosystem-scale CO_2 responses to environmental drivers? High temporal resolution flux measurements from 19 eddy covariance flux towers over lakes and reservoirs representing six climatic zones and wide gradients of nutrient and color were synthesized. This is a first multi-site and multi-temporal analysis of eddy CO_2 fluxes. Fluxes of CO_2 and environmental drivers were used to investigate the patterns of CO_2 flux at daily to seasonal time scale and how environmental controls change as a function of time. Comparison across diverse ecosystems was used to examine the role of ecosystem-specific characteristics in modulating these driver responses. Based on empirical data, the CO_2 fluxes were up-scaled to evaluate lakes and reservoir contribution to the global carbon budget.

In Chapter 5, I synthesize the results and address the questions: What are the multi-temporal drivers of CO_2 flux, how do they change with time scale, and how do ecosystem feedbacks to environmental drivers? I also discuss the uncertainties attributed to estimating CO_2 in freshwaters and how they may affect our ability to predict ecosystem responses to global change. Together, these findings are used to provide a pathway for future research and pathways for the discipline.

CHAPTER 2

Large uncertainty in estimating pCO_2 from carbonate equilibria in lakes

AUTHORS

Malgorzata Golub, Ankur R. Desai, Galen A. McKinley, Christina K. Remucal, Emily H. Stanley

KEY POINTS

- pCO_2 random error varies by input parameter pairs and lake alkalinity groups
- Systematic uncertainty dominates random errors in pCO_2 estimation
- Comparison to directly observed pCO_2 reveals poor precision and accuracy of calculated pCO_2

ABSTRACT

Most estimates of carbon dioxide (CO_2) evasion from freshwaters rely on calculating the partial pressure of CO_2 (pCO_2) from two CO_2-related parameters using carbonate equilibria. Thus, input parameter errors drive uncertainty of pCO_2 estimates. We quantified random errors in the parameters pH, dissolved inorganic carbon and alkalinity from North Temperate Lakes Long Term Ecological Research paired observation time series, and using a bootstrap approach, propagated the errors onto pCO_2 calculated from three carbonate equilibria in four lake groups across a broad gradient of chemical composition. We also compared the error magnitudes between direct and estimated pCO_2 observations. The empirical random errors of the three parameters were mostly below 2% of the median, although the measurements in low alkalinity lakes were more uncertain. Depending on the alkalinity group and choice of input parameter pairs, random pCO_2 errors ranged

from 3.7% to 31% of the median. However, when compared with direct pCO_2 measurements, all parameter combinations produced biased pCO_2 estimates with only 3%-31% of total errors explained by random pCO_2 errors indicating that systematic uncertainties dominated pCO_2 calculations. We demonstrate poor precision and accuracy of pCO_2 estimates derived from any combination of two CO_2-related parameters and recommend direct pCO_2 measurements instead. These results indicate that historical observations of carbon system parameters are unlikely to provide robust estimates of mean or temporal trends in pCO_2. To reduce uncertainty in CO_2 emissions from freshwater components of terrestrial carbon balances, future efforts should focus on improving accuracy and precision of CO_2-related parameter (including direct pCO_2) measurements and associated pCO_2 calculations.

2.1 INTRODUCTION

Outgassing of carbon dioxide (CO_2) from inland waters has been estimated to offset approximately 60% of net uptake of carbon into the terrestrial biosphere. However, this calculation is based on estimates of source strength at the air-water interface that is highly uncertain [*Ciais et al.*, 2013; *Raymond et al.*, 2013]. One of the largest unknowns is the accuracy and precision of freshwater partial pressure of CO_2 (pCO_2) estimates. Improving understanding and comprehensive evaluation of how observational uncertainties propagate onto pCO_2 estimation is therefore a key step towards achieving robust estimates CO_2 emissions from freshwater components of terrestrial carbon balances with improved confidence in detection of long-term change.

The net air-water CO_2 exchange is calculated as a product of the CO_2 gas transfer velocity (k), the CO_2 solubility constant (K_0) and the gradient between pCO_2 in the atmosphere and water (ΔpCO_2). The aquatic component of ΔpCO_2 in current estimates of carbon evasion from inland waters relies on calculating pCO_2 using carbonate equilibria due to scarcity of direct pCO_2

measurements at regional and global scales [*Atilla et al.*, 2011; *Butman and Raymond*, 2011; *McDonald et al.*, 2013; *Raymond et al.*, 2013]. Carbonate equilibria use temperature and the combination of two CO_2-related parameters (i.e., pH, alkalinity (ALK), dissolved inorganic carbon (DIC)) to calculate pCO_2 in surface waters [*Parkhurst and Appelo*, 1999; *van Heuven et al.*, 2011]. Therefore, the knowledge on the magnitudes and sources of parameter errors is necessary to quantify the effect of those uncertainties on estimates of aquatic pCO_2.

Oceanographers have made significant efforts to standardize and reduce errors, resulting in thermodynamically consistent measurements of CO_2-related parameters, highly precise and accurate estimates of the seawater carbonate system [*Lueker et al.*, 2000; *Millero*, 2007], and thus of the ocean sink for anthropogenic carbon [*Sabine et al.*, 2004; *Ciais et al.*, 2013b; *Khatiwala et al.*, 2013]. Similar efforts however have not been undertaken for the carbon dioxide system in freshwaters. Although there would be an additional challenge of addressing the more diverse chemical composition of inland waters [*Dickson and Riley*, 1978], an error analysis for freshwaters is critical to identify key uncertainties in measurements of CO_2-related parameters and pCO_2 calculations.

Given the high accuracy and precision of atmospheric pCO_2 measurements [*Andrews et al.*, 2014], uncertainties attributed to measurement errors in aquatic carbon system parameters are likely the largest source of uncertainty in ΔpCO_2 calculated from carbonate equilibria. The measurement errors include systematic errors and random errors. Systematic errors (e.g., instrument limitations and methodological errors) affect the accuracy of the measurements [*Skoog et al.*, 2014] and lead to directional (i.e., positive or negative) biases in the measurements of pH, ALK, and DIC concentration [*Herczeg and Hesslein*, 1984; *French et al.*, 2002; *Lozovik*, 2005]. Although systematic errors are likely to cause biased pCO_2 estimates in surface waters [*Herczeg*

and Hesslein, 1984; *Butman and Raymond*, 2011; *Abril et al.*, 2015], their contributions to regional and global CO_2 emissions from freshwaters have not yet been quantified [*Raymond et al.*, 2013]. Fully accounting for systematic biases and quantifying their effect on the accuracy of pCO_2 estimates will however require information on instrumentation and analytical procedures used among researchers. Such information is not currently available for freshwater systems.

Random errors are always present in carbonate system parameter observations but must be considered during data analysis and result interpretation [*Aubinet et al.*, 2012]. Difficult to control factors (e.g., fluctuations of temperature or barometric pressure) or insufficient understanding of errors in analytical procedures cause data to scatter around the mean values and affect the parameter precision and accuracy [*Skoog et al.*, 2014]. The measurement precision is characterized by estimating the standard deviation from multiple measurements collected under different conditions (reproducibility) or from a pair of independent measurements made under identical conditions (repeatability), assuming normally distributed errors [*ISO*, 2010]. Unlike in atmospheric and oceanic studies [*Millero*, 2007; *Andrews et al.*, 2014], acceptable precision levels have not been quantified for freshwater systems. However, quantifying errors is necessary to estimate uncertainty around pCO_2 means and temporal trends. To our knowledge, there is no comprehensive study on how random errors in pH, ALK and DIC affect the precision of pCO_2 calculated from multiple carbonate equilibria in freshwaters, contributing to current uncertainties in estimating pCO_2.

In view of increasing use of carbonate equilibria to estimate pCO_2 and C flux from freshwater systems, we asked: What are the uncertainties attributed to pCO_2 calculations from carbonate equilibria using two CO_2-related parameters? This is currently the most commonly used approach of estimating pCO_2 but quantitative studies on uncertainties propagating through

equilibria remains scarce. To help rectify this knowledge gap, we conduct a comprehensive error analysis of historical observations at North Temperate Lake Long Term Ecological Research (NTL LTER) site. We quantify random errors in pH, DIC, ALK measurements to demonstrate how these propagate onto uncertainties in pCO_2 estimated from three carbonate equilibria in four lake groups across a broad gradient of water chemical composition. Although our study primarily focuses on random error analysis, we also compare uncertainties in direct and estimated pCO_2 observations to determine whether random pCO_2 errors are a dominant source of uncertainty in pCO_2 calculations.

2.2 MATERIAL AND METHODS

Study site and data collection

We quantified random error using observations from the NTL LTER data set for years 1986 – 2011 (NTL LTER website). Carbonate system parameters have been measured since 1986 in seven lakes located in northern Wisconsin, USA, and in four lakes in southern Wisconsin since 1996. The northern lakes are located in the Northern Highland Lake District (NHLD) which has a mosaic of mixed, hardwood, and coniferous forests (~53 % of total area), wetlands (28%), lakes (13%), and other land coverages [*Buffam et al.*, 2010]. Soils in the NHLD are dominated by sandy gravel and gravelly sand with dominance of silicate over carbonate [*Attig*, 1985]. The southern lakes are located in the Yahara River Lake District (YRLD), which is dominated by agriculture (65%), urban (20%) land uses and the remainder for forest, wetland, or water bodies [*Carpenter et al.*, 2007]. Soils in YRLD are dominated by glacial tills, most commonly sand, silt and clay accumulated over dolomite and limestone parent geology [*Clayton and Attig*, 1997].

The carbon system parameters: pH, total alkalinity (ALK), and dissolved inorganic carbon (DIC), and water temperature (WT) were measured biweekly (WT), monthly (pH and DIC), or quarterly (ALK). Depending on the lake maximum depth and thermocline depth, the samples were taken from one to six depths per sampling. On each sampling occasion, blind-paired samples were collected for all variables except water temperature from a randomly selected depth. To ensure valid comparison across the three combinations of input parameters, we used only data with paired measurements for all three CO_2-related parameters. This limited the analysis to quarterly measurements at one depth per lake.

To prevent CO_2 loss or entrainment, water samples for determination of CO_2-related parameters were gently collected, avoiding splashing and air exposure. The bottles were rinsed with the water to be sampled, then filled to the top including overflow, and carefully screwed on the displacement cap. Bottles were checked for the presence of air bubbles by inverting the bottles. If bubbles were present, water samples were discarded and refilled again.

Water samples for pH measurements were collected with a peristaltic pump and tubing to 20 ml scintillation vials with displacement caps to exclude air from the vial. In this study we used the air-excluded pH samples only. The samples were stored in a cold and dark container minimize biological activity until just before analysis, and then warmed up in the same container to room temperature. The pH samples were analyzed the same day using a potentiometric method in two laboratories: Hasler Lab in Madison (water samples from southern lakes) and Trout Lake Station Lab (water samples from northern lakes). The electrode syringe barrel sealed with teflon tape around the electrode was conditioned with lake water to be analyzed for at least 15 minutes. After uncovering the electrode filling solution hole, the conditioning solution was removed from the barrel using the three-way valve and aspiration system. The electrode chamber was flushed in and

out for several times with 2-ml water samples to be measured. The bottles for pH determination were opened just before analysis to draw of 2-ml aliquots of the water sample for several runs of measurements. The measurements were repeated until two consecutive millivolt readings were within 1 mV. Last mV reading was recorded. After analyzing all samples, the mV readings for three buffer solutions: pH 10.00, 7.00, and 4.00 were obtained. The recorded buffer and sample mV values were used to calculate pH values. The pH meters were changed from PHM84 Research pH meter to Orion model 720 pH meter in 1988. Since July 2010, pH was measured using a Radiometer combination pH electrode and Orion 4Star pH meter. The dates of pH electrode replacement were unavailable. The relative accuracy of all pH meters was ±0.002 according to the manufacturers' specifications.

Dissolved inorganic carbon (DIC) samples were collected with the peristaltic pump, tubing and in-line filtered through 0.40-micron polycarbonate filter into 24 ml glass vials capped with septa, leaving no head space. The samples were not poisoned prior storage analysis. The samples were refrigerated at 4˚C and sent in the shipper to Hasler Lab via Fed Ex overnight delivery. The samples were stored refrigerated and analyzed within two-to-three weeks. After phosphoric acid addition, the samples were analyzed with OI Model 700 Carbon Analyzer (before May 2006) or a Shimadzu TOC-V-csh Total Organic Carbon Analyzer (to date). The detection limit for DIC was 0.15 ppm for the analytical measurement range of 60 ppm. The accuracy and precision of Shimadzu's Analyzer was 1.5% according to manufacturer' specification.

Total alkalinity (ALK) samples were collected with the peristaltic pump and tubing to 20 ml HDPE plastic containers with conical caps. The ALK samples were not poisoned prior storage and analysis. The samples were stored refrigerated at 4˚C and then sent to Hasler Lab in Madison via Fed Ex overnight delivery. The sample were stored refrigerated at 4˚C until determination,

which typically occurred within two weeks. Prior to analytical determination, samples were brought to room temperature. ALK was determined by titrating water samples to an endpoint pH of circa 3.557 by adding 10 μL increments of 0.05N HCL to 16-ml sample from southern lakes or 0.01N HCL to 4-ml sample from northern lakes. Between February 1986 and November 2001, the alkalinity measurements in four lakes (Trout Lake, Sparkling Lake, Allequash Lake and Big Muskellunge Lake) were made using a Brinkmann 636 Titroprocessor. The detection limit for the gran alkalinity titration was approximately 5 μeq. L^{-1}, for the analytical range spanning to 4000 μeq. L^{-1}. The accuracy of manual alkalinity titration is unavailable.

Random errors in CO_2-related parameters

To minimize the impact of outlying observations on distribution and statistical properties of random errors, we removed paired measurements with chemical composition differences larger than 15% following the NTL LTER QA/QC protocol. Many of removed observations were already flagged for other quality control reasons. Quality control led to removal of 8% (58/709) of pH observations in antilog scale, 9.5% (68/709) of ALK measurements, and 2.4% (14/709) of DIC observations.

Because carbonate chemistry data in NTL LTER lakes varied over 1-3 orders of magnitude (Table 2.1), the lakes were grouped into four groups based on ALK and dissolved organic (DOC) concentrations: two bog lakes with low ALK but high DOC (hitherto called "LB_{ALK}", one clearwater lake with low ALK and low DOC ("LC_{ALK}"), four lakes with moderate ALK and low DOC ("M_{ALK}"), and four lakes with high and moderate DOC ("H_{ALK}"). Grouping lakes also allowed having large enough populations of paired observations to generate reasonable resampling distribution [*Chernick and LaBudde*, 2011] for error analysis.

To quantify random uncertainties from paired samples, we followed the approach described in *Hollinger and Richardson* [2005]. For a given parameter (P_i) we used a pair of independent measurements (X_1, X_2) that were made under identical conditions. Because every measurement (X_i) is subject to uncertainties, each parameter value represents the best estimate of the measured constituent plus the random (ε) and systematic (δ) errors. While random errors cause scatter around the mean value, systematic errors underestimate or overestimate the mean value. Since no information on systematic errors in CO_2-related parameters at NTL LTER site were available for the majority of the records, we initially focused on the effect of random errors only while neglecting the effect of systematic uncertainties on the pair. Thus, ε was an approximation of the random variable with mean 0 and standard deviation σ(ε). Since the mean difference between two independent measurements (X_1–X_2) was close to zero and random uncertainties were independent and identically distributed, the standard deviation σ(ε) can be determined from equation 1:

$$\sigma(\varepsilon) = \frac{1}{\sqrt{2}}\sigma(X_1 - X_2) \qquad \text{(Eq. 1)}$$

Therefore, random errors of each parameter, $\varepsilon_{(P_i)}$, were quantified as the standard deviation of the difference of repeated pairs of measurements.

Finally, distributions of parameter errors were characterized by fitting and characterizing the probability density functions (pdf) using the fitdist function in Matlab R2014b and open-source codes. For each pdf, the mean, the scaling, and if applicable, the shape parameters, skewness and kurtosis were calculated. We used Shapiro-Wilk test to evaluate the normality of each distribution.

The effect of random parameter errors on pCO_2 *estimates*

To assess random uncertainty attributed to pCO_2 estimation, we propagated errors onto pCO_2 derived from two CO_2-related parameters. We used three combinations of two input parameters: pH-DIC (pCO_2-pH-DIC equilibrium), pH-ALK (pCO_2-pH-ALK equilibrium), and ALK-DIC (pCO_2-ALK-DIC equilibrium). All three thermodynamic equilibria calculated pCO_2 from pH and DIC; however, the calculations in two equilibria (pCO_2-pH-ALK and pCO_2-ALK-DIC) required an additional step of estimating of DIC and pH, respectively.

The mass-conservation equation for DIC calculations was defined as:

$$[\mathrm{DIC}] = [\mathrm{H_2CO_3^*}] + [\mathrm{HCO_3^-}] + [\mathrm{CO_3^{2-}}] \quad \text{(Eq. 2)}$$

Where $\mathrm{H_2CO_3^*}$ is the sum of aqueous CO_2 and carbonic acid (H_2CO_3). The alkalinity equation neglected the contribution of non-CO_2 species and was defined as:

$$[\mathrm{ALK}] = [\mathrm{HCO_3^-}] + 2[\mathrm{CO_3^{2-}}] + [\mathrm{OH^-}] - [\mathrm{H^+}] \quad \text{(Eq. 3)}$$

For pCO_2 calculations, we used *in-situ* water temperature, the dissociation constants for freshwaters after *Millero* [1979], and barometric pressure at 1 atmosphere. The influence of ionic strength was neglected and all calculations were performed in pH NBS scale. Calculations were performed with the MATLAB-version of the CO_2 System Calculations [i.e., CO2SYS, *van Heuven et al.*, 2011]. The sets of equations for three parameter pairs are described in [*Dickson, A.G., Sabine, C.L., Christian*, 2007].

A bootstrap method was used to propagate parameter errors onto carbonate equilibria equations to estimate random pCO_2 errors. This approach uses empirical data and does not introduces any assumptions about error population distributions [*Chernick and LaBudde*, 2011]. It also provides more realistic estimates of random uncertainty because allows partial cancelation of errors. At each iteration, the random error for each parameter were bootstrapped with substitution

from the error pools specific for each alkalinity group. The parameters' error terms were simultaneously applied to the entire population of observations within each ALK group representing a full spectrum of chemical and temperature ranges observed in lakes. Applying errors to all observations at once permitted to investigate errors propagating through equations, not errors in individual observations [*Yanai et al.*, 2010]. Since parameter measurements were independent, the covariance between two parameters was assumed zero and random errors uncorrelated [*Bevington and Robinson*, 2003]. Therefore, random errors for each parameter were propagated independently.

We propagated random parameter errors 10000 times, and at each iteration, computed the population pCO_2 median. For highly-skewed or heavy-tailed distributions, similar to distributions found for both parameters and random errors (Table 2.2, Figure S1), the sample median is considered a good measure of central tendency [*Chernick and LaBudde*, 2011]. From histogram of 10000 population pCO_2 medians, we inferred the properties of random pCO_2 error distribution. The population median described the best estimate of population center within each ALK group. The uncertainty in the estimate of population median were described as the standard error of the median. For each ALK group, we propagated random errors in three runs, one run with errors in both parameters, and two runs with errors in each parameter separately. The uncertainty attributed to bootstrapping accounted for <1% in all three carbonate equilibria.

Although our goal was to demonstrate uncertainty propagating onto pCO_2 derived from two carbonate parameters, we also acknowledge that using just two CO_2-related parameters may result in spurious pCO_2 estimates in some ALK groups. Therefore, we also run additional simulations after correcting organic acids contribution to total alkalinity in the LB_{ALK} group and after considering ionic strength influences in the H_{ALK} group. In the LB_{ALK} group, 1 μM of ALK

was subtracted for each 1 mg L^{-1} of DOC before running ALK-based equilibria. The pool of observations for pCO_2 calculations decreased by 30% as negative ALK observations were removed before simulations. Additionally, we corrected thermodynamic constant for influences of ionic strength before pCO_2 calculations in the H_{ALK} group. Only one hardwater lake (Lake Wingra) had major ions measurements and the same ionic strength was assumed for other lakes within H_{ALK} group. Estimated ionic was calculated from a Debye-Hückel equation [*Brezonik and Arnold*, 2011] and accounted for I=0.0091 M. The activity coefficients were calculated from an extended Debye-Hückel equation [*Brezonik and Arnold*, 2011].

The estimates of random uncertainty in pCO_2 estimation were conservative because they did not take into account temperature effect on pCO_2 errors. Temperature effect can be large as it affects non-state variables (i.e., pCO_2 and pH) and calculations of two dissociation constants of carbonic acid and [*Lueker et al.*, 2000; *Atilla et al.*, 2011]. Our dataset does not have paired observations of water temperature to estimate the stochastic error in temperature measurements and poses limitations of this study

The pCO_2 values estimated from pCO_2-ALK-DIC equilibrium in LC_{ALK}, M_{ALK}, and H_{ALK} groups were also biased relative pCO_2 calculated from pCO_2-pH-DIC and pCO_2-pH-ALK equilibria because observations with DIC concentrations smaller than ALK concentrations (DIC<ALK) were removed. Exclusion of DIC<ALK observations enabled pCO_2-ALK-DIC equilibrium to solve for pH over 10000 iterations in this ALK groups. A single model iteration revealed that removing DIC<ALK (more alkaline) observations increased the median pCO_2 estimates by 22, 123, 1448 μatm in the LC_{ALK}, M_{ALK}, and H_{ALK} groups, respectively. Removed observations accounted for 4 (4.2%) observations in LC_{ALK} group, 77 (11.7%) in M_{ALK} group, and

101 (34.6%) in H_{ALK} group (Text S2.1, Fig. S2.1). Negative ALK observations were also removed before propagating errors in pCO_2-pH-ALK and pCO_2-ALK-DIC equilibria.

Comparison of uncertainties in direct and indirect pCO_2 measurements

To determine how much uncertainty between direct and indirect measurements can be explained by random error propagating though three carbonate equilibria, we took direct measurements of pCO_2 together with carbonate chemistry measurements for a limited number of observations (n=17). The measurements of CO_2-related parameters were taken according sampling and handling protocols described above. The mole fraction of CO_2 (ppmv) at 0.1 m depth was directly measured using a non-dispersive infrared Vaisala CARBOCAP CO_2 probe enclosed in waterproof, gas permeable polytetrafluoroethylene (PTFE) membrane following the *Johnson et al.*, [*Wilcox*, 2010] approach. Each measurement was taken over 16 minutes, first allowing the probe to equilibrate to environmental conditions (which generally occurred within 15 minutes), and then taking a one-minute measurement at one second intervals.

The probes were calibrated against gas standards in the laboratory before each field campaign to evaluate if the probe performs within the manufacturers' accuracy specifications and to identify potential sensor drifts. The average of the last 60 records was assumed to represent field CO_2 concentration. The measured CO_2 values were linearly fitted to calibration curves. The post-measurement corrections of calibrated values were applied to compensate temperature and barometric pressure differences relative to manufacturer's factory settings (i.e., 1013 hPa at 25°C), 1.5 ppmv CO_2 values increases per 1 hPa barometric pressure decrease and 3 ppmv declines per 1°C water temperature decrease. These corrections were derived empirically by the manufacturer. Additionally, the CO_2 values were lowered by 14.7 ppm to compensate for greater pressure on

probes at 10 cm measurement depth [*Johnson et al.*, 2010]. The partial pressure of CO_2 in μatm (pCO_2) were calculated as a product of mole fraction and barometric pressure at 1 atmosphere.

The probe accuracy and precision were 1.5% of the range and 2% of the reading at 25° C and 1 atmosphere for a range of 0-3000 ppm according to manufacturer specification and consistent with our calibration results. The paired observations of direct pCO_2 measurements were not taken, hence the precision of field measurements were unquantified.

Finally, for each data point, we used the combination of corresponding paired measurements of pH, DIC, and ALK to calculate pCO_2. The lake-specific random parameter errors were propagated onto each pCO_2 observation over 10000 iterations; each pCO_2 estimate and its random error constitute the median and standard deviation of 10000 medians. The random error in direct measurements was set to 2% following the manufacturer specifications.

2.3 RESULTS

Random errors in CO_2-related parameters

The analysis of nearly 600 paired samples showed that most random errors in CO_2-related parameters measurements were relatively small relative to parameters' medians when pooled by alkalinity group (Table 2.1-2.2). The random error standard deviation (σ_n), the estimate of measurements' precision, in pH measurements were ±0.02 across all ALK groups and were below 0.4% of the median. Unlike errors in pH, the random errors in ALK and DIC measurements increased with the magnitude of parameters' measurements. The random ALK errors ranged from ±0.3 μM in LC_{ALK} group to ±56.4 μM in H_{ALK} group. Similarly, the smallest random DIC errors were in LC_{ALK} group, ±3.4 μM, while the largest errors were in H_{ALK} group, ±83 μM. However, when expressed in relative measures, the random uncertainty was the largest in low ALK groups,

accounting for 15.94% of the median ALK in LB_{ALK} group and 5.5% of the median DIC in LC_{ALK} group. The parameter error magnitudes were also independent of the season, year, water temperature, and measurement depth (Fig. S2.3).

The empirical distributions of random parameter errors were generally symmetrical around the mean with skewness values close to zero (Table 2.2, Fig. S2.2). Although the kurtosis for pH across all ALK groups was close to kurtosis values observed in normally distributed data (typically <3), the errors in ALK and DIC were strongly leptokurtic with characteristic high peaks near the mean difference and heavy tails. The Gaussian distributions were confirmed for random pH errors in LB_{ALK} and LC_{ALK} groups only (Shapiro-Wilk test, $p<0.05$). Hence, σ_n would inadequately characterize the parameters' error dispersion in ALK and DIC measurements.

A t location-scale distribution (tLocat) best characterized distribution of random errors in ALK and DIC (Fig. S2.2). This distribution has an additional, shape parameter (ν) where small values indicate heavy tails in error distributions and sensitivity to outliers. Low ν values (<2) were found in DIC error distributions across all ALK groups and in ALK error distributions in medium to high ALK groups (Table 2.2). However, the tLocat distribution provided only a slightly better fit compared to normal distribution in pH uncertainties and approached a normal distribution in the H_{ALK} group. Other probability density functions which can accept negative values of random parameter errors did not improve the data fit (data not shown).

The effect of random parameter errors on pCO_2 estimates

Random pCO_2 errors propagating through ALK-based equilibria were always higher than pCO_2 errors propagating through pCO_2-pH-DIC equilibrium (Table 2.3). We found only two cases where random pCO_2 errors were comparable, with pCO_2-pH-DIC and pCO_2-pH-ALK equilibria

differing by 10% in the M_{ALK} group and by 8% in the H_{ALK} group. In contrast, the random pCO_2 errors derived from pCO_2-ALK-DIC equilibrium were 5 and 30 times higher in M_{ALK} and H_{ALK} groups compared to errors propagating through pCO_2-pH-DIC equilibrium. In the LC_{ALK} group, the random pCO_2 errors were 2 times (pCO_2-pH-ALK equilibrium) and 0.5 times (pCO_2-ALK-DIC equilibrium) higher relative to random pCO_2 errors derived from pCO_2-pH-DIC equilibrium. The pCO_2-pH-ALK and pCO_2-pH-DIC equilibria in the LB_{ALK} group showed 6 and 0.2 times higher sensitivities to random parameter errors relative to pCO_2-ALK-DIC equilibrium.

Across the lake alkalinity gradient, random pCO_2 errors calculated from pCO_2-pH-DIC equilibrium were the highest (±166 μatm) in LB_{ALK} group, but remained similar (~40 μatm) across the remainder of ALK groups (Table 2.3). Similarly, random errors propagating through pCO_2-pH-ALK equilibrium were also highest (±1026 μatm) in the LB_{ALK} group, though the error decreased steadily down to ±41 along ALK groups. The pCO_2 errors calculated from pCO_2-ALK-DIC equilibrium ranged from ± 59 μatm in the LC_{ALK} group to ± 1156 μatm in H_{ALK} group. Extreme pCO_2 errors corresponded to unrealistically high estimates of median pCO_2: 15225±1026 μatm (10999±935 μatm after adjustment) derived from pH and ALK in the LB_{ALK} group, and 3725±1156 μatm (3129±985 μatm after adjustment) calculated from pCO_2-ALK-DIC equilibrium in the H_{ALK} group (Table 2.3).

Regardless of carbonate equilibrium used, random pCO_2 errors were exponentially proportional to the median pCO_2 (Fig. 2.1). Random pCO_2 errors decreased along pH gradient in pCO_2-pH-DIC and pCO_2-pH-ALK equilibria, with greatest pCO_2 error decline per pH unit change in acidic waters (pH<5.5) (Fig. 2.1). Unlike in pH-based equilibria, the random pCO_2 errors propagating through pCO_2-ALK-DIC equilibrium were higher at both ends of pH gradient with

minimum error at pH around 6.5. Changes in pCO_2 errors along DIC and ALK gradients depended on the carbonate equilibrium used.

Adjusting for contribution of organic acids to total alkalinity in humic lakes (LB_{ALK} group) and for ionic strength in highly buffered lakes (H_{ALK} group) generally resulted in lower random pCO_2 errors (Table 2.3). The random pCO_2 error decreased by 9%, from ±1026 μatm to ±935 μatm in pCO_2 derived from pH and ALK in LB_{ALK} group. However, adjusted values were still 5 times more sensitive to random parameter errors relative to pCO_2 errors derived from pH and DIC. Adjusting pCO_2 in pCO_2-ALK-DIC equilibrium nearly doubled uncertainty from ±198 μatm to ±391 μatm. Correcting for ionic strength in HALK groups decreased random pCO_2 errors by 15% across three carbonate equilibria.

Comparison of uncertainties in direct and indirect pCO_2 measurements

The spread of random pCO_2 errors in indirect observations, expressed here as mean absolute deviation, accounted for at least 33, 10, 7, 36 μatm in LB_{ALK}, LC_{ALK}, M_{ALK}, and H_{ALK} groups, respectively (Table 2.4). Random error deviation in direct pCO_2 measurements in these groups were 7, 3, 4, and 5 μatm, respectively. The largest random pCO_2 errors in direct and indirect observations cumulatively explained less than 16%, 32%, 12%, 27% of the root-mean-square errors (RMSEs) between direct and indirect pCO_2 observations in LB_{ALK}, LC_{ALK}, M_{ALK}, and H_{ALK} groups, respectively. The global RMSEs were explained by random pCO_2 errors by <8% in pCO_2-pH-DIC equilibrium, <5% in pCO_2-pH-ALK equilibrium, and <20% in pCO_2-ALK-DIC equilibrium (Fig. 2.2, Table 2.4).

Although measurements of carbonate parameters were taken at the same time as direct pCO_2 measurements, the calculated pCO_2 always failed to reproduce direct pCO_2 (Fig. 2.2, Table 2.4). Equilibria pCO_2-pH-DIC and pCO_2-pH-ALK tended to overestimate pCO_2, while pCO_2-

DIC-ALK equilibrium generally underestimated pCO_2 (Fig. 2.2). The largest mismatch with directly measured pCO_2 occurred for observations in the LB_{ALK} group calculated from pCO_2-pH-ALK equilibrium and in the H_{ALK} group calculated all from any combination of parameters had. These discrepancies persisted even after adjusting pCO_2 values for influences of organics acids and ionic strength.

2.4 DISCUSSION

Random errors in CO_2-related parameters

Most random errors were relatively small relative to median parameter values when pooled by lake type (Table 2.1-2.2). The standard deviations of carbonate parameter measurements derived for a normal distribution (σ_n) reported in Table 2.2 compare our estimates of parameter repeatability with published values of precision. The precision in the pH measurements ranged from ±0.01 to ±0.17 pH units, thus pH precision values were among the most precise potentiometric pH measurements reported for freshwaters [*Herczeg and Hesslein*, 1984; *French et al.*, 2002; *Phillips et al.*, 2015]. More precise pH measurements are achieved using spectrophotometric methods with precision ranging from ±0.008 to ±0.002 pH units [*French et al.*, 2002; *Lynch et al.*, 2010]. The reported repeatability in DIC and ALK measurements in low to medium ALK groups agreed with precision values ranging <12 μM [*Wilkinson et al.*, 1992; *Baehr and DeGrandpre*, 2002; *Abril et al.*, 2015]. However, random errors in highly buffered waters (H_{ALK} group) were approximately four-fold higher for ALK and sevenfold for DIC (Table 2.2) than ever reported.

The empirical error distributions deviated from the normal distribution assumption in the majority of carbonate parameters' measurements in this study (Fig. S2.2, Table 2.2), similarly to CO_2-related studies showing non-Gaussian distributions of random errors [*Richardson and*

Hollinger, 2005; *Ciais et al.*, 2013b; *Cueva et al.*, 2015]. The fitted probability density functions imply more frequent small errors around the mean parameter errors (around zero) and also more frequent high errors compared to errors that would otherwise be derived from normal probability density functions (Table 2.2, Fig. S.2). Hence, the errors derived from normal distribution will underestimate both small and large random errors at the heavy distribution tails.

Although the tLocat distribution provided better fit over Gaussian in ALK and DIC observation coming from M_{ALK} to H_{ALK} groups, neither of these two distributions nor any other probability density functions fitted provided good data fit in some ALK groups (i.e., pH in M_{ALK}, Fig. S2.2). Moreover, the variance was defined only for shape parameter values of $\nu>2$ in tLocat distribution (Table 2.2). These results influenced our choice of the method to propagate random parameter errors onto carbonate equilibria, the bootstrap approach over the Monte Carlo approach, as no assumptions regarding error distributions were required. The variety of error distribution also limits the use of statistical and modeling techniques (i.e., assuming normal distribution) to describe pCO_2 uncertainties.

The heavy tails in the PDFs of random parameters' errors might also be indicative of a quality control problem that warrants further evaluation of NTL LTER data. The outlying observations with large concentration differences between duplicates (expressed as high kurtosis and low tLocat shape parameter ν, Table 2.2) were present despite prior-analysis removal of duplicate pairs that differed more than 15% (Fig. S2.2). These results suggest that samples chemical composition can significantly change between samples collection and analytical analysis (from several hours for pH to two-three weeks for ALK and DIC samples). Potential sources behind changing constituents' composition include lack of sample poisoning to stop biological activity [*Dickson, A.G., Sabine, C.L., Christian*, 2007; *Åberg and Wallin*, 2014], taking unfiltered ALK

samples with substantial amount of acid-neutralizing particles [*Abril et al.*, 2015], DOC interference with pH electrode [*Herczeg and Hesslein*, 1984], transport of samples to another lab or long shelfing time between duplicate samples analysis. Many of enlisted potential errors are systematic, and unlike random uncertainties, cannot be evaluated from duplicate samples. This warrants further targeted efforts towards quantifying and reducing errors in NTL LTER site.

The increased uncertainty of certain measurements in some ALK groups might also indicate that the behavior of systematic errors may vary under certain conditions. For example, the measurements of ALK in humic lakes (LB_{ALK} group) and pH in highly buffered and productive lakes (H_{ALK} group) were particularly vulnerable, with 46% and 17% of paired observations failing QA/QC criterion. Furthermore, even though the random parameter errors were generally below 2% of the median, the uncertainties in ALK and DIC measurements exceeded 5% in low ALK groups (Table 2.1-2.2). These results may suggest the presence of systematic biases in the measurements in these groups (and likely in other ALK groups) and potential challenges for correcting historical observations for these biases.

4.1. The effect of random parameter errors on pCO_2 estimates

The cumulative effect of random parameter errors on pCO_2 calculations across alkalinity gradient in NTL LTER site showed that sensitivity to errors varied by the choice of input parameter pairs and alkalinity group. Although the parameter errors were generally below ±2% of parameters' median values across all ALK groups (Table 2.1-2.2), unadjusted pCO_2 errors ranged from ±3.7% to ±31.5%, depending on parameter pairs and lake ALK group (Table 2.3). Our repeatability estimates for pCO_2-pH-DIC (±3.7%-5.5%) were within range of the few existing studies for freshwaters, where the precision of pCO_2 calculated ranged from 3% to 5% [*Herczeg and Hesslein*, 1984; *Baehr and DeGrandpre*, 2004].

Among the three equilibrium models, the pCO_2-pH-DIC equilibrium was always least sensitive to random errors in the input parameter pairs (Table 2.3). The highest attainable precision of pCO_2 estimates was ±36 μatm (5.5%) in the LC_{ALK} group and ±45 μatm (3.7%) in the M_{ALK} group. The pCO_2 estimates calculated from ALK and DIC were most uncertain. Similar patterns of propagated random pCO_2 uncertainty was found in seawater studies [*Dickson and Riley*, 1978; *Millero*, 2007], however our lowest pCO_2 errors were at least 20 times higher than in seawaters [*Millero*, 2007]. Although findings from *Millero* [2007] cannot be directly applied to chemically heterogeneous freshwaters [*Dickson and Riley*, 1978], our results imply low precision of pCO_2 estimates based on historical pH, DIC and ALK data from our study lakes.

Single-parameter random error propagation identified that dominant terms contributing to random pCO_2 uncertainty changed along water chemical composition (across ALK groups). In pCO_2-pH-DIC and pCO_2-pH-ALK equilibria, the dominance of DIC and ALK uncertainty in contribution to pCO_2 uncertainty switched to pH uncertainty with increasing ALK (Table 2.3). The "break point" fell between LC_{ALK} and M_{ALK} groups which corresponded to transition from slightly acidic to slightly alkaline waters (Table 2.1). The largest single-parameter contribution to pCO_2 error was observed at both ends of buffering capacity gradient, in LB_{ALK} and H_{ALK} groups. For example, although random pH errors were the same across all ALK groups (Table 2.2), the pH effect on pCO_2 derived from pCO_2-pH-DIC equilibrium increased from ~30% in the LB_{ALK} group to ~90% in the H_{ALK} group (Table 2.3).

The pCO_2 calculations from ALK and DIC were overall highly uncertain (Table 2.3) and also likely obscured by reduced number of observations in all ALK groups except for the LB_{ALK} group (removed observations with DIC<ALK concentrations (Fig. S2.1), negative alkalinity, failing QA/QC criteria).

The random error propagation showed that the lower the median pCO_2, the higher the precision of pCO_2 estimates (Fig. 2.1, Table 2.3). For example, uncertainties generally declined after adjusting for ionic strength in the H_{ALK} group or for organic acid contribution in the LB_{ALK} group since applying corrections resulted in lower median pCO_2 estimates and accordingly lower random pCO_2 errors (except for pCO_2 derived from ALK and DIC in the LB_{ALK} group). Doubled pCO_2 uncertainty (from pCO_2-ALK-DIC equilibrium) in bog lakes could partly be explained by 13% increase in median pCO_2 due to removal observations with negative alkalinity. Since this equilibrium is also highly prone to errors due to similar DIC and ALK values [*Dickson and Riley*, 1978], we likely introduced additional errors in pCO_2 calculations by assuming non-carbonate concentrations equated DOC concentrations without verifying by charge balance of major ions. The proportionality of random error to median pCO_2 also implies that any inaccuracies in estimating median pCO_2 will be reflected in random pCO_2 estimates.

Comparing random pCO_2 errors across ALK groups also allowed to assess how error magnitudes propagated through three carbonate equilibria with changing water chemical composition. pCO_2 errors showed largest declines were in these waters and overall inversely proportional to pH (Fig. 2.1, Table 2.3) since low pH and low ALK waters had highest median pCO_2 derived from pH-based equilibria. This is not surprising given DIC species concentrations in carbonate equilibria are a function of the pH [*Brezonik and Arnold*, 2011]. Nonlinear relationship with increasing pH and pCO_2 errors were in pCO_2-ALK-DIC equilibrium where largest uncertainties were in hardwater and humic lakes. Nonlinearities of pCO_2 errors in DIC-based equilibria corresponded to high pCO_2 errors in low ALK, high DOC waters (humic lakes).

The comparison of pCO_2 errors within ALK groups permitted us to examine if three carbonate equilibria showed similar sensitivities to random parameter errors under the same water

chemical composition. While all three equilibria should produce similar pCO_2 values and errors, the comparisons of pCO_2 estimated showed large differences in a vast majority of lake ALK groups (Table 2.3). These results indicate that certain combinations of parameters produced more uncertain pCO_2 estimates relative to other equilibria. Using pCO_2-pH-ALK equilibrium to calculate pCO_2 in LB_{ALK} and LC_{ALK} groups, for example, always resulted in elevated pCO_2 values and errors, particularly in bog lakes (even after organic acids adjustment). Therefore, pH and ALK observations should not be used in this groups. In M_{ALK} and H_{ALK} groups, pCO_2 values and errors derived from pH-based equilibria were similar within random error uncertainty contrary to extremely high uncertainty of pCO_2 calculated from ALK and DIC. While rather availability of given parameter pairs, not errors pCO_2 estimates, determines the choice of carbonate equilibrium, the knowledge on uncertainties associated with pCO_2 calculations helps evaluate the results. Lack of agreement of pCO_2 estimates within each ALK groups may also indicate significant systematic biases affecting pCO_2 calculations.

4.2. Comparison of uncertainties in direct and indirect pCO_2 measurements

Random errors in directly measured pCO_2 were at least several times lower than uncertainty in any pCO_2 estimated from carbonate equilibria (Fig. 2.2, Table 2.4). After considering potential 2-3-fold increase of probe's random errors due to difficult to control factors in field measurements, the comparable uncertainties between direct and indirect pCO_2 measurements would occur only in pCO_2 derived from pH-based equilibria in LC_{ALK} and M_{ALK} groups. Therefore, our findings indicate poor precision of virtually all pCO_2 derived from any carbonate equilibrium and across all ALK groups.

Small proportion of explained root mean square errors (RMSEs) between direct and indirect pCO_2 estimates that random errors are minor source of uncertainty in pCO_2 estimation.

When considering the highest achievable precision of unadjusted pCO_2 estimates only, the proportion of unexplained variation for pCO_2 ranged from 69% to 97% (Table 2.4, Fig. 2.2). Since RMSE measures the accuracy of model predictions, our findings demonstrate poor accuracy of pCO_2 estimates from any carbonate equilibrium and across all ALK groups.

Deviation from a theoretical 1:1 line between calculated and observed pCO_2 showed the directionality of biases in pCO_2 calculations (Fig. 2.2). All pCO_2 values showed positive biases (i.e., overestimated) except for pCO_2 estimated from pCO_2-ALK-DIC equilibrium in LC_{ALK} and M_{ALK} groups which showed negative biases (Fig. 2.2, Table 2.4). The underestimated pCO_2 occurred for observations with ALK>DIC (Fig. S2.1). These findings imply a widespread presence of systematic errors, either in input parameters or in pCO_2 calculations, which cause overestimation of pCO_2 concentrations from all three carbonate equilibria in surface waters.

The pCO_2 calculations from pH and ALK are currently most commonly used carbonate equilibrium in freshwater systems. We showed larger discrepancies between direct and indirect pCO_2 observations were when pCO_2 was calculated from pCO_2-pH-ALK equilibrium (Fig. 2.2, Table 2.4). The average pCO_2 overestimation ranged from 164% in the LC_{ALK} group to 625% (470% adjusted) in the LB_{ALK} group. Similarly highly overestimated pCO_2 values were previously reported for pCO_2-pH-ALK equilibrium, particularly in poorly buffered waters and with high DOC contribution [*Butman and Raymond*, 2011; Wallin et al, 2014, *Abril et al.*, 2015]. However, we also show highly overestimated pCO_2 in the H_{ALK} group, 570% and 460% before and after adjustment (Table 2.4).

The pCO_2-pH-DIC equilibrium produced overestimated pCO_2 values across all ALK groups, however, the overestimation increased along alkalinity and pH gradients, from on average 1% in the LB_{ALK} group to 560% (470% in pCO_2 adjusted) in the H_{ALK} group (Table 2.4). Published

discrepancies between direct and indirect pCO_2 for this equilibrium differed by study. The pCO_2 estimates were either unbiased [*Cole et al.*, 1994] or underestimated in bog lakes (i.e., LB_{ALK} group in this study) [*Riera et al.*, 1999], or agreed within 8% with direct pCO_2 observations in a lake with chemistry closest to M_{ALK} group [*Baehr and DeGrandpre*, 2004]. Our findings suggest larger than previously reported biases in pCO_2 calculation from pCO_2-pH-DIC equilibrium.

Adjusting for organic acids in the LBALK groups and for ionic strength in the HALK group emphasizes high uncertainty of pCO_2 estimated derived from any combination of carbonate parameters in these ALK groups (Fig. 2.2, Table 2.2-2.3). Relative to pCO_2 estimated from two CO_2-related parameters, adjusted pCO_2 values were generally lower and showed improved reliability of pCO_2 calculations expressed as decreased RMSEs by 22% in the pCO_2-pH-ALK equilibrium, 26-30% in the pCO_2-pH-ALK equilibrium, and 8% in the pCO_2-ALK-DIC equilibrium. To make pCO_2 adjustments, however, additional measurements were required in pCO_2 calculations: dissolved organic carbon (or major ions) to estimate non-carbonate alkalinity in humic lakes, and major ions (or specific conductance or total dissolved solids) to approximate ionic strength and activity coefficients in highly buffered lakes. Such measurements can be unavailable but their omission in pCO_2 calculations introduces an additional source of error

Despite improved reliability of pCO_2 calculations after adjusting for organic acids and ionic strength, the adjusted pCO_2 values remained biased relative to direct pCO_2 measurements. The positive bias in the LB_{ALK} group accounted for on average 470% in pCO_2 calculated from pH and ALK and 2% in pCO_2 calculated from ALK and DIC (Table 2.4). The overestimated pCO_2 vales were in the H_{ALK} group: 470% (from pCO_2-pH-DIC equilibrium), 460% (pCO_2-pH-ALK), and 270% in pCO_2-ALK-DIC. These findings highlight difficulty of estimating pCO_2 in humic

lakes from pCO_2-pH-ALK equilibrium and in hardwater lakes from all three carbonate equilibrium and likely introduce additional uncertainty in regional carbon balances.

A number of factors could cause field measurements of CO_2-related parameters to fail to reproduce directly measured pCO_2. First, consider biases in the measurements. As we discussed in the 3.1 section, the carbonate parameters' concentrations significantly changed between sampling and analytical determination (Fig. S2.2, Table 2.2). Consequently, although all measurements were taken under identical conditions, the pCO_2 estimated from carbonate equilibria reflected the changed concentrations relative to direct pCO_2 measurements. Furthermore, the systematic biases in carbonate parameter measurements are present in freshwaters systems [*Herczeg and Hesslein*, 1984; *Metcalf et al.*, 1989; *French et al.*, 2002, *Lozovik*, 2005] and likely cause biased pCO_2 estimates [*Herczeg and Hesslein*, 1984; *Butman and Raymond*, 2011; *Abril et al.*, 2015]. The accuracy of pCO_2 probe used in this study comprised 1.5% of the reading potentially contributing 20-30 μatm to overall uncertainties. Likewise, potential probe's precision decreases in the field measurements could add additional uncertainty. All of these factors likely impacted large discrepancies between direct and indirect pCO_2 measurements, however, their contribution remained unquantified for our lakes due lack information on systematic errors.

The observed mismatch between direct and indirect pCO_2 observations can also be attributed to systematic errors in pCO_2 calculations from carbonate equilibria. Adjusting for organic acids contribution in the LB_{ALK} group and for ionic strength in the H_{ALK} group significantly improved the estimated pCO_2 (Fig. 2.2, Table 2.3-2.4) suggesting significant uncertainty attributed to *a priori* assumptions about carbonate equilibria equations approximating the CO_2 system (Fig. 2.1-2.2). The equations also ignored the contribution of non-CO_2 acid-bases

(i.e., borate, phosphate, arsenate, ammonia, silicate) to ALK and the inference of calcium forming ions with DIC mass balance and likely produced biased pCO_2 estimates in freshwaters [*Gelbrecht et al.*, 1998]. The pCO_2 biases can also be attributed to errors in calculation of the two dissociation constants of carbonic acid and bicarbonate (i.e., pK_{a1} and pK_{a2}), as it was shown in oceanic studies [*Millero, Pierrot, Lee, et al.*, 2002; *Lueker, Dickson, and Keeling*, 2000; *Millero*, 2007], or using outdated and likely untested in many heterogeneous freshwater systems dissociation constants.

At present, we cannot elucidate which systematic errors contributed to observed mismatch between direct and indirect pCO_2 measurements. While further investigation on a larger pool of observations is necessary to validate the accuracy of pCO_2 calculations, we conclude the effect of random parameter errors on pCO_2 was rather small compared to dominant systematic errors. Given all sources of uncertainty in pCO_2 calculations, it is clear that having just two field measurements of CO_2-related parameters (plus temperature) was insufficient to produce thermodynamically consistent estimates of pCO_2 in our lakes, regardless of the combination of input parameters used. Direct pCO_2 measurements are therefore recommended.

4.4 Implications for estimating pCO_2 from carbonate equilibria in freshwaters

To illustrate importance of considering pCO_2 errors in results interpretation, we propagated random and systematic parameter errors and uncertainties due to different time series beginnings and endings onto the time series at Crystal Lake (LC_{ALK} group) (Fig. 2.3). Uncertainty around median pCO_2 ranged from ±24 to ±40 μatm, and in some cases, made in impossible to determine whether lake was classified as undersaturated or supersaturated with respect to atmospheric pCO_2. The trend line indicated an insignificant pCO_2 decrease -2 ±26 μatm per year owing high overall uncertainties around the trend line. Given a growing number of studies using carbonate equilibria to estimate pCO_2 and C flux from inland waters [*Butman and Raymond*, 2011; *McDonald et al.*,

2013; *Raymond et al.*, 2013], and temporal trends of inorganic carbon species [*Jones*, 2003; *Raymond and Cole*, 2003], it is necessary to perform error analysis to determine the bounds of uncertainty around pCO_2 estimates and determine which method is sensitive enough to detect long-term change.

The systematic pCO_2 errors additionally affected the median pCO_2 estimates and the accuracy of pCO_2 predictions. While we determined the presence of non-negligible systematic errors (δ) additionally affecting the median pCO_2 estimates, further targeted effort is essential to identify the sources and behavior of systematic errors. Such information is necessary to correct for systematic biases in pCO_2 calculations from historical observations of pH, DIC, and ALK, and to improve the accuracy of measurements and pCO_2 predictions in the future. Since pCO_2 estimates and random pCO_2 errors were proportionally related (Fig. 2.2, Table 2.3), the random pCO_2 errors also reflected systematic errors propagating through biased pCO_2 medians. Therefore, the improved accuracy of pCO_2 calculations from carbonate equilibria will likely increase the precision of pCO_2 estimates.

Despite using consistent methodology of sample collection, handling, analytical determination, and quality control, the results from NTL-LTER site indicate large uncertainties arising from pCO_2 estimation from carbonate equilibria. More research is needed to determine how our result extrapolate to other datasets and freshwater systems, although our findings are generally supported by previous studies. To fully account for systematic biases and quantify their effect on the uncertainty of pCO_2 estimates at global scales, it will require information on instrumentation, analytical procedures used among researchers, and reporting uncertainties attributed to pCO_2 estimation. Such information is currently unavailable for freshwater systems. Given bounds of uncertainty in global C emissions from lakes and reservoirs (0.32 Pg C yr^{-1}) range

from 0.06 to 0.84 Pg C yr^{-1}, and from rivers and streams (1.8 Pg C yr^{-1}) vary from 1.5 to 2.1 Pg C yr^{-1} [*Raymond et al.,* 2013], freshwater researchers must make significant efforts to standardize and reduce errors in pCO_2 predictions.

Unlike atmospheric and oceanographers, the freshwater community has not determined the acceptable levels of precision and accuracy of carbonate parameter measurements to achieve pCO_2 estimates with uncertainty level permitting to detect long-term pCO_2 changes. Overall uncertainty of atmospheric CO_2 measurement account for <0.2 ppm [*Andrews et al.,* 2014]. Current laboratory measurements of seawater, for example, have precision and accuracy ±1 μmol kg^{-1} and ±2 μmol kg^{-1} for DIC, ±1 μmol kg^{-1} and ±3 μmol kg^{-1} for ALK, and ±0.0004 and ±0.002 for pH measurements to produce fugacity CO_2 (fCO_2 values are a few μatm lower than pCO_2 after accounting for non-ideal nature of gas phase) estimates with uncertainty ±6 μatm or higher [*Millero,* 2007]. Similar levels of uncertainty must be determined for direct pCO_2 measurements. While above analytical uncertainties are incomparable with errors estimates of in our lakes (Table 2.2-2.3), they serve as a gold standard that sets the bar for improving freshwater measurements of CO_2-related parameters.

Adapting solutions already developed for seawater could potentially advance methodological improvements of the CO_2 system measurements in freshwater systems. The certified reference materials (CRM) of CO_2 measurements in oceans contributed most towards development of fully calibrated dataset with uniformly calculated estimates [*Key et al.,* 2004; *Sabine et al.,* 2004]. The CRM samples were prepared in one certified laboratory and distributed among laboratories to serve as an independent measurement quality test. Furthermore, a unified quality assurance and quality control procedure was applied to compare the results from different research groups and identify laboratories having problems with accuracy and precision. Finally,

an unambiguous guide on best practices on CO_2 measurements [*Dickson and Goyet*, 1994; *Dickson, A.G., Sabine, C.L., Christian*, 2007] provided up-to-date information on the chemistry of the CO_2 system in seawater, well-tested analytical methods of analyzing parameters, and standard operating procedures. If using carbonate equilibria from two CO_2-related parameters continued to be the most common method of estimating pCO_2 in freshwaters, developing similar solutions is urgently needed.

Since none of the selected input parameter pairs produced thermodynamically consistent pCO_2 estimates across all ALK groups, an important question on the suitability of carbonate equilibria to estimate pCO_2 in freshwaters arises. While pCO_2 in humic systems were previously excluded from regional and global carbon balances due to unreliable pCO_2 estimates [*Cole et al.*, 1994; *Raymond et al.*, 2013; Wallin et al, 2014], our findings demonstrate more widespread problems. Given current uncertainties in pCO_2 estimation, the carbonate parameters should not be used to estimate pCO_2 from carbonate equilibria, although these parameters are still essential to characterize chemical composition of freshwater systems. However, accounting for systematic uncertainties in pCO_2 estimates might be still insufficient to derive sound pCO_2 estimates. Despite having highly precise and accurate measurements of carbonate parameters of seawater, the pCO_2 derived from any choice of input parameters generally gives pCO_2 estimates more uncertain relative to directly measured pCO_2, [*Dickson and Riley*, 1978; *Dickson, A.G., Sabine, C.L., Christian*, 2007; *Millero*, 2007]. Therefore, oceanographers recommend using direct pCO_2 measurements in CO_2-related studies, especially if two carbon system parameters cannot be precisely constrained [*Dickson and Riley*, 1978; *Dickson, A.G., Sabine, C.L., Christian*, 2007; *Millero*, 2007]. We agree that direct pCO_2 measurements are key to constraining CO_2 flux from diverse aquatic components of terrestrial carbon balances.

2.5 CONCLUSIONS

Due to increasingly frequent use of carbonate equilibria to estimate pCO_2 and C emissions from freshwater systems, we evaluated uncertainties attributed to pCO_2 estimation from carbonate equilibria using two CO_2-related parameters. We quantified random parameter errors in pH, dissolved inorganic carbon, and total alkalinity measurements in four lake groups encompassing a broad gradient of water chemical composition (humic, poorly buffered clearwater, moderate alkalinity, and hardwater) to determine how these errors propagate onto uncertainties in pCO_2 estimated from three carbonate equilibria: pCO_2-pH-DIC, pCO_2-pH-ALK, and pCO_2-ALK-DIC. The results presented here indicate that relatively low random parameter errors can produce random pCO_2 error up to one third of estimated median pCO_2, depending on the choice of input parameter pairs and lake alkalinity group. The comparison of direct and indirect pCO_2 observations reveals that all parameter combinations produces biased pCO_2 estimates. Large proportion of unexplained uncertainty imply dominance of systematic errors in pCO_2 estimation from carbonate equilibria.

Given all sources of uncertainty in pCO_2 calculations, we demonstrate that none of the choice of input parameter pairs provides reliable and reproducible pCO_2 estimates. Therefore, we recommend direct pCO_2 measurements in studies aiming estimation of pCO_2 and C flux from inland waters. Questions remain regarding how our results extrapolate to other data sets and freshwater systems, what is the contribution of random and systematic errors to regional and global pCO_2 estimates, what are the acceptable levels of precision and accuracy of pCO_2 estimates to achieve robust pCO_2 estimates that are comparable at global scales and sensitive enough to detect temporal changes, and whether using carbonate equilibria to estimate pCO_2 is a suitable method for freshwaters. However, regardless which method is going to be used to estimate pCO_2 and C

flux from inland waters, freshwater community urgently needs to standardize and reduce errors in aquatic pCO_2 estimation.

ACKNOWLEDGEMENTS

We are grateful to the North Temperate Lakes Long-term Ecological Research (LTER) staff that has collected and analyzed data over the past 26 years. We also thank J. Thom, K. Xu, L. Loken for their assistance in the field measurements and calculations. We are also grateful for the critical and useful comments of two anonymous reviewers. This research was supported by funding from the National Science Foundation LTER Program for North Temperature Lakes LTER (NSF DEB-1440297, NTL LTER) and NSF DEB-0845166, and University of Wisconsin Anna Grant Birge Memorial Award For Graduate Research awarded to M. Golub. This manuscript contains Supporting Information file together with data used in this study, which are available online.

2.6 TABLES

Table 2.1 Chemical characteristics within lake alkalinity groups (low to high); the values represent the median and 5th and 95th percentiles

Variable	LB_{ALK}[1]	LC_{ALK}[2]	M_{ALK}[3]	H_{ALK}[4]
pH	5.03 (4.58-5.52) (n = 2136)	6.32 (5.62 – 7.06) (n = 1543)	7.44 (6.65 – 8.38) (n = 6016)	8.31 (7.44 – 9.08) (n = 3631)
ALK (μM)	15 (-16 - 102) (n = 754)	29 (11 – 77) (n = 498)	797 (388 – 997) (n = 2025)	3524 (2608–4196) (n = 1021)
DIC (μM)	263 (45-644) (n = 2060)	62 (30-292) (n = 1508)	855 (429 – 1227) (n = 5826)	3612 (2475 - 4499) (n = 3149)
DOC (mgL^{-1})	16.36 (8.09 – 28.37) (n = 2055)	1.90 (1.36 – 2.54) (n = 1492)	3.38 (2.48 – 4.73) (n = 5782)	6.12 (4.65 – 8.56) (n = 3129)
TP (μgL^{-1})	8 (3 - 32) (n = 2107)	23 (9-106) (n = 1446)	11 (4 - 90) (n = 5840)	61 (13 - 463) (n = 4477)
TN (μgL^{-1})	193 (105 - 463) (n = 2112)	721 (360 – 1889) (n = 1537)	311 (166 - 885) (n = 5948)	920 (610 – 2540) (n = 1537)

[1] – Lakes grouped in LB_{ALK} group are: Crystal Bog, Trout Bog
[2] –LC_{ALK} group includes Crystal Lake
[3] – Lakes grouped in M_{ALK} group are: Allequash Lake, Big Muskellunge Lake, Sparkling Lake, Trout Lake
[4] – Lakes grouped in H_{ALK} group are: Fish Lake, Lake Mendota, Lake Monona, Lake Wingra

Table 2.2 Statistical properties of random errors in carbon system parameters within four alkalinity groups calculated from paired observations. The reported values were rounded according to significant figure convention[1].

Lake group	Parameter	Normal distribution parameters		Skewness	Kurtosis	t location-scale distribution parameters		
		[μ]	[σ_n]			[μ]	[σ_t]	[ν]
LB_{ALK} (n=55)	pH[2]	0.002	0.018	0.021	3.2	0.002	0.016	10.3
	ALK (μM)	0.1	2.4	2.0	12.9	0.2	1.1	2.1
	DIC (μM)	1.4	12.3	1.8	7.7	-0.9	5.5	1.8
LC_{ALK} (n=48)	pH[2]	0.002	0.017	-0.114	3.7	0.002	0.013	4.3
	ALK (μM)	0.3	0.3	0.282	4.4	0.2	1.1	3.3
	DIC (μM)	0.9	3.4	1.62	7.7	0.5	1.3	1.6
M_{ALK} (n=331)	pH	0.003	0.015	-0.143	4.8	0.003	0.009	2.6
	ALK (μM)	0.6	11.7	1.4	12.8	-0.3	3.6	1.4
	DIC (μM)	-0.3	13.8	-0.4	9.1	-0.4	3.9	1.2
H_{ALK} (n=150)	pH	0.003	0.019	0.022	3.0	0.003	0.019	56.2
	ALK (μM)	6.8	56.4	0.517	13.0	4.6	13.7	1.2
	DIC (μM)	6.1	83.0	-0.44	13.0	4.3	34.7	1.9

[1] the significant figures convention reports all certain digits plus the first uncertain digit.

[2] the variable is normally distributed at significance level 0.05 according to Shapiro-Wilk test

Table 2.3 The random parameter error effect on pCO_2 calculations using three carbonate equilibria in four alkalinity groups shows that pCO_2 sensitivity to parameter errors depends on the choice of input parameter pairs and lake group. Values reported represent best estimates of the median pCO_2 at 1 atmosphere with error propagated over 10000 simulations. The random errors of median pCO_2 are expressed as standard error (SE) of the median (standard deviation of 10000 medians) and relative standard error of the median (RSE).

Equilibrium	Input Parameter	LB_{ALK}			LC_{ALK}			M_{ALK}			H_{ALK}		
		pCO_2 [µatm]	SE [µatm]	RSE [%]	pCO_2 [µatm]	SE [µatm]	RSE [%]	pCO_2 [µatm]	SE [µatm]	RSE [%]	pCO_2 [µatm]	SE [µatm]	RSE [%]
pCO_2-pH-DIC	Both	**3554**	**±166**	**±4.7**	**653**	**±36**	**±5.5**	**1212**	**±45**	**±3.7**	**795**	**±38**	**±4.8**
	Both adj.	n/a	n/a	n/a	n/a	n/a	n/a	n/a	n/a	n/a	**661**[3]	**±32**	**±4.8**
	pH		±46	±1.3		±9	±1.4		±34	±2.8		±34	±4.3
	pH adj.		n/a	n/a		n/a	n/a		n/a	n/a		±28	±5.1
	DIC		±165	±4.6		±35	±5.4		±28	±2.3		±17	±2.1
	DIC adj.		n/a	n/a		n/a	n/a		n/a	n/a		±14	±2.1
pCO_2-pH-ALK	Both	**15225**	**±1026**	**±6.7**	**900**	**±69**	**±7.7**	**1281**	**±50**	**±3.9**	**866**	**±41**	**±4.7**
	Both adj.	**10999**[2]	**±935**	**±8.5**	n/a	n/a	n/a	n/a	n/a	n/a	**719**[3]	**±35**	**±4.9**
	pH		±716	±4.7		±36	±4.0		±43	±3.4		±38	±4.4
	pH adj.		±694	±6.3		n/a	n/a		n/a	n/a		±31	±4.3
	ALK		±629	±4.1		±58	±6.4		±25	±2.0		±14	±1.6
	ALK adj.		±638	±5.8		n/a	n/a		n/a	n/a		±12	±1.7
pCO_2-ALK-DIC	Both	**2546**	**±198**	**±7.8**	**580**[1]	**±59**	**±10.2**	**1437**[1]	**±230**	**±16.0**	**3725**[1]	**±1156**	**±31.0**
	Both adj.	**2867**[2]	**±391**	**±13.6**	n/a	n/a	n/a	n/a	n/a	n/a	**3129**[1,3]	**±985**	**±31.5**
	ALK		±68	±2.7		±25	±4.3		±166	±11.6		±870	±23.4
	ALK adj.		±375	±13.1		n/a	n/a		n/a	n/a		±866	±27.7
	DIC		±198	±7.8		±55	±9.5		±207	±14.4		±1031	±27.7
	DIC adj.		±285	±9.9		n/a	n/a		n/a	n/a		±1027	±32.8

[1] presented pCO_2 estimates are only for observations when DIC concentrations were larger than ALK concentrations (*see Material and Method, and Supporting Information for more details*)

[2] calculations after correcting for organic acids contribution to total alkalinity

[3] calculations after adjusting thermodynamic constants for ionic strength

Table 2.4 Comparison of the mean pCO_2 and mean absolute deviation (MAD) of the random errors in direct pCO_2 measurements and indirect pCO_2 derived from three carbonate equilibria across four alkalinity groups. Abbreviation n/a indicates not applicable.

Measured/ Calculated pCO_2	**LB_{ALK}** (n = 4)		**LC_{ALK}** (n = 2)		**M_{ALK}** (n = 8)		**H_{ALK}** (n = 3)		**Global** (n = 17)	
	Median pCO_2 [μatm]	MAD [μatm]	Median pCO_2 [μatm]	MAD [μatm]	Median pCO_2 [μatm]	MAD [μatm]	Median pCO_2 [μatm]	MAD [μatm]	Median pCO_2 [μatm]	MAD [μatm]
Direct	1873	±7	341	±3	706	±4	410	±5	717	±9
pCO_2-pH-DIC	1893	±53	383	±10	1152	±7	2299	±52	1242	±75
pCO_2-pH-DIC adj.	n/a	n/a	n/a	n/a	n/a	n/a	1928[2]	±45	1242[2]	±73[2]
pCO_2-pH-ALK	11712	±633	630	±20	1501	±15	2354	±48	1756	±386
pCO_2-pH-ALK adj.	8799[1]	±654[1]	n/a	n/a	n/a	n/a	1891[2]	±36	1756[2]	±600[2]
pCO_2–ALK-DIC	2052	±33	157	±14	18	±81	1091	±883	204	±344
pCO_2–ALK-DIC adj.	1921[1]	±43[1]	n/a	n/a	n/a	n/a	1102[2]	±12005	204[2]	±3117[2]

[1] calculations after correcting for organic acids contribution to total alkalinity

[2] calculations after adjusting thermodynamic constants for ionic strength

2.7 FIGURES

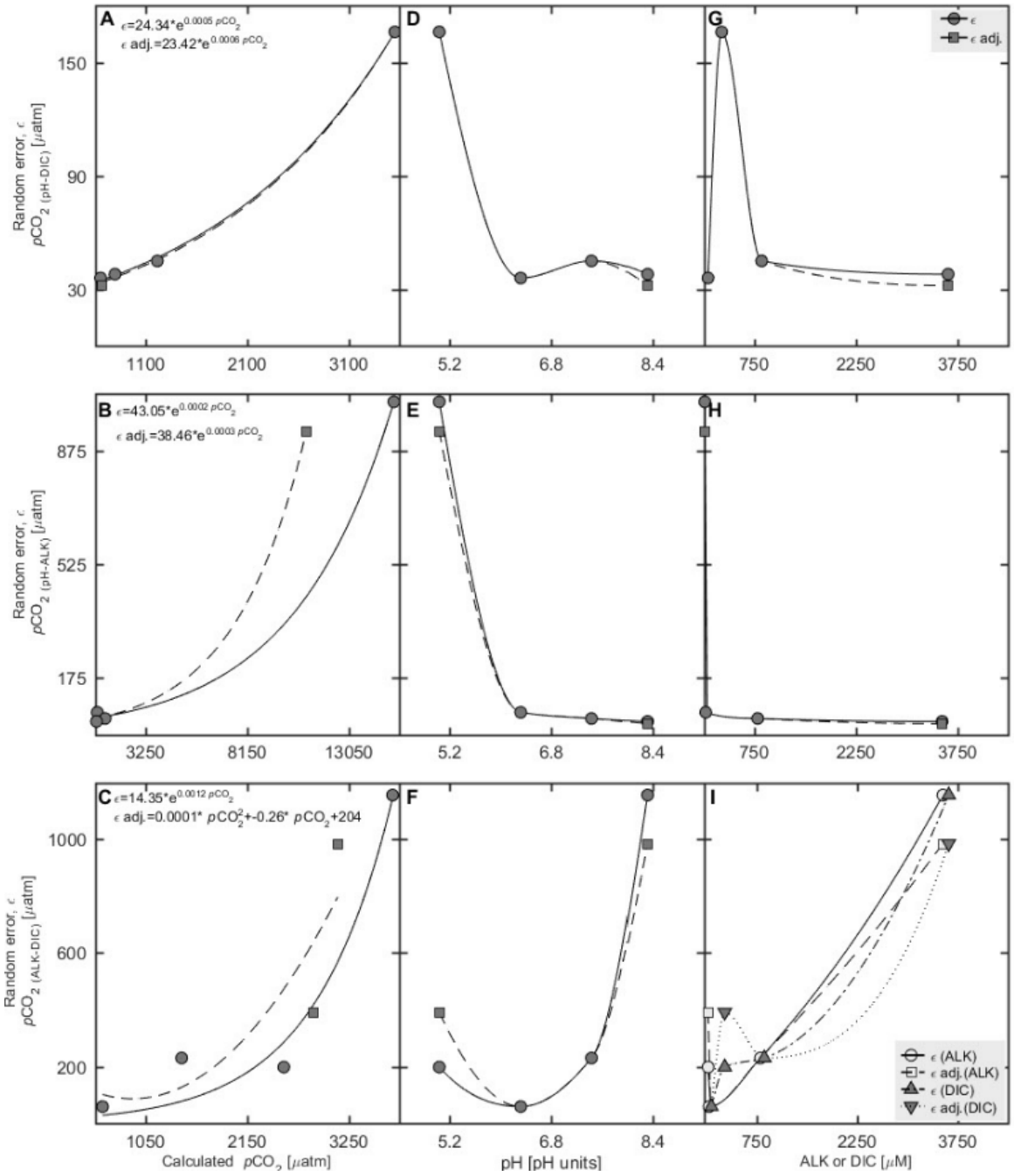

Figure 1.1 Random pCO_2 errors across median pCO_2 estimates (A-C), pH gradient (D-F), and ALK/DIC gradients (G-I) shows that pCO_2 errors were exponentially proportional to median pCO_2 estimates across three carbonate equilibria. Random pCO_2 errors were inversely proportional to pH gradient in pCO_2-pH-DIC and pCO_2-pH-ALK equilibria, and proportional to ALK/DIC in the pCO_2-ALK-DIC equilibrium. Note different scales of y-axes between panels. In cases where regression failed to produce a significant fit, the likes shown are piecewise interpolation.

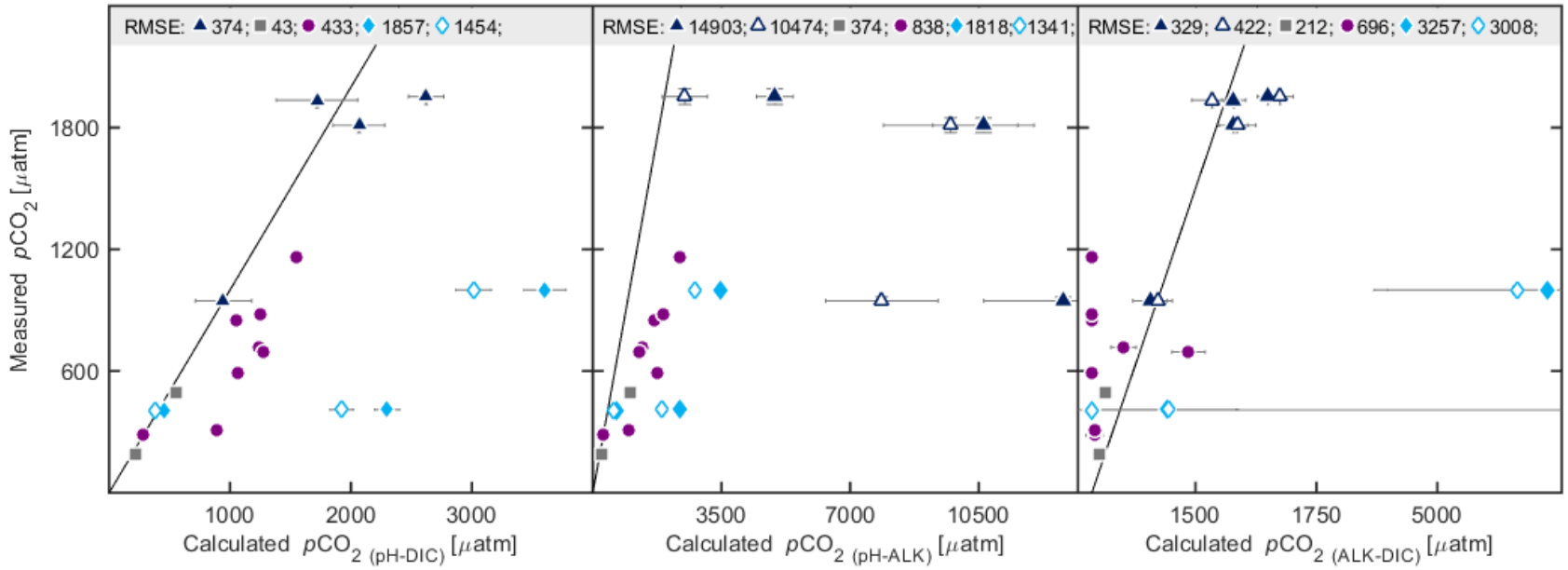

Figure 2.2 The comparison of directly measured pCO_2 and pCO_2 estimated from three equilibria: pCO_2-pH-DIC (left), pCO_2-pH-ALK (middle), and pCO_2-DIC-ALK (right), shows high uncertainty and directionality of biases attributed to pCO_2 estimation. Horizontal error bars represent standard error of the median, while vertical error bars represent 2% of the median. The global root mean square error (RMSE) accounted for 1094 (994 after adjustments), 7700 (5563), and 1741 (1659) μatm, respectively. The diagonal line represents a theoretical 1:1 relationship. The observations coding: L_{BALK} group – navy triangles; L_{BALK} group adjusted – open triangles; LC_{ALK} group – grey squares; M_{ALK} group - purple circles; H_{ALK} group – blue diamonds; H_{ALK} group adjusted – open diamonds.

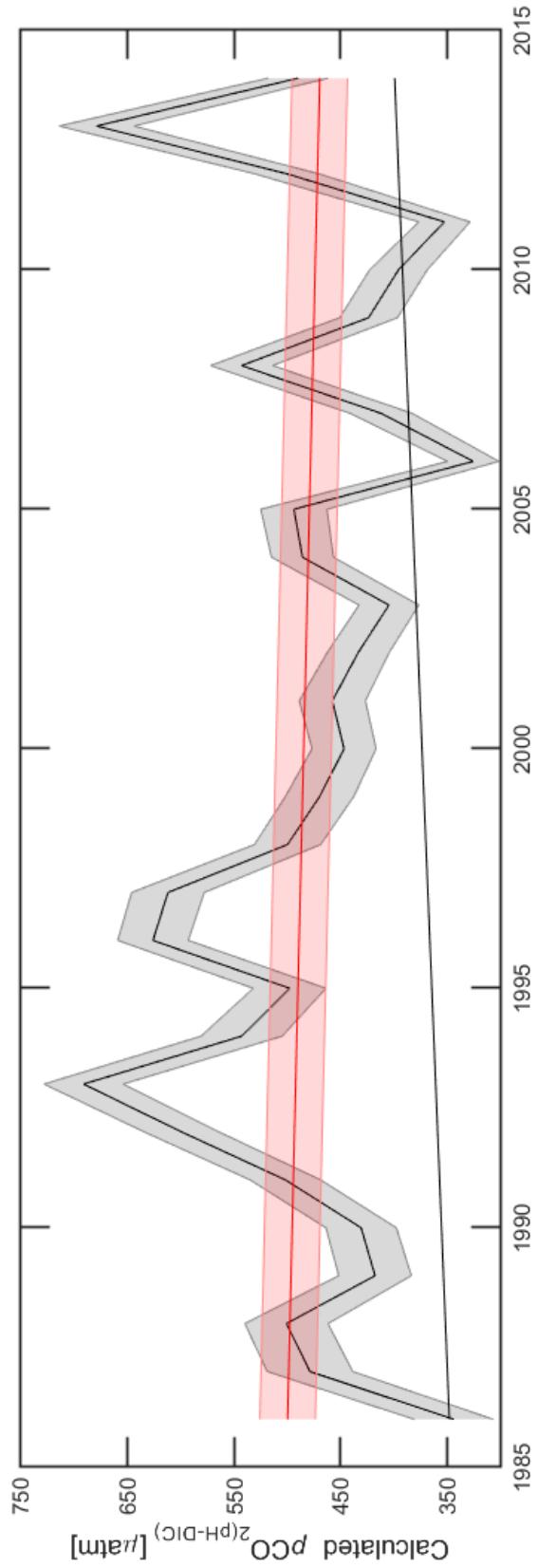

Figure 2.3 The time-series of pCO_2 estimates with propagated uncertainties attributed to random and systematic errors and different beginnings and endings of time series demonstrates the scatter around best pCO_2 estimates (median of 10000 median values) and fitted trend line (median of 10000 fitted linear regression). Confidence intervals represent standard error of the median for near-monthly observation (light gray) and trend (light red). Black solid line represents mean annual atmospheric CO_2 at 1 atmosphere. Slope line indicates statistically insignificant decline of 2±26 μatm per year.

2.8 APPENDIX I

SUPPORTING INFORMATION for:

Large uncertainty in estimating pCO_2 from carbonate equilibria in lakes

Malgorzata Golub, Ankur R. Desai, Galen A. McKinley, Christina K. Remucal, Emily H. Stanley

Text S2.1. *Problems with estimating pCO_2 using pCO_2-ALK-DIC equilibrium*

The pCO_2-ALK-DIC equilibrium was sensitive to DIC/ALK concentration imbalances. When DIC concentrations were smaller than ALK concentrations (DIC<ALK), pCO_2-ALK-DIC overestimated the median pH by 1.81 pH units (9.22 in DIC<ALK group and 7.41 in DIC>ALK), resulting in largely underestimated median pCO_2 (47 µatm in DIC<ALK group and 1,577 µatm in DIC>ALK, Fig. S1). We found DIC<ALK observations mainly in epilimnetic waters and in 1/3 of observations in eutrophic lakes (high ALK group), indicating that DIC/ALK imbalance was due to photosynthetically-driven DIC drawdown and non-carbonate alkalinity contribution to total alkalinity.

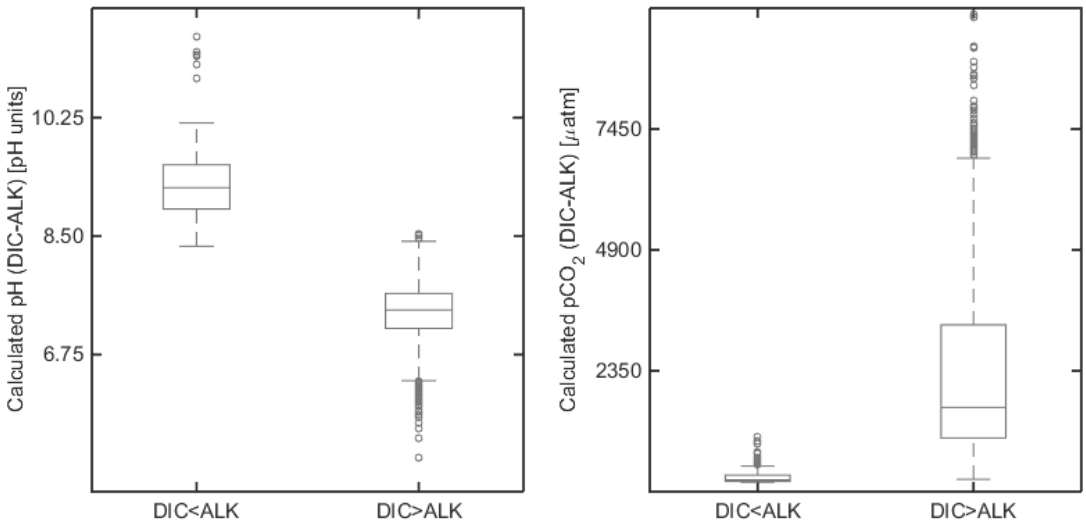

Figure S2.1. The calculations of pH (left panel) and pCO_2 using pCO_2-ALK-DIC equilibrium (right panel) in two groups of observations: DIC<ALK and DIC>ALK demonstrate that DIC/ALK concentration imbalances below one resulted in erroneously high pH predictions and low pCO_2 concentrations compared to predictions in DIC/ALK>1. Extreme outliers: pH>12 in DIC<ALK group (n=6) and pCO_2 > 10000 µatm in DIC>ALK (n = 12) were omitted.

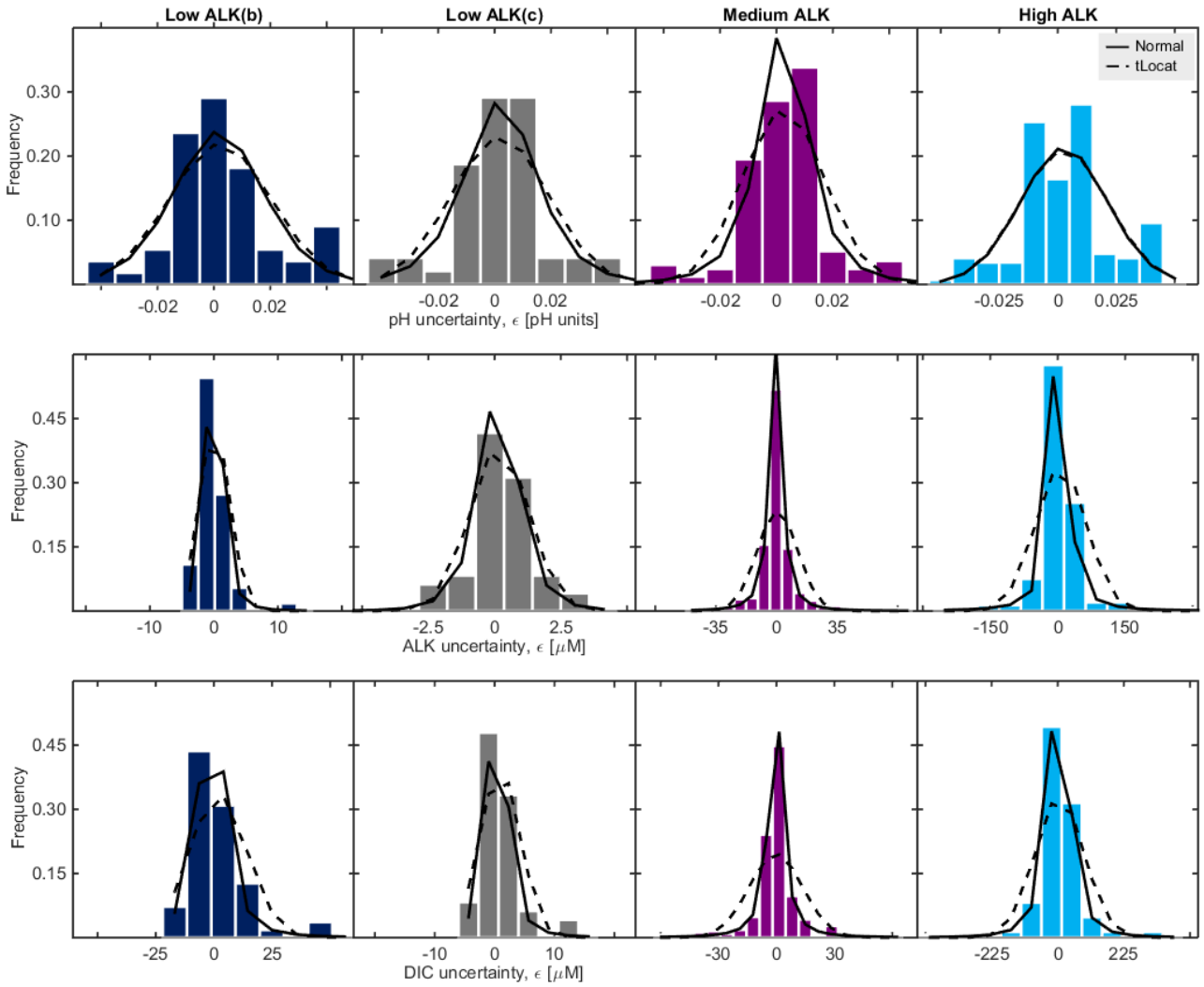

Figure S2.2. Probability distribution functions (PDF) of a normal distribution and a t location-scale distribution fitted to random uncertainties inferred from paired observation in three carbonate parameters in four alkalinity lake groups. Statistical properties of each PDF in table 2.2.

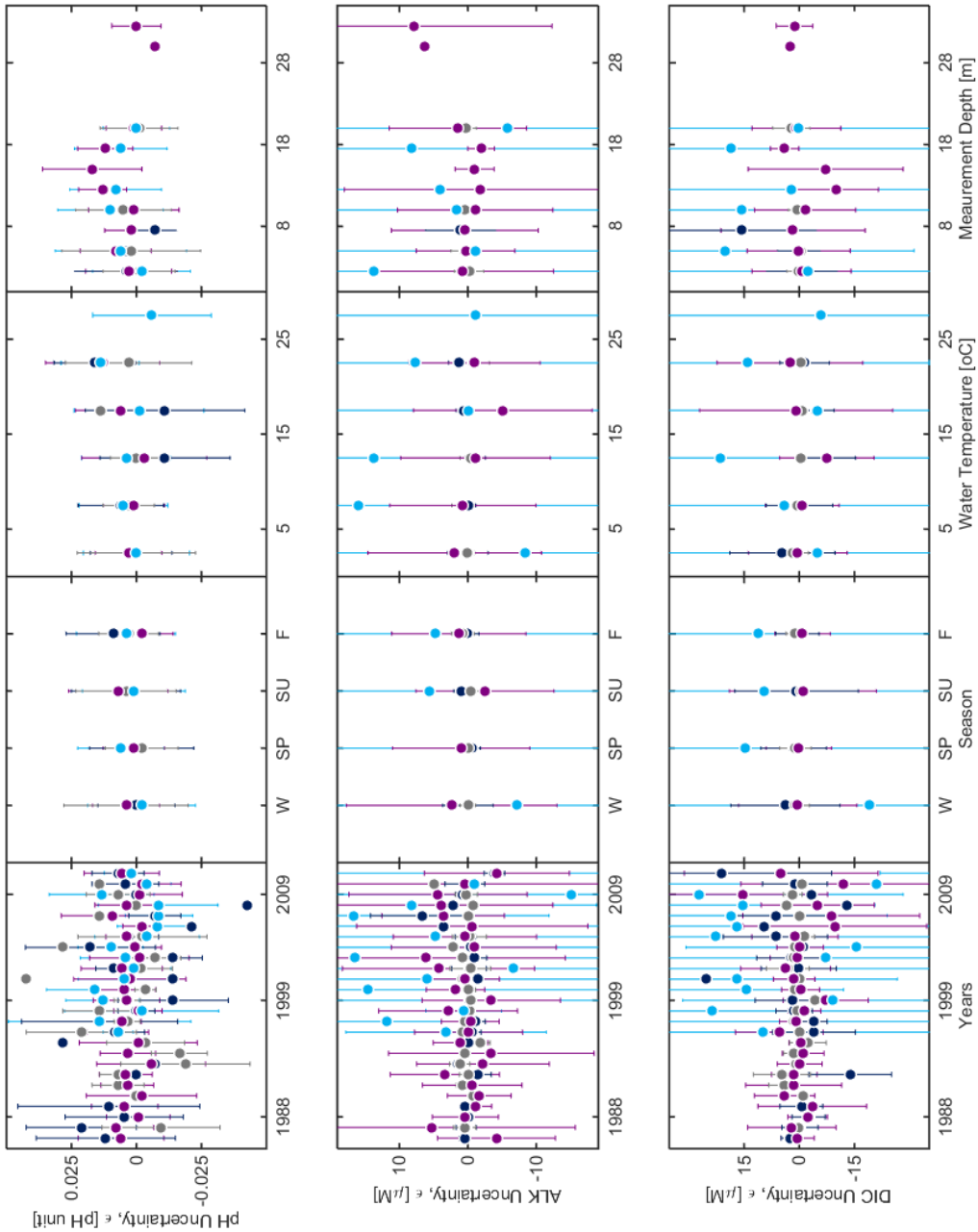

Figure S2.3. Random error in three carbonate parameters in four alkalinity lake groups grouped by year, season, water temperature, and depth show independence of error from these variables. Error bars represent standard deviation of random errors within a given group. Abbreviations: W-winter, SP-spring, SU-summer, F-fall. Colors represent ALK groups: navy –LB_{ALK}, grey – LC_{ALK}, purple – M_{ALK}, blue – H_{ALK}

CHAPTER 3

Limited role of ice duration and thermal stratification on interannual variability CO_2 efflux from seasonally ice-covered lakes

AUTHORS

Malgorzata Golub, Ankur R. Desai[1]

ABSTRACT

Climate warming has induced widespread ice cover loss and warming temperature in seasonally ice-coved lakes. While ice duration dynamics has cascading effects on lake physical and biogeochemical processes, little is known on ice-CO_2 emission feedbacks, primarily due to lack of long observational time series. Here, we evaluate ice feedbacks on interannual variability of pCO_2 with a nearly three-decade-long time series for seven lakes from the North Temperate Lake Long Term Ecological Research program. There was no relationship between interannual, under-ice pCO_2 accumulation and springtime pCO_2 with ice cover duration. While one day of ice cover loss corresponded to on average 4°C increase in summer water temperature, temperature increases did not enhance summer pCO_2. We did not observe hypolimnetic pCO_2 build-up and higher fall emissions due to longer thermal stratification and higher temperature on annual basis. An artificial warming experiment in Crystal Lake revealed that temperature-mediated pCO_2 increases were small and within carbonate equilibria parameter uncertainties, and were likely lost to other geochemical effects on pCO_2. Our results demonstrate that under-ice pCO_2 is more dynamic than

previously assumed, predicting springtime emissions from ice is unreliable, and detecting climate warming impact on pCO_2 calculated from carbonate equilibria is difficult.

3.1 INTRODUCTION

Outgassing of carbon dioxide (CO_2) from inland waters offsets approximately 60% of net uptake of carbon into the terrestrial biosphere [*Ciais et al.*, 2013]. However, these up-scaled estimates of carbon emissions from lakes and reservoirs do not generally include ice cover dynamics [*Aufdenkampe et al.*, 2011; *Raymond et al.*, 2013], which comprise a significant proportion of a year in temperate, boreal and Arctic lakes [*Karlsson et al.*, 2013; *Ducharme-Riel et al.*, 2015]. Therefore, it is uncertain how the source carbon strength from inland waters will respond to warming climate, hindering prediction of carbon fate in lakes carbon balances [*Phillips et al.*, 2015; *Hasler et al.*, 2016] and contribution to regional and global carbon balances. Here we investigate interannual variability of pCO_2 in relation to ice cover dynamics in seven north temperate lakes in Northern Wisconsin.

A warming atmosphere would first manifest on lakes by changing the lake physical environment: shortening lake cover duration [*Magnuson*, 2000; *Weyhenmeyer et al.*, 2011], increasing variability of ice phenology [*Benson et al.*, 2012], warming water temperature [*Winslow et al.*, 2014; *O'Reilly et al.*, 2015] and changing lake thermal structure [*Austin and Colman*, 2007]. Lake annual CO_2 balances in seasonally ice-covered lakes are tightly linked to these ice dynamics [*Striegl et al.*, 2001; *Karlsson et al.*, 2013] and temperature-mediated effects [*Finlay et al.*, 2015]. Thus, there is good reason to expect that a changing physical environment, such as ice cover, influence lake chemistry and productivity.

Lake-ice prevents the exchanges of CO_2 at air-water interface and determines the amount of CO_2 accumulated under ice and further outgassing magnitudes after ice break-up [*Riera et al.*, 1999; *Striegl et al.*, 2001; *Demarty et al.*, 2010]. These springtime emissions account for a significant proportion of CO_2 balances in seasonally ice-covered lakes [*Riera et al.*, 1999; *Karlsson et al.*, 2013]. Although ice cover duration is a poor predictor of under-ice CO_2 in boreal and subarctic lakes at regional scale, lake-ice might play more important role in CO_2 dynamics at local and temporal timescales [*Denfeld et al.*, 2015]. In the case of dimictic lakes, the timing and length of thermal stratification closely follows lake-ice phenology [*Austin and Colman*, 2007], and CO_2 accumulated in deep waters over summer is then outgassed during fall turnover [*López Bellido et al.*, 2009; *Karlsson et al.*, 2013; *Ducharme-Riel et al.*, 2015]. However, the linkages between ice dynamic and the timing and strength of springtime and fall CO_2 emissions remain unexplored because the majority of studies cover one season only. Therefore, to establish the role of ice cover dynamics in CO_2 evasion variability, we need multi-year and multi-lake observation.

A warming climate would imply shorter length of ice cover for lakes. Shorter ice cover leads to longer exposure to heat during growing season, and hence, contributes to warmer water temperature in the following season, and earlier onset and strength of thermal stratification [*Austin and Colman*, 2007; *Posch et al.*, 2012]. Ice cover contributes to widespread warming trends of surface temperature across in ice-covered lakes [*Schneider and Hook*, 2010; *O'Reilly et al.*, 2015]. Lake thermal stratification also suppresses turbulence in water column, modulating CO_2 exchanges at air-water interface [*MacIntyre et al.*, 2010], and decouples hypolimnetic waters from gas exchanges with atmosphere for prolonged time. Temperature, in turn, mediates processes regulating CO_2 balances such as CO_2 gas solubility in water [*Weiss*, 1974], metabolic rates, especially ecosystem respiration [*Yvon-Durocher et al.*, 2012; *Marotta et al.*, 2014], and

hypolimnetic accumulations rates [*Ducharme-Riel et al.*, 2015]. Therefore, the effect of ice variability on lake CO_2 variability might span beyond springtime and fall emissions but persist across years.

In this view of climate-warming induced loss of ice cover and risk of permanent lake ice loss in many regions [*Weyhenmeyer et al.*, 2011], it is critical to improve our understanding of ice-CO_2 emission feedbacks. Here we analyzed a long-term multi-lake dataset of lake ice cover and CO_2 and asked: How does interannual variability in lake-ice phenology affect phenology of CO_2 emissions from lakes? To answer this question, we collected and harmonized over three-decade-long records for seven lakes studied under North Temperate Lake Long Term Ecological Research program. Our working hypotheses are that shorter ice cover (1) reduces under-ice CO_2 accumulation and springtime efflux, (2) increases CO_2 emissions during an open water season through longer exposure to heat, and (3) increases fall pulses of CO_2 due to prolonged thermal stratification and warmer water temperature in hypolimnion. By testing these hypotheses, we can improve our predictive understanding on responses of CO_2 emission from aquatic systems to declining ice cover.

3.2 MATERIAL AND METHODS

Study area and data collection

Seven lakes are located in the Northern Highland Lake District (NHLD) in northern Wisconsin, USA. NHDL has a mosaic of mixed, hardwood, and coniferous forests (~53 % of total area), wetlands (28%), lakes (13%), and other land coverages [*Buffam et al.*, 2010]. Soils in the NHLD are dominated by sandy gravel and gravelly sand with dominance of silicate over carbonate [*Attig*, 1985].

The limnological data are collected under North Temperate Lake Long Term Ecological Research (NTL-LTER) program since 1981. The core lakes include two seepage humic lakes: Crystal Bog (CB) and Trout Bog (TB); one seepage clearwater lake (Crystal Lake); two lakes with intermediate landscape position: Big Maskellunge Lake (BM) and Sparkling Lake (SP); and two lakes with low landscape position: Allequash Lake (AL) and Trout Lake (TR). Lake area ranges from to 0.6 ha in CB to 1565.1 ha in TR. The mean depth ranges from 1.7 m in CB to 14.6 m in TR. Ice cover duration is ~ 145 days across all lakes and varies by lake and calendar year. Lake morphometric characteristics are in Table 3.1.

Ice cover observations are made every other day around ice freezing and melting period. A lake is regarded as ice-covered when the sampling boat cannot reach the deepest point in the lake. Days of year with first ice and with first open water were set as freeze and break-up dates. Ice cover duration was calculated as a number of days between freeze and break-up dates.

Water temperature is measured bi-weekly during open water season and every 6 weeks during ice-covered season. The measurements are made in the deepest part of each lake at 1-m depth intervals. Water temperature was averaged for epilimnion and hypolimnion.

Nutrient chemistry is measured at the same station at several depths: the top and bottom of the epilimnion, mid-thermocline, and top, middle, and bottom of the hypolimnion. Parameters characterizing chemistry of lakes used in this study include: pH, dissolved inorganic carbon (DIC), total dissolved nitrogen (TN), total phosphorus (TP), dissolved organic carbon (DOC). The chemical composition parameters were averaged for epilimnion and hypolimnion. Statistical properties of lake chemical composition are summarized in Table 3.1.

Mixing and stratification indices

The indices of mixing and stratification for each lake was modelled from water temperature, wind speed, and lake bathymetry, using Lake Analyzer for MATLAB [*Read et al.*, 2011] and available through Global Lake Ecological Observatory Network GitHub website (http://github.com/GLEON). Onset of stratification is set to one week with temperature gradient larger than 1°C. End of stratification is set to day of year when entire water column is fully mixed and water column is isothermal.

Variability of CO_2

Concentration of CO_2 and other inorganic carbon species from lakes was modeled from observations of pH, DIC, and water temperature using dissociation constants for freshwaters [*Millero*, 1979]. The carbonate equilibrium model based on pH and DIC enables the comparison of CO_2 concentration across NHDL without producing erroneous values for humic lakes, and also showed highest precision of CO_2 estimates (3.6-5.5% of the median) compared to other carbonate equilibria models [*Golub et al, in review*). The influence of ionic strength was neglected and all calculations were performed in pH NBS scale. Calculations were performed with the MATLAB-version of the CO_2 System Calculations [i.e., CO2SYS, *van Heuven et al.*, 2011].

Time series with carbon data spanned period of 1986-2014. Under ice measurements, for example, were made around 18, 56, and 90 days of year. Although we estimated CO_2 concentrations for each sampling period, we were particularly interested in interannual variation of CO_2 concentrations at four characteristic periods of CO_2 emissions in ice-covered lakes: under-ice, spring emissions after ice break-up, summer emissions, and fall emissions after autumn turnover.

We examined the relationship between ice duration and pCO_2 to test hypothesis that shorter ice cover leads to lower under-ice pCO_2. We compared pCO_2 values all under-ice observations and calculated ice duration at time of measurement (number of days since ice-on). Therefore, CO_2 concentrations from at least two last measurements before ice-out was considered as representative for estimating under-ice CO_2 accumulation rate and as a proxy of springtime emissions. Because sampling periods just before and after ice melt and freeze are dangerous for sampling, these periods were particularly under-sampled and we relied on linear extrapolations until ice-off and ice-on dates. Second comparison comprised within-year observations for which we fitted 29 annual curves, and linearly extrapolated to ice-melt days. We assumed no air-water CO_2 exchanges through ice, linear CO_2 build-up over winter, and no under-ice convective mixing and biotic uptake.

To test hypothesis that shorter ice cover leads to greater hypolimnetic CO_2 accumulation via prolonged lake thermal stratification and warmer temperature, we analyzed CO_2 concentration in summer months (June, July, and August). The measurements below thermocline were averaged to hypolimnetic CO_2 concentrations. No CO_2 exchange between epilimnion and hypolimnion was assumed. For the same months (JJA) we estimated summer emission and correlated with ice duration to verify hypothesis that longer open water season contributes to higher pCO_2.

3.3 RESULTS

Lake-ice variability effect on lake mixing and temperature regimes

Lake-ice showed similar dynamics across all seven lakes (Table 3.1). Shallower lakes had longer ice cover, around 150 days, while deeper lakes had about 12 days shorter (~137 days). Interannual variability of ice duration was coherent across all lakes, ranging from 14 to 17 days. The effect of interannual variability of ice on mixing regimes varied by stratification index and lake (Table 3.2).

Ice cover duration showed a significant positive relationship with onset of stable stratification in four, mostly deep lakes (Table 3.2). In two lakes, TB and CR, longer ice cover also corresponded to prolonged stable stratification. The length of open water season was negatively correlated with ice duration across all lakes. Additionally, shorter ice duration corresponded to higher summer water temperature both in epilimnion and in hypolimnion (Table 3.2, Fig. 3.1). The loss of ice cover by one day translated into slopes around 0.4°C in summer water temperature, coherently across of all lakes. The intercepts of ice duration-water temperature relationship corresponded with depth of mixed layer, with fastest warming rates found in bog and in shallow lakes, however the relationship was insignificant.

Lake-ice variability effect on under-ice accumulation and prediction of springtime pCO_2

When considering under-ice pCO_2 accumulation from pooled under ice observations, pCO_2 gradually accumulated with longer ice cover duration (Fig. 3.2). Except for Trout Bog Lake, all lakes showed significant, positive relationships of under ice pCO_2 and ice duration (R^2adj. at $p<0.05$ for AL, BM, CB, CR, SP, TR lakes accounted for 0.15, 0.30, 0.12, 0.27, 0.32, 0.34, respectively). The rates of under-ice pCO_2 accumulation were 4 μatm d^{-1} in CR, 6 μatm d^{-1} in TR, 9 μatm d^{-1} in AL, BM, SP, and 18 μatm d^{-1} in CB.

However, under-ice pCO_2 also showed high interannual and between-sampling-dates variability across all lakes (Fig. 3.2). In SP, for example, the pCO_2 standard deviation accounted for 436, 405, and 552 μatm at first, second, and third sampling dates (around 15, 50, and 90 day of year), respectively. Moreover, nearly a half of interannual observations showed pCO_2 decline or nonlinear relationship with ice duration. Most nonlinear pCO_2 responses to ice duration showed under-ice pCO_2 build-up between first and second sampling points, but pCO_2 decline between second and thirds sampling points. Also, the rates of pCO_2 change were several times slower at

the end of ice cover. Similar nonlinearities and declines of pCO_2 with ice duration were observed across all lakes.

Springtime pCO_2 calculated from both cumulative and annual under-ice data showed different ranges of interannual variability at ice-off (Fig. 3.2-3.3). In SP, for example, the pCO_2 standard deviation was 186 μatm for cumulative and 990 μatm for annual data. Annual pCO_2 data predicted 4-6 times more variable springtime pCO_2 than cumulative data in non-bog lakes. The root mean square errors (RMSE) between these two methods of springtime pCO_2 estimation ranged from 468 μatm in CR to 2853 μatm in CB. Differences in the springtime pCO_2 means estimated from two methods were within 15%, however, pCO_2 predicted from cumulative under-ice pCO_2 tended to be overestimated. There was no relationship between springtime pCO2 calculated from annual under-ice data and ice duration across all lakes (Fig. 3.2-3.3). The observed (within two weeks since ice-melt) were significantly lower than estimated pCO_2, except for TB (Table 3.3).

Lake-ice variability indirect effects on lake CO_2 concentrations

The temperature-mediated effects on pCO_2 were season showed no or negative relationships with water temperature (Fig. 3.1) except for a weak relationship between pCO_2 and water temperature in CR. Stratification length played an important role in summer hypolimnetic pCO_2 build-up in three deep lakes, BM, TR, and SP, explaining 59%, 40% and 20% of pCO_2 variability respectively (Fig. 3.5, Table 3.3). The pCO_2 accumulation rates accounted for 34, 22, and 19 μatm d^{-1}, respectively. Like under-ice pCO_2 accumulation (Fig 3.2), however, 60% annual data showed linear increases, linear decreases, non-linear increases and declines along length of stable stratification (Fig. 3.4). Nearly two third of with-in year summer seasonal pCO_2 data showed non-nonlinear responses to stratification length. When extrapolated till end stratification season,

the fall were unrelated to length of thermal stratification. Fall pCO_2 values in non-bog lakes were similar to springtime pCO_2 magnitudes (Table 3.3).

3.4 DISCUSSION

Lake-ice variability effect on lake mixing and temperature regimes

Here we used interannual variability to test coupling ice cover dynamics to water temperature and pCO_2 in seasonally ice-covered lakes, allowing us to test hypothesis related to warming climate effects on ice and ecosystem responses at shorter time frame and independently of long term trends [*Austin and Colman*, 2007]. Shorter ice cover duration corresponded to earlier onset of stratification in three deep lakes and one meromictic lake, and to warmer summer water temperature in epilimnion and hypolimnion (Table 3.2, Fig. 3.1). These results agree with observed warming trends in lakes [*Hanson et al.*, 2006; *Austin and Colman*, 2007; *O'Reilly et al.*, 2015] and to variation in stratification metrics [*Austin and Colman*, 2007]. An ice-albedo feedback was proposed to explain these relationships where dark water absorb more heat relative ice-coved waters [*Austin and Colman*, 2007]. Ice cover duration was found as one of the best exploratory variable responsible for warming trends in seasonally ice-covered lakes [*O'Reilly et al.*, 2015].

Interestingly, all lakes had similar slopes of relationship between summer water temperature and ice duration, which corresponded with lake depth (Fig. 3.1, Table 3.1). Given all lakes were affected by the same climatic conditions and heat capacity is the same across lakes was the same, shallower and brown lakes warmed up faster than deeper lakes Recent studies indicate an interplay of morphometric characteristics in response to warming climate [*Winslow et al.*, 2014; *O'Reilly et al.*, 2015]. However, our results partly agree with, warming trends in non-bog lakes in this study [*O'Reilly et al.*, 2015], who although found the highest warming rates were in the

shallowest Lake Allequash (0.85°C decade^{-1}), the second shallowest lake, Lake Big Muskellunge had the slowest warming rates across non-bog lakes (0.56°C decade^{-1}).

Lake-ice variability effect on under-ice CO_2 and prediction of springtime pCO_2

Our first hypothesis that shorter ice cover leads to lower CO_2 accumulation, however, was partly falsified as we did detect significant relationships with cumulative under-ice CO_2 but insignificant relationship for within-year data (Fig. 3.2). In contrast to our finding, lack of ice duration with under-ice relationship was found in Swedish and Finnish lakes [*Denfeld et al.*, 2015]. However, as we showed on SP lake example (Fig. 3.2), observation of the within-year variability of under-ice pCO_2 suggests influences of other factors on under-ice CO_2 accumulation. Other studies shown that pCO_2 concentration correlated with nutrients and dissolved organic concentration, suggesting hydrological influences as the dominant influence over ice blocking CO_2 exchange with atmosphere [*Denfeld et al.*, 2015]. Moreover, under-ice CO_2 can be sequestered when solar radiation penetrates though ice and under-ice turnover brings nutrient-rich water to the epilimnion [*Baehr and DeGrandpre*, 2004]. As a result of potential confounding factors, there is no convincing evidence that length of ice increases pCO_2 build-up, and that in turn, ice durations as a proxy of under-ice pCO_2 accumulation and springtime emissions. These results imply that approximating spring emissions based on under-ice pCO_2 as has been done in some studies [*Denfeld et al.*, 2015; *Ducharme-Riel et al.*, 2015] may introduce biases in CO_2 emissions. In the case of our study lakes, the RMSEs of springtime pCO_2 at the ice melt ranged from 468 μatm to 2853 μatm (Fig. 3.3).

Lake-ice variability indirect effects on lake CO_2 concentrations

Summer temperature had either a flat or negative relationship of pCO_2 for both epilimnetic and hypolimnetic temperature. We attribute this to relative small temperature effect on pCO_2

relative to non-temperature effects (i.e., chemical and biological, Fig. 3.1). Henry's law implies that all else being equal, pCO_2 should increase as solubility constant goes down with increasing temperature. However, temperature-mediated pCO_2 increases were likely overridden by other factors. Similarly confounding relationships were found in large lakes [*Alin and Johnson*, 2007] and possibly in global databased on lake chemistry [*Sobek et al.*, 2005]. Such responses would not be expected here, as the lakes in this study generally had low productivity, except for highly productive epilimnetic waters in bog lakes (Table 3.1). However, given ecosystem respiration generally exceeded gross primary production in these lakes [*Hanson et al.*, 2003], it is likely that CO_2 production was sufficient to offset temperature-dependent increases. Consequently, we falsified hypotheses 2 and 3 that pCO_2 increases were attributed to ice cover variability.

High variability of pCO_2 in summer temperature in bog lakes (Fig. 3.1) might suggest influences of other factors affecting CO_2 interannual variability. We assumed the absence of long-term trends in input parameters and pCO_2 while analyzing interannual variability. However, over the study period, we bserved non-monotonic variability in pCO_2 across years in some lakes, mostly in bog lakes. We detected no trends in wintertime measurements, implying limited atmospheric change as winter is assumed to be a dormant season and chemical composition is least affected by biology. However, prolonged open waters season in years with shorter ice cover could also have resulted in increased influx of nutrients and dissolved organic carbon during precipitation events [*Sobek et al.*, 2005; *Tranvik et al.*, 2009]. For example, Finnish annual CO_2 fluxes showed a positive relationship with precipitation [*Rantakari and Kortelainen*, 2005]. However, CO_2 trends in bog study lakes, were coherent rather with chlorophyll *a* than precipitation at least at shorter temporal scales [*Hanson et al.*, 2006], suggesting the impact of nutrient delivery with precipitation.

Another factor of the lack of pCO_2 relationship with hypolimnetic temperature is attributed to the presence of anoxic conditions and methane production instead of carbon mineralization to CO_2 [*Tranvik et al.*, 2009]. However, this is unlikely in this study, as most lakes in this study are unproductive or polimictic to experience prolonged or any anoxic conditions. Additional analyses using dissolved oxygen in addition to CO_2 would help disentangle that effect.

To illustrate difficulty in estimating temperature-effect on pCO_2 derived from the pCO_2-pH-DIC equilibrium, we used data for Crystal Lake in years 2011-2014, in which thermal stratification was artificially perturbed to eradicate an invasive, cold water rainbow smelt [*Gaeta et al.*, 2012; *Lawson et al.*, 2015]. Thermal de-stratification occurred in 2012-2013 while 2011 and 2014 were used as reference points. Assuming no major external events affecting lake chemistry and temperature during the experiment, the mean summer (June-August) epilimnetic water temperature increased by 3.64°C, a twofold increase relative to interannual variability of seasonal means. The pCO_2 and DIC increased by 266 μatm and 15 μM, while pH declined by 0.13 units. These changes corresponded to nearly fivefold increase compared to interannual variation of pCO_2 and equal to interannual variation in pH and DIC. To quantify pCO_2 sensitivity to parameter changes, the reported single-parameter values were perturbed on long-term summer parameter averages (Fig. 3.5). Despite higher water temperature, pCO_2 increased by 22 μatm and was within random parameter uncertainties (±42 μatm) around long-term pCO_2 mean. The pH and DIC influences on pCO_2 accounted for +64 μatm and +111 μatm, respectively.

These results suggest that detecting the effect on pCO_2 from an average 0.4°C increase per 1 day of ice loss (+8 μatm) was rather unlikely, given high pCO_2 sensitivity to pH and DIC. While many researchers suggest temperature independence of pCO_2 and CO_2 flux [*Sobek et al.*, 2005; *Weyhenmeyer et al.*, 2015], we find instead that while temperature does have a large effect on

pCO_2, it is generally overridden by biotic effects. Thus, the regression analyses typically show no or negative temperature-pCO_2 relationships [*Alin and Johnson*, 2007] Separating temperature and non-temperature effects on pCO_2 [*Takahashi et al.,* 2002; *Atilla et al.*, 2011] would be beneficial for quatifying temperature effects on pCO_2 with climate warming.

3.5 CONCLUSIONS

To answer question of "How does interannual variability in ice phenology affect phenology of CO_2 emissions from lakes?", we tested CO_2 connections to changing ice feedbacks on nearly-three-decade long time series for seven seasonally ice-covered lakes.

Although cumulative under-ice pCO_2 observations were positively correlated with ice duration in six lakes, within-year pCO_2 showed high temporal variability, especially in the second part of winter. Interannual springtime pCO_2, predicted from under-ice pCO_2, was hence uncorrelated with ice duration. We also found that longer exposure to heat with shorter ice duration significantly increased water temperature but did not resulted in temperature-mediated pCO_2 increases in epilimnion and hypolimnion. Earlier onset of thermal stratification corresponded to shorter ice cover, and played an important role in hypolimnetic accumulation of pCO_2 in deep lakes. However, high within-year temporal pCO_2 variability resulted in pCO_2 unrelated to the length of thermal stratification at the end of summer. Moreover, all lakes showed elevated fall pCO_2 regardless of lake morphometry and presence of stratification. Therefore, the contribution of hypolimnetic CO_2-rich waters to CO_2 pulse during autumn turnover was insufficiently explained by the length of thermal stratification. Warming experiment results coupled with model simulations revealed that even extreme temperature warming (corresponding to warming trends spanning several decades) effect on pCO_2 remained undetected because of high pCO_2 uncertainty calculated from pH and DIC.

Linking temporal pCO_2 variability to direct (shorter ice-covered periods) and indirect (warmer waters and/or longer thermal stratification) effects of climate-induced ice cover loss proved to be difficult from existing long-term records. Our results imply more biogeochemically dynamic processes regulating wintertime pCO_2 than previously assumed and inability to predict the magnitudes of spring CO_2 pulses from ice duration itself. Limited role of water temperature and thermal stratification in summer and fall pCO_2 indicates an unresolved interplay of physical and biogeochemical processes modulating temporal pCO_2 variability. Given that pCO_2 calculated from pH-based carbonate equilibria is currently most commonly used to estimate CO_2 flux from freshwaters, our results imply difficulty in detecting pCO_2 variability and change due to climate warming.

ACKNOWLEDGEMENTS

We are grateful to the North Temperate Lakes Long-term Ecological Research (LTER) staff that has collected and analyzed data over the past 26 years. This research was supported by funding from the National Science Foundation LTER Program for North Temperature Lakes LTER (NSF DEB-1440297, NTL LTER).

Table 3.1 Limnological characteristics of seven lakes studied; the values (except morphological characteristics) represent annual volume-integrated mean, standard deviation, and 5th and 95th percentiles

Characteristics	CB[1]	TB[1]	CR[1]	BM[1]	SP[1]	AL[1]	TR[1]
pH	5.18±.23	4.94±.28	6.31±.47	7.22±.50	7.46±.57	7.57±.55	7.58±.48
	(4.80-5.56)	(4.53-5.46)	(5.62-7.06)	(6.53-8.08)	(6.69-8.33)	(6.89-8.61)	(6.87-8.40)
DIC (μM)	202±194	339±222	97±107	546±168	786±210	1020±223	958±110
	(39-553)	(48-704)	(29-291)	(396-900)	(604-1202)	(797-1471)	(825-1169)
TP (μgL^{-1})	22±20	44±55	13±19	33±47	23±48	33±48	13±28
	(8-52)	(12-142)	(3-32)	(4-134)	(3-85)	(7-102)	(3-31)
TN (μgL^{-1})	714±397	968±698	230±183	479±288	398±404	429±284	270±149
	(340-1418)	(409-2232)	(105-463)	(264-1026)	(165-1153)	(193-841)	(140-526)
DOC (mgL^{-1})	9.93±2.11	21.03±5.30	1.92±.42	3.84±0.57	3.34±.96	4.08±1.07	2.88±1.01
	(7.73-14.05)	(13.49-30.55)	(1.36-2.53)	(3.21-4.46)	(2.63-4.45)	(2.57-5.18)	(2.37-3.38)
Temperature	13.1±7.2	7.5±3.2	10.6±5.0	11.1±5.2	10.8±5.2	12.9±6.7	8.4±3.9
(°C)	(2.0-22.9)	(2.8-12.2)	(1.1-24.1)	(2.6-18.2)	(1.2-24.1)	(2.5-21.8)	(1.7-13.8)
Ice Duration	152±15	154±14	139±15	140±16	137±16	146±17	134±17
(days)	(122-176)	(129-177)	(107-158)	(111-160)	(109-160)	(115-173)	(107-154)
Lake Area (ha)	0.6	1.0	37.5	363.4	63.7	164.2	1565.1
Mean Depth (m)	1.7	5.6	10.4	7.5	10.9	2.9	14.6
Max. Depth (m)	2.5	7.9	20.4	21.3	20	8	35.7

[1] – Lakes names are: Crystal Bog (CB), Trout Bog (TB), Crystal Lake (CR), Big Muskellunge Lake (BM), Sparkling Lake (SP), Allequash Lake (AL), and Trout Lake (TR)

Table 3.2 Interannual variability of lake physical environment attributed to ice duration interannual variability. The abbreviations indicate: slopes of linear regression (β_1), adjusted coefficients of determination (R^2adj.), root-mean-square errors (RMSE). The significance levels at $p<0.05$, otherwise indicates as insignificant (ns). Lake names as in table 3.1.

Lake	Onset of stratification (days)			Length of stable stratification (days)			Length of open water season (days)			Ice freeze date (days)			Summer surface water temperature (°C)			Summer bottom water temperature (°C)		
	β_1	R^2 adj.	RMSE	β_1	R^2 adj.	RMSE	β_1	R^2 adj.	RMSE	β_1	R^2 adj.	RMSE	β_1	R^2 adj.	RMSE	β_1	R^2 adj.	RMSE
CB	ns	ns	ns	ns	ns	ns	-.74	.50	11.5	ns	ns	ns	-.03	.14	1.21	-.06	0.33	1.32
TB	.52	.56	7.0	-.56	.43	9.7	-.78	.50	11.2	-.2	.09	8.0	-.05	.36	1.01	-.02	0.32	0.45
CR	.39	.18	11.8	-.36	.13	12.8	-.84	.57	10.6	ns	ns	ns	-.04	.29	.88	ns	ns	ns
BM	ns	ns	ns	ns	ns	ns	-.77	.51	11.9	ns	ns	ns	-.05	.47	.80	-.04	0.21	1.33
SP	.27	.12	11.3	ns	ns	ns	-.76	.52	11.1	ns	ns	ns	-.05	.51	.81	-.05	0.37	1.04
AL	ns	ns	ns	ns	ns	ns	-.67	.44	12.4	ns	ns	ns	-.04	.33	.89	-.06	0.22	1.88
TR	.31	.14	13	ns	ns	ns	-.70	.48	12.9	ns	ns	ns	-0.5	.67	.65	-.03	0.20	0.98

Table 3.3 Summary statistics for partial pressure of CO_2 (pCO_2) in four periods: under-ice, springtime (defined as period between ice melt and May 31), summertime (defined as June-August), and fall (defined as September 1 till last measurement in November). The values represent the mean and mean absolute deviation of interannual variation.

Lake	**Under-ice pCO_2 (μatm)**	**Springtime pCO_2 (μatm)**			**Summer pCO_2 (μatm)**		**Fall pCO_2 (μatm)**
		Cumulative	Annual	Observed	Epilimnetic	Hypolimnetic	Observed
CB	4074±1459	5084±282	5781±2906	3363±2409	1613±685	5596±1848	1882±1301
TB	4434±1383	4484±13	4582±2335	5554±3050	2750±2267	7308±2083	5877±3324
CR	1182±282	1456±80	1400±507	625±546	317±134	910±688	649±427
BM	2376±534	2987±149	2870± 628	2056±2002	557±520	4231±1594	2436±2553
SP	2001±503	2555±186	2276±990	1835±2093	362±402	3246±2365	2536±2556
AL	3418±671	3969±192	3479±699	1324±1572	416±478	4192±1252	1041±829
TR	1635±351	2039±133	2067±484	1533±1526	333±222	3034±1469	2377±1969

3.7 FIGURES

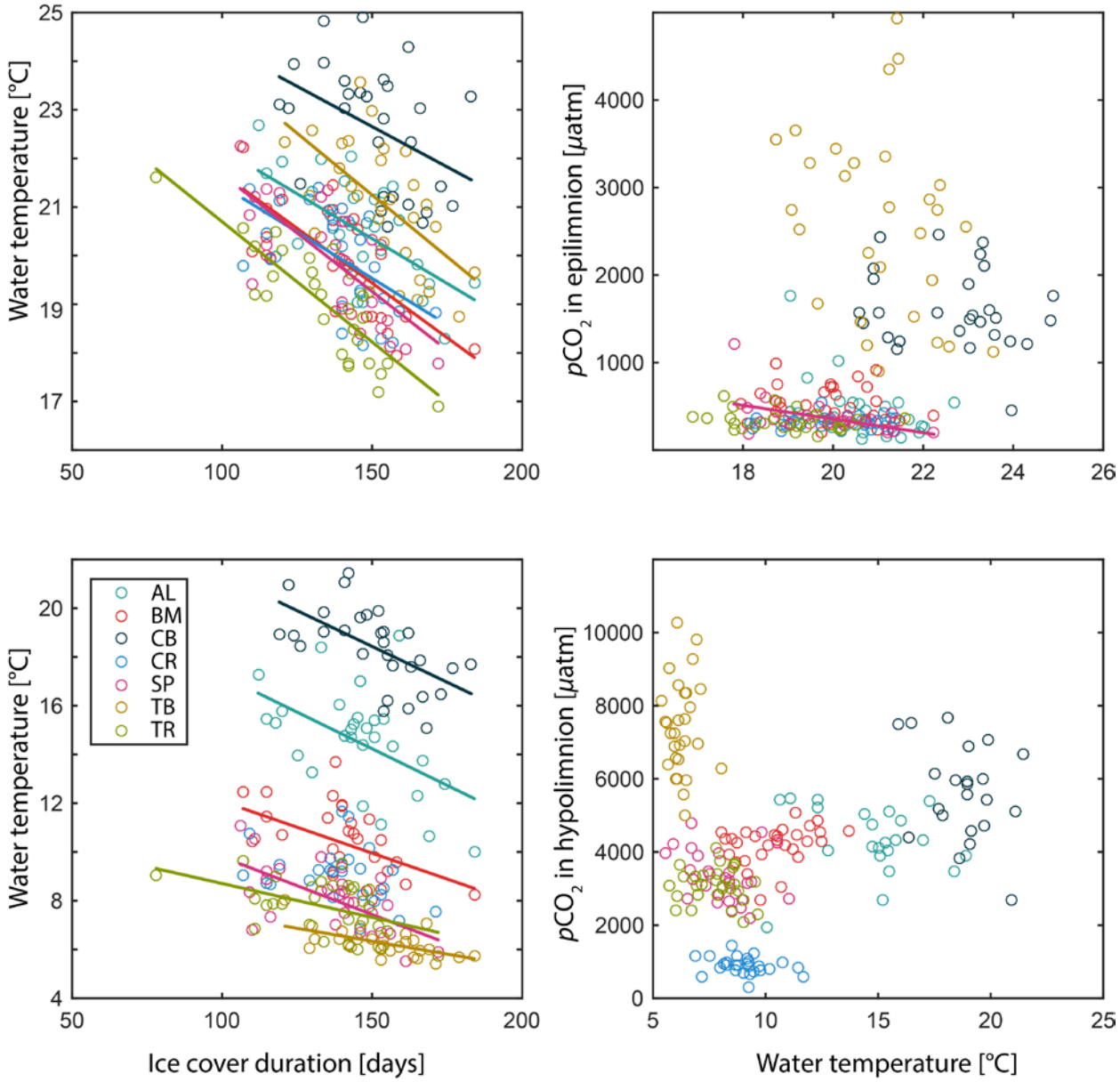

Figure 3.1 Relationship between ice cover duration and mean summer water temperature indicates significantly warmer temperature due to loss of ice cover (both left panels) however temperature increases did not translate to temperature-modulated pCO_2 increases (both right panels). The statistics for fitted regression lines are in table 3.2.

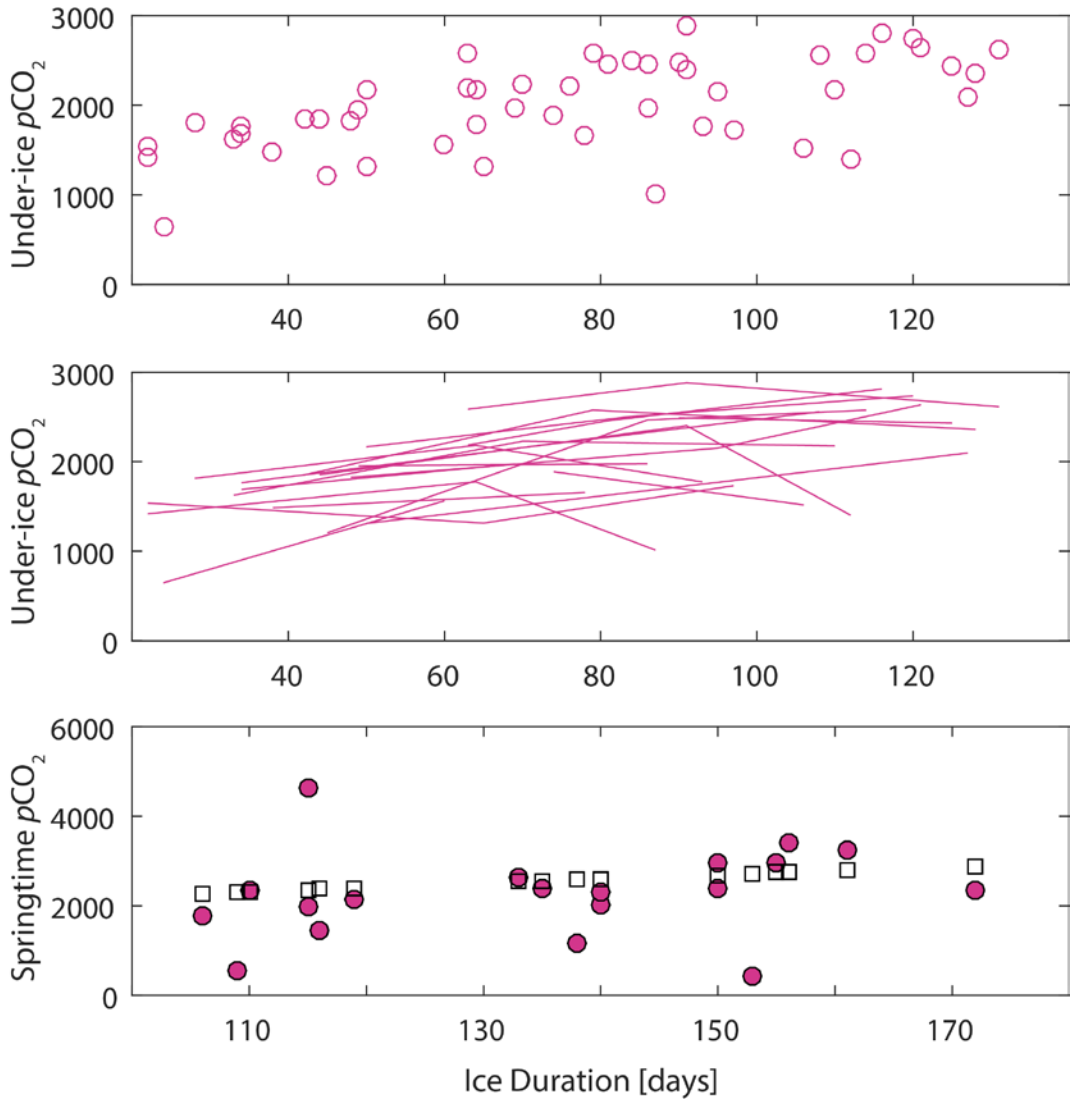

Figure 3.2 Under-ice and springtime pCO_2 in relation to ice cover duration in Sparling Lake. Cumulative under-ice pCO_2 (upper panel), within-year under-ice pCO_2 (middle panel), and springtime pCO_2 predicted from cumulative (open squares) and within year (filled magenta circles) pCO_2 under-ice data (bottom panel).

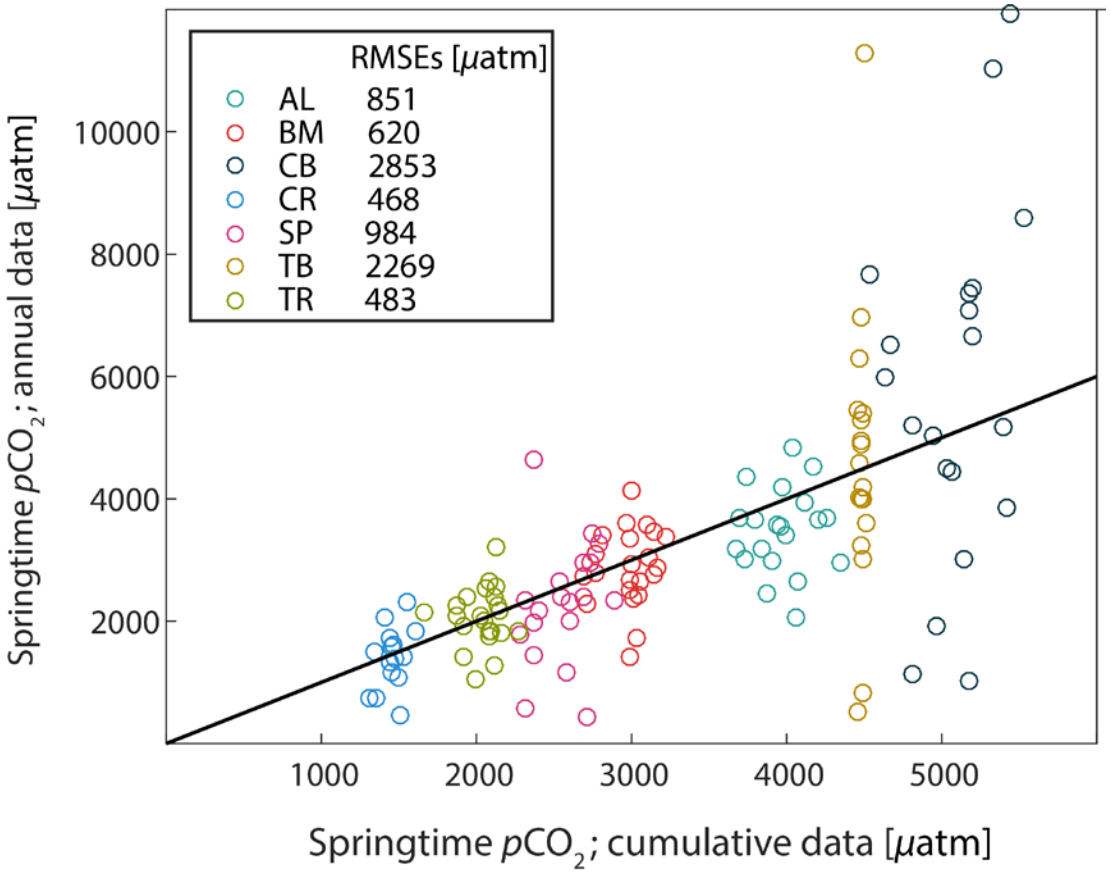

Figure 3.3 Comparison of springtime error prediction from two approaches (cumulative and within-year) to estimating springtime pCO_2 from ice records for seven analyzed lakes. RMSEs indicate the root mean square errors.

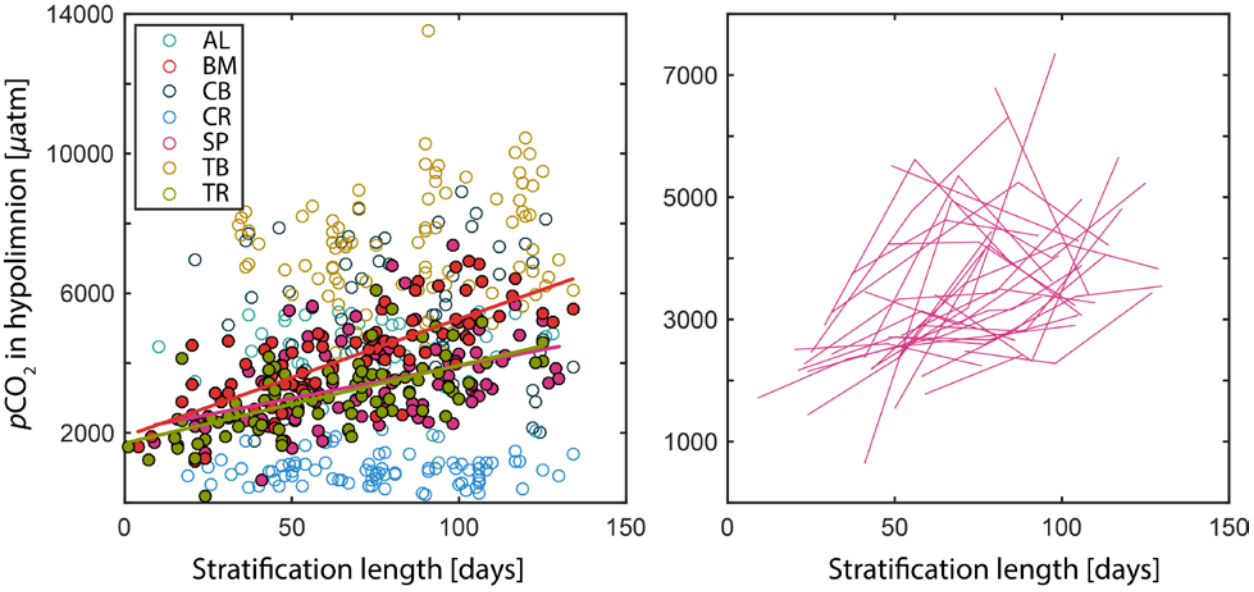

Figure 3.4 Relationship between the length of thermal stratification and pCO_2 accumulation in hypolimnion (left panel), and single-lake relationship with highlighted within-year variability of pCO_2 in Sparkling Lake (right panel). Filled circles indicted statistically significant relationship in three deep lakes (SP, TR, BM).

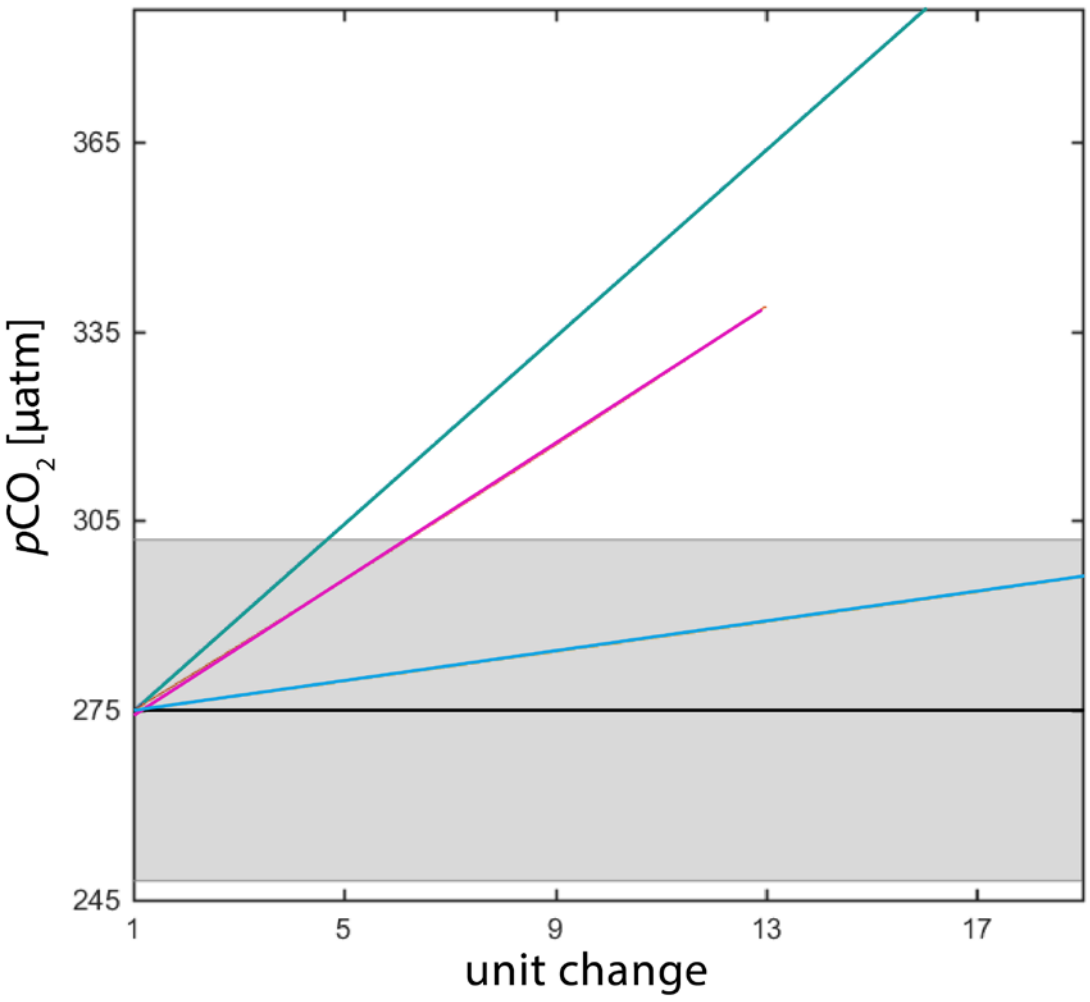

Figure 3.5 The parameter sensitivity of pCO_2 calculated from carbonate equilibrium equations (pH - magenta line, dissolved inorganic carbon - cyan line, and temperature - blue line in comparison with long-term summer pCO_2 - black line) in Crystal Lake during warming experiment. Shaded region indicates confidence interval after 10000 random and systematic error propagation.

CHAPTER 4

Multi-temporal patterns and environmental drivers of CO_2 fluxes in lakes and reservoirs

AUTHORS

Malgorzata Golub, Ankur R. Desai, Timo Vesala, Ivan Mammarella, Gil Bohrer; Chandra Shekhar Deshmukh; Jan Elbers; Werner Eugster; Daniela Franz; Stephan Glatzel; Frederic Guérin; Jouni Heiskanen; George Kling; Elyn Humphreys; Mathilde Jammet; Anders Jonsson; Vuorenmaa Jussi; Jan Karlsson; Xuhui Lee; Heping Liu; Annalea Lohila; Erik Lundin; Anne Ojala, Tim Morin; Anna Rutgersson; Torsten Sachs; Erik Sahlee; Dominique Serça; Changliang Shao; Gus Shaver; Ian Strachan; Gesa Weyhenmeyer; Wei Xiao;

ABSTRACT

Current emission rates from the aquatic components of the global terrestrial carbon balance are highly uncertain owing to the scarcity of direct CO_2 flux measurements. Here, we combine high temporal resolution eddy covariance CO_2 flux data from 19 globally distributed lakes and reservoirs representing six climatic zones and wide gradients of nutrient and color to quantify empirical emission rates and examine which environmental controls drive patterns and dynamics of CO_2 efflux at multiple temporal scales. CO_2 flux ranged from -1.12 gC m^{-2} d^{-1} to 1.69 gC m^{-2} d^{-1}, with mean CO_2 flux was 0.30 gC m^{-2} d^{-1}, and did not show spatial variability with latitude, mean annual temperature and precipitation. Despite differences in lake characteristics in trophic state, color, and thermal stratification, most waterbodies showed coherent responses to environmental controls at daily to seasonal timescales. Temperature, solar radiation, and wind speed were among environmental drivers best predicting CO_2 fluxes. Most striking result was a

consistent 20-30-day oscillatory CO_2 flux pattern across all lakes. Applying a simple upscaling to these direct observations, we estimated annual emission rate from lakes and reservoirs at 0.23±0.19 PgC, 40% less compared to current emission rate for lentic systems. Our results indicate that greater temporal sampling from diverse aquatic sites can significantly alter our understanding and quantification of lake and reservoir CO_2 contribution to global carbon balances.

4.1 INTRODUCTION

Despite covering small proportion of Earth's land [*Lehner and Döll*, 2004; *Downing et al.*, 2006], inland waters have been estimated to emit 1 PgC yr^{-1} to the atmosphere, an amount nearly equal to cumulative anthropogenic carbon release due to net land use change [*Ciais et al.*, 2013]. However, this source strength is typically based on limited temporal sampling and thus poorly constrained [*Ciais et al.*, 2013]. Depending on the study, lakes and reservoirs CO_2 emissions only range from 0.32 to 0.64 PgC yr^{-1} at the global scale [*Cole et al.*, 2007; *Tranvik et al.*, 2009; *Aufdenkampe et al.*, 2011; *Raymond et al.*, 2013]. To improve assessment of the role of lakes and reservoirs in global carbon balances and to evaluate CO_2 emissions feedbacks to global change, we make a first synthesis of continuous, direct CO_2 flux estimates over 19 globally distributed lakes and reservoirs.

Exchange of CO_2 at water-air interface reflect net carbon-related processes in the waterbody, including direct CO_2 uptake [*Balmer and Downing*, 2011], biological and phytochemical mineralization of terrestrially-derived organic carbon [*McCallister and del Giorgio*, 2012], advected soil respiration [*Eugster et al.*, 2003], groundwater inputs [*Stets et al.*, 2009; *McDonald et al.*, 2013], and internal CO_2 production [*Weyhenmeyer et al.*, 2015]. Ecosystem respiration exceeds gross ecosystem productivity for most waterbodies [*del Giorgio et al.*, 1997; *Hanson et al.*, 2004], therefore inland waterbodies are generally supersturated with CO_2

and net sources of CO_2 to atmosphere [*Cole et al.*, 2007; *Tranvik et al.*, 2009; *Raymond et al.*, 2013]. Because of tight aquatic-terrestrial linkages, inland waters directly and indirectly integrate influences from watersheds [*Williamson et al.*, 2008]. It is postulated that influences on aquatic systems will be mediated rather through delivery of solutes from watershed than temperature [*Sobek et al.*, 2005; *Hanson et al.*, 2006]. Hence CO_2 flux measurements can be used to assess the role of inland waters in terrestrial system [*Cole et al.*, 2007; *Battin et al.*, 2009; *Raymond et al.*, 2013]. To better understand the role of inland of waters in regional and global carbon balances, however, we need the reliable estimates of CO_2 flux from those ecosystems.

The major obstacle in reducing uncertainty in global estimates of carbon emissions from lakes and reservoirs is scarcity of continuous and direct CO_2 measurements [*Raymond et al.*, 2013]. Current estimates are based only 1% on direct measurements, while the remainder rely on extrapolation from point measurements and modelling from carbonate equilibria [*Raymond et al.*, 2013], which have been shown to grossly overestimate CO_2 concentrations, particularly in systems with high dissolved organic carbon content [*Abril et al.*, 2015, Golub et al., in review]. Only one study synthesizes published direct CO_2 measurements in global small ponds to date [*Holgerson and Raymond*, 2016]. However, even these direct CO_2 estimates are prone to uncertainties attributed to parameterization of gas transfer velocities [*Wanninkhof et al.*, 2009; *MacIntyre et al.*, 2010].

In contrast, the eddy covariance (EC) technique is the only method providing direct measurements of CO_2 exchanges at the water-air interface [*Wanninkhof et al.*, 2009; *Aubinet et al.*, 2012], and in combination with measurements of CO_2 concentrations, also gas transfer velocities [*MacIntyre et al.*, 2010; *Heiskanen et al.*, 2014]. Already several dozens of towers provide high resolution measurements of CO_2 exchanges over aquatic systems in six climatic

zones, though most of these have only published short time records of the observations [*Eugster et al.*, 2003; *Vesala et al.*, 2006; *Lee*, 2014; *Shao et al.*, 2015; *Katul et al.*, 2016]. Therefore, synthesis of results from multiple eddy towers over multiple years gives unprecedented opportunities for combining high temporal resolution of EC measurements with benefits of space-for-time substitution over ecosystems in broader geographical scale to compare magnitudes of CO_2 flux from diverse lakes and reservoirs.

Time series of CO_2 fluxes allow us to investigate which drivers govern CO_2 flux at hourly to centennial time scales [*Hanson et al.*, 2006; *Vesala et al.*, 2006; *Perga et al.*, 2016]. At shorter time scales, air-water CO_2 flux is hypothesized to be regulated through kinetic forcing on gas transfer velocities (including wind shear, convection, waves, rain, bubbles, fetch [*Cole and Caraco*, 1998; *Wanninkhof et al.*, 2009; *MacIntyre et al.*, 2010; *Vachon and Prairie*, 2013], and thermodynamic forcing on ΔpCO_2 (the difference between pCO_2 in air and water), including ecosystem metabolism, irradiance, temperature, mixing, and transport, [*Hanson et al.*, 2006; *Atilla et al.*, 2011; *Yvon-Durocher et al.*, 2012; *Mammarella et al.*, 2015]. The regulators of CO_2 concentrations at longer timescales include climate, nutrients and organic carbon delivery [*Hanson et al.*, 2006; *Maberly et al.*, 2013; *Finlay et al.*, 2015; *Perga et al.*, 2016].

Moreover, the same driver may affect different physical, chemical and biological processes at different time scales [*Hanson et al.*, 2006], and the importance of different drivers and their contribution to CO_2 flux change over time [*Sturtevant et al.*, 2015; *Perga et al.*, 2016]. The ecosystem-scale CO_2 feedbacks also may significantly vary depending on nutrient, color, connectivity with landscape, waterbody morphometry [*Blenckner*, 2005; *Webster et al.*, 2008]. Finally, the impact of global threats, such as eutrophication, climate change, invasive species, building water infrastructures [*Smith*, 2003; *Lehner et al.*, 2011; *Attermeyer et al.*, 2016],

additionally affects freshwater systems and interacts with “natural” environmental controls. Therefore, temporarily-resolved observations to inform mechanistic models [*Hasler et al.,* 2016] are urgently needed to improve our understanding of multi-temporal CO_2 ecosystem feedbacks to biotic and abiotic factors and to predict future trajectories of change.

In view of limited understanding of meteorological controls of air-water CO_2 exchange in freshwater ecosystems, we synthesize the eddy covariance from globally distributed 19 lakes and reservoirs. We asked: How do observed diurnal and seasonal patterns of CO_2 flux vary by lake and meteorological characteristics? What consistent climatic and biotic drivers best predict ecosystem level CO_2 responses? How does full temporal sampling of all hours and seasons influence estimates of global net evasion of CO_2 from inland lakes and reservoirs compared to published indirect approaches? By answering these questions, we can improve our predictive understanding on responses of CO_2 emission from aquatic systems to environmental drivers at multiple time scales.

4.2 MATERIAL AND METHODS

Study sites

We analyzed multi-temporal patterns of air-water CO_2 exchange and environmental drivers across globally-distributed 19 sites with direct eddy covariance flux towers. The sites included 13 lakes and 6 reservoirs, and were characterized in terms of morphometric type, nutrient and dissolved organic carbon concentrations, and climatic zones whenever possible (Fig. 4.1, Table 4.1). Most sites were located between 40-68°N of latitude, which coincides with the largest area of Earth's land surfaces covered with lakes. To our knowledge this study is the first large-scale synthesis of direct CO_2 observations in lakes and reservoirs.

Eddy covariance data

The eddy covariance (EC) technique directly measures air-water exchange of CO_2, H_2O, energy, and momentum. It does not disturb the water-air interface and captures all sources of turbulent gas exchange across a lake flux footprint (i.e., an upwind area "seen" by the tower). EC flux is computed as a products of the mean air density and the covariance between turbulent fluctuations of mixing gas ratio and vertical wind speed [*Aubinet et al.*, 2012]. The measurements were generally measured at 10 Hz frequencies which were further integrated into half-hourly averages of ecosystem carbon dioxide, water vapor, and energy fluxes by site principle investigators (PIs). Raw data processing, quality screening, flux computation was performed by PIs according to methodologies applicable to each site. Although no standard data processing protocol for freshwater systems has been developed yet, the reliable flux computation procedures developed for terrestrial systems over nearly three decades were applied [*Baldocchi*, 2014], significantly reducing cross-site flux uncertainty due to methodological differences. Length of time series

reported varied from a few days to several year-long observations, however most data were collected over multiple (up to seven) open water periods (Table S4.1).

Data were further harmonized to the same data format and units, screened for fetch, and de-spiked. The number of daytime and nighttime observations retained varied across sites but with on average data gaps comprised 69% (daytime) and 73% (nighttime) of time series (Table S4.1). The largest gaps were due to excluding out-of-lake tower footprints or sensors malfunctioning. Tower footprints (i.e., an upwind areas visible to tower instruments) were calculated using two dimensional model [*Kljun et al.*, 2015] to estimate lake surface area contributing to half-hourly flux measurements (at least >80% lake surface area within footprint) or observations were excluded based on prevailing wind direction provided by PIs.

We applied a consistent approach to gap-fill climatic (air temperature, incoming solar radiation, photosynthetically active radiation, wind speed, friction velocity, relative humidity, barometric pressure, net radiation, vapor pressure deficit) and in-water (water temperature at 0m and 1m depths, partial pressure of CO_2) variables across all sites using an enhanced look up table (LUT) approach [*Reichstein et al.*, 2005] using REddyProc package (https://www.bgc-jena.mpg.de/bgi/index.php/Services/REddyProcWebRPackage). To gap-fill sensible and latent heat, and CO_2 fluxes, we first tested two approaches: LUT modified for our purposes and artificial neural network (ANN, [*Morin et al.*, 2014]). In LUT approach, we used wind speed, air temperature, and incoming solar radiation to gap-fill CO_2 flux. In ANN approach, we included variables of fuzzy diurnal and seasonal cycles, three decomposed signals of NEE with highest spectral energies, and all climatic variables with statistically significant relationship with the flux [*Papale and Valentini*, 2003; *Morin et al.*, 2014]. The ANN algorithm could iteratively choose variables, consequently each lake had different sets of variables used to gap-fill. Because we

modified LUT source code for our purposes we could not estimate uncertainty and biases due to gap-filling, however it has previously been noted that the LUT approach tends to overestimate annual flux values [*Franz et al.*, 2016]. The average root-mean-square-error in ANN approach accounted for 0.35 μM m^{-2} s^{-1}. Single-site uncertainty estimate are in table S4.1. Although both approaches generally led to similar magnitudes and patterns of fluxes, LUT approach resulted in a smaller number of end-gaps and always used the same variables for gap-fill across all sites. Therefore, we used LUT to gap-fill fluxes as it also proved to be suitable in other limnetic sites [*Shao et al.*, 2015; *Franz et al.*, 2016] but used the ANN results to interpret potential drivers. Linear interpolation was used to gap fill reminder gaps.

Auxiliary data

Global distribution and surface area of lakes and reservoirs for CO_2 flux upscaling were obtained from Global Lakes and Wetlands Database (GLWD, [*Lehner and Döll*, 2004]). Data levels 1 and 2 of GLWD contains lakes and reservoirs >0.10 km^2. Ice-free days were estimated from mean annual air temperature, air temperature amplitude, and latitude following equations 4 and 5 [*Weyhenmeyer et al.*, 2011]. Monthly bias-corrected CRU-NCEP gridded temperature and precipitation data for year 2010 were produces as part of Multi-scale Synthesis and Terrestrial Model Intercomparison Project [*Wei et al*,. 2014]. Monthly values were aggregated into annual values.

Data analysis

To identify time scales with largest spectral energies in CO_2 flux and environmental controls, we used continuous wavelet transform (CWT) with the Morlet wavelet to decompose signals. The wavelet was applied as bandpass filter to the time series, which was then stretched in time by

varying its scale and normalizing it to have unit energy [*Grinsted et al.*, 2004]. The CWT is useful in extracting features from noisy geophysical time series [*Grinsted et al.,* 2004]. It also suitable for nonstationary data which are frequent in ecological systems [*Cazelles et al.,* 2008]. The Morlet wavelet is well localized both in scales and frequencies [*Grinsted et al.,* 2004]. Because Morlet wavelet is sensitive to edge effects at both ends of time series [*Cazelles et al.,* 2008], we used symmetrical zero padding to extend signals. However, it is impossible to totally eliminate the edge effect, and therefore areas outside of coin of influence should not be taken into account [*Cazelles et al.,* 2008]. Another limitation of using CWT is a length of eddy covariance measurements, typically over an open water season, which limits CWT detection ability from monthly (in case of shorter time series) to half a yearly time scales. Consequently, we focused the analysis here on hourly, daily, weekly, monthly, and seasonal timescales.

We examined which environmental driver controls CO_2 flux at multiple timescales using robust non-linear regression at half-hourly time scale (binned and un-binned) and wavelet coherence at hourly to seasonal timescales. This technique detects time-localized oscillations common to two signals and is a measure of correlation in time frequency space [*Grinsted et al.,* 2004]. Gaussian quadratic least-squares fit was used to derive equation to estimate CO_2 efflux along latitude.

4.3 RESULTS

Spatial patterns of CO_2 *flux*

The distribution of daily sums of net ecosystem exchange of CO_2 (NEE) for open water seasons showed a range of patterns and magnitudes across the study lakes (Fig. 4.2). Average daily emission for all water bodies ranged from -1.12 gC m^{-2} d^{-1} to 1.69 gC m^{-2} d^{-1} with the average daily NEE of 0.30 gC m^{-2} d^{-1}across all lakes. A vast majority of lakes released carbon to

atmosphere during an open water season. One lake, Lake Erie, was on average sink of carbon with average NEE accounting for -0.12 gC m^{-2} d^{-1}. Three other lakes, Lake Mendota and Lake Taihu (both eutrophic), and Lake Villasjon (humic with submerged vegetation) were on average near-neutral, slightly above equilibrium with atmosphere. The largest carbon emissions were in a humic boreal lake (Lake Kuivajarvi, 0.68 g C m^{-2} d^{-1}) and two reservoirs: tropical Nam Theun2 (1.10 gC m^{-2} d^{-1}) and temperate Maneesward (0.74 g C m^{-2} d^{-1}). When daily CO_2 fluxes were divided by lake groups, low-to-moderate productivity, high productivity, humic, and reservoirs waterbodies outgassed on average 0.24, 0.12, 0.39, and 0.47 gC m^{-2} d^{-1}, respectively.

Almost all lakes showed high NEE variability during an open water season. While majority of water bodies had mean NEE corresponding to the peak of highest probability NEE (mode), some of the lakes (like Lake Taihu or Lake Kuivajarvi) exhibited an apparent bimodal distribution with mean flux falling between two peaks. Fifteen out of nineteen (80%) lakes sequestered atmospheric CO_2 at some point of an open water season, regardless of lake trophic state.

Table 4.2 compares cumulative NEE over a common summer period (199-342 day of year), a 36 period with overlapping observations for a majority (n=16) of the sites. Seasonal cumulative values ranged from -4.6 gC m^{-2} 36 $days^{-1}$ in shallow with submerged vegetation Lake Villasjön to 28.6 gC m^{-2} 36 $days^{-1}$ in Reservoir Maneswaard. Most water bodies released CO_2 to atmosphere over this period, on average 12.67 gC m^{-2} 36 $days^{-1}$ or 10.94 gC m^{-2} 36 $days^{-1}$ (after averaging within-site interannual variability). Higher NEE relative to summer average were found in reservoirs and humic lakes, while smaller fluxes were found in productive lakes. Although Lake Taihu was a highly productive lake, over the 36-day common period, it emitted CO_2 comparable in magnitude to the mean CO_2 flux.

Mean daily NEE across for 36-day period was 333 mgC m^{-2} day^{-1} across lakes and ranged from -174 mgC m^{-2} d^{-1} to 772 mgC m^{-2} d^{-1} (Table 4.2). Again, lower CO_2 flux magnitudes were observed in eutrophic and unproductive water bodies, while larger in humic lakes and reservoirs. These CO_2 flux averages were higher or lower relative to open water averages (Fig. 4.2) depending on the lake. Daytime hourly flux magnitudes were, on average, 45% lower relative to nighttime hourly flux (Table 4.2).

We observed no linear pattern of NEE along latitude or to gradients of mean annual precipitation or mean annual air temperature (Fig. 4.3), indicating an importance of lake-specific characteristics in modulating ecosystems' response to climatic drivers. The only obvious pattern was that emissions between 30-40°N and >62°N were lower relative to CO_2 flux in 50-60°N.

Temporal patterns: Diurnal cycle

When diurnal NEE variations are compared for each month, we found consistent patterns of daytime minima and nighttime mixima except for the flushing reservoir Estmain (Fig. 4.4). Estmain Reservoir had the highest NEE during the day. The amplitude of midday NEE drawdown varied across lakes and across open water season. In August, for example, the highest diurnal uptake was in productive lakes Zarnekow and Mendota, at 1.34 and 0.88 µM m^{-2} s^{-1}, respectively. The smallest diurnal drawdown was in a humic lake (Valkea-Kotinen), 0.15 µM m^{-2} s^{-1}. In fall months, the diurnal variability generally decreased and patterns were irregular among lakes. Moreover, NEE showed little or no mid-day drawdown in September in deep, stratified lakes (Mendota and Valkea-Kotinen). In October, small midday dips were observed in almost all waterbodies. Despite predominant effect of lake metabolism at daily timescales, a clear trend of gradually increasing NEE during water-warming months was observed in almost all lakes.

Temporal patterns: Seasonal cycle

Seasonal variations were pronounced and dominant across of lakes and reservoirs (Fig. 4.5). Most water bodies are net sources of carbon to atmosphere thought the open water season. Across all lakes, NEE ranged from -0.3 gC m^{-2} d^{-1} to 0.6 m^{-2} d^{-1} in spring, while in the fall, NEE ranged from 0 gC m^{-2} d^{-1} to 1 gC m^{-2} d^{-1}. Like in diurnal cycle, there is a gradual increase (reduced sink, increased emission) of NEE across open water season.

In additional to variation across seasons, regular oscillations at 20-30 day intervals were present in all time series. In waterbodies with vegetation, NEE oscillated around a mean of -0.2 gC m^{-2} d^{-1} (Lake Villasjon) and 0.5 gC m^{-2} d^{-1} (Reservoir Zarnekow) until late August, when daily emissions nearly doubled in Reservoir Zarnekow and Lake Villasjon switched from sink of carbon to source of carbon. NEE in deep lakes (Lake Valkea-Kotinen and Lake Mendota) also reached emission maxima in late summer/early fall but gradually decreased towards the end of season, reaching values comparable to the seasonal average.

Drivers of lake CO_2 flux

Half-hourly time scale

Scatterplots of half-hourly observations of NEE and drivers for an open water season were very scattered and generally showed no or weak relationships (data not shown). To reduce scatter from noise and secondary drivers, NEE data were binned in intervals, whereby fitted lines revealed several NEE responses to micrometeorological drivers (Fig. 4.6). Among all environmental controls, water-air temperature difference (ΔT) best correlated with NEE, explaining on average 58% of binned NEE variability. Of these regressions, shallow lakes showed a higher r^2 than deeper lakes. Air temperature was a better predictor of NEE variability (average r^2 was 0.36) than water

temperature (0.08). Net radiation (Rnet), latent heat (LE), and water-air vapor pressure deficit (VPD) were also among the most consistent controls of NEE, explaining on average 55%, 44%, and 42% of variability, respectively. Wind speed (U) and friction velocity (U_*) explained on average 29% and 17% of NEE variability. Influx of photosynthetically active radiation (PAR) poorly correlated with binned NEE, excluding the productive reservoir with emergent vegetation. For six sites having water pCO_2 data, the water-air pCO_2 difference (ΔpCO_2) was an important driver of NEE, with r^2 ranging from 0.05 in Lake Merasjarvi to 0.74 in Lake Valkea-Kotinen. Figure 6 shows highly variable sensitivity to drivers among sites and incoherent latitudinal gradient of these sensitivities. In many cases, binned NEE also often had nonlinear responses to environmental drivers.

Multi-temporal drivers based on wavelet coherence

Environmental controls again showed inconsistent patterns with NEE at timescales longer than daily across all lakes (Fig. 4.7). At daily timescale, temperature-related variables showed highest spectral energies (i.e., variability), with air temperature (T_{air}) having highest coherence with CO_2 flux, followed by ΔT (not shown because it mirrors T_{air}), sensible heat (H) and water temperature (T_w). All these variables also showed high coherence one with another (>0.7). While signals of CO_2 and Tair in lakes Zarnekow and Tamnaren had strongest coherence across open-water season, it had little or no coherence in Estmain Reservoir and Lake Erie. Among wind and shear driven drivers, NEE and u* and U (not shown) signals showed transient and alternating periods of high and low coherence, indicating a temporal oscillation to wind driven CO_2 emissions in most lakes, except throughout the open-water season in Zarnekow Reservoir, which was consistently coherent.

Among potential signals of biotic interaction, the strongest and most coherent relationship of NEE with LE was in waterbodies with emergent and submerged macrophytes, suggesting

photosynthetic control of CO_2 uptake. In deeper lakes, the coherence between NEE and LE was more transient, with consistent high coherence period confined to late August and September. Similar to LE, the strongest NEE coherence with PAR was in shallow productive lakes with vegetation (Zarnekow and Tamnaren, and Villasjon until October). Except Lake Erie, PAR was an important driver in all lakes with periods of high and low coherence. Only three lakes had continuous ΔpCO_2 data, and those lakes showed alternating periods of high and low coherence with CO_2 flux. Water level in Zarnekow Reservoir highly correlated with CO_2 signal during summer.

At longer temporal timescales, the coherence between CO_2 flux and environmental drivers varied by lakes and time periods of open water season (Fig. 4.7). At weekly to monthly time scales, highly coherent episodes were infrequent relative to daily time scale. NEE coherence with temperature-related variables were more frequent in shallower lakes (Villasjon, Tamnaren, Douglas). At seasonal time scale, Tair became incoherent to NEE signal in contrast to more coherent signals of ΔT and LE (Fig. 4.7). Water level was consistently coherent with NEE signal Zarnekow Reservoir. Lake productivity indicators, PAR and ΔpCO_2, were coherent with NEE in productive lakes Erie and Mendota, however over different parts of the open water season.

4.4 DISCUSSION

We used a time-for-space approach to estimating carbon emission from 19 ecosystems representing diverse ecosystems types. By subsetting our study sites to only those with multiple seasons of eddy covariance (EC), we are able evaluate the reliability of previous indirect and infrequently sampled based estimates of CO_2 flux. Though the total number of study lakes is small, the total number of independent observations is significantly larger relative to more “traditional” limnological studies. Major findings and implications are discussed below.

Human-made waterbodies emit more carbon than lakes

Consistent with earlier studies, CO_2 flux magnitudes from reservoirs were larger than natural lakes (Fig. 4.2, Table. 4.2). The mean daily NEE in a young tropical reservoir Nam Theun 2 were nearly twice as high as fluxes in reservoirs in other climatic zones. Our estimates for tropical reservoirs agreed with another EC study [*Guérin et al.*, 2007], though were 35% higher [*Barros et al.*, 2011] or 320% lower [*St. Louis et al.*, 2000] than others. Tropical reservoirs had higher CO_2 emissions likely because of higher temperature-mediated mineralization raters, higher organic content relative to mid- and high latitude waterbodies, thermally enhanced gas transfer velocities, water level fluctuations, short residence times [*Guérin et al.*, 2007; *Roland et al.*, 2010; *Barros et al.*, 2011; *Polsenaere et al.*, 2013; *Franz et al.*, 2016].

NEE observed by eddy covariance from reservoirs in other climatic zones range from three times lower [*St. Louis et al.*, 2000] to 40% higher [*Barros et al.*, 2011] of those indirect estimates reported in the literature. The largest discrepancies between our and published estimates were for boreal Eastmain Reservoir where maximum daily flux (2.6 times higher than mean flux) was 0.43-1.5 fold lower than published values for the same reservoir [*Teodoru et al.*, 2011]. These differences were likely because of different surface area sampled (the reservoir has large patchiness of pre-flooding area with large emission differences, [*Teodoru et al.*, 2011]), decline of emissions with reservoirs aging [*Barros et al.*, 2011], flux overestimation when using chamber measurements [*Eugster et al.*, 2003], and limited number of chamber samples compared to continuous sampling by the tower. It is worth noting that [*St. Louis et al.*, 2000] study was used to upscaling fluxes from reservoirs [*Raymond et al.*, 2013], indicating one likely source of flux biases in contribution of reservoirs to global efflux from lakes and reservoirs.

Our eddy covariance daily CO_2 flux magnitudes for lakes were in agreement with indirect measurements for ponds <100 km^2 [*Holgerson and Raymond*, 2016] and fluxes derived from pH, DIC for US waterbodies [*McDonald et al.*, 2013]. However, CO_2 fluxes calculated from pH, ALK for Swedish lakes were nearly twice higher than for Scandinavian lakes in our data set [*Weyhenmeyer et al.*, 2015] and a few times lower relative to CO_2 fluxes derived from pH, DIC for Finnish lakes [*Rantakari and Kortelainen*, 2005]. Though this is not a comprehensive flux magnitudes revision, the differences in CO_2 estimates highlight a core difficulty in synthesizing NEE across methods for global upscaling.

Reconciling NEE estimates with other CO_2 flux measurements

That said, there is good reason to believe that flux tower approaches can be a viable method for estimating lake CO_2 fluxes more continuously and reliably than chambers. Simultaneous measurements of CO_2 using eddy covariance (EC) with indirect methods (chamber or models of surface renewal and boundary layer) showed good agreement between flux estimates [*Eugster et al.*, 2003; *Vesala et al.*, 2006], though other studies found flux underestimation [*Jonsson et al.*, 2008; *Podgrajsek et al.*, 2014a; *Xiao et al.*, 2014] or overestimation [*Eugster et al.*, 2003; *Guérin et al.*, 2007] of eddy covariance compared to indirect methods, while others showed variable periods of agreement and disagreement [*Podgrajsek et al.*, 2014a]. Largest discrepancies tend to be found between EC and floating chamber measurements [*Eugster et al.*, 2003; *Podgrajsek et al.*, 2014a], where chambers typically overestimate CO_2 flux. Continued analysis of multi-method flux estimation is critical to detecting biases and factors contributing to flux discrepancies.

Although majority of published eddy covariance studies are included in this study, we found our re-analyzed the NEE estimates agreed with literature estimates for some lakes [*Vesala et al.*, 2006; *Jonsson et al.*, 2008; *Huotari*, 2011], but were larger [*Eugster et al.*, 2003; *Podgrajsek*

et al., 2014b; Shao et al., 2015; *Franz et al.*, 2016] or smaller [*Franz et al.*, 2016], indicating that consistent post-processing of data and protocols for doing so are essential to move forward on aquatic eddy covariance. Here, we applied a consistent post-processing and gap-filling approach across all lakes in this study, therefore, we attribute discrepancies in daily CO_2 flux estimates to different periods being compared (i.e., summer, monthly, convective or stratified periods), gap-filling approached, statistics (i.e., ranges, median, means), and interannual variability in time series covering multiple seasons.

Reconciling aquatic and terrestrial latitudinal gradients of climatic data

The lack of linear latitudinal, mean annual precipitation and temperature gradients were likely attributed to ecosystem differences and their effect on fluxes. Although latitudinal gradient of CO_2 emission is useful in assessing the impact of climate as latitude integrates multiple variables like annual insolation, air temperature, precipitation, ice-cover duration [*Blenckner*, 2005], we found a quadratic relationship with latitude in our lakes, with highest emissions between 50-62°N (Fig. 4.2-4.3). Previous studies found declining CO_2 fluxes or aquatic pCO_2 (a proxy of CO_2 flux) with latitude in lakes and/or reservoirs [*Alin and Johnson*, 2007; *Marotta et al.*, 2009; *Barros et al.*, 2011] or cubic relationship in ponds [*Holgerson and Raymond*, 2016]. While temperature-mediated C mineralization rates were highest in tropics [*Kosten et al.*, 2010; *Barros et al.*, 2011] and pCO_2 increased with temperature [*Marotta et al.*, 2009; *Barros et al.*, 2011; *Kosten et al.*, 2014], another study found a negative relationship with pCO_2 and CO_2 flux [*Alin and Johnson*, 2007]. Since pCO_2 should increase with temperature increases, confounding factors like lake productivity [*Alin and Johnson*, 2007], overridden the latitudinal temperature effect on CO_2 flux.

Lack of linear latitudinal gradient of CO_2 flux could also be attributed to incomplete representation of lake types in major climatic zones. Therefore, highest emissions fall between 50-62°N latitude where most humic lakes and reservoirs were located (Fig. 4.2-4.3). It also reflected overrepresentation of US/Canada and Scandinavian sites and largely underrepresentation of subtropical and tropical lakes, not mentioning lack of any lakes from Southern Hemisphere.

Lake nutrient – color content indicates NEE sign and magnitude

Unlike latitude, lake trophic status and humic contents were better in explaining differences in CO_2 flux waterbodies (Fig. 4.2, Table 4.2). Eutrophic waterbodies had reduced CO_2 efflux (or even influx of CO_2) relative to unproductive or humic lakes, similarly to CO_2 flux studies [*Riera et al.*, 1999; *Hanson et al.*, 2004; *Balmer and Downing*, 2011]. For example, net autotrophic lakes sequestered CO_2 with median carbon uptake of -77 mgC m^{-2} d^{-1} while net heterotrophic lakes emitted at 253 mgC m^{-2} d^{-1} in boreal lakes [*Bogard and del Giorgio*, 2016]. Eddy covariance studies also showed that humic lakes emit 2-3 times more CO_2 than unproductive lake and up to 6 times more than productive lake [*Vesala et al.*, 2006; *Jonsson et al.*, 2008; *Huotari et al.*, 2011; *Podgrajsek et al.*, 2015]. Therefore, the nutrient-color paradigm [*Williamson et al.*, 1999; *Webster et al.*, 2008] appears to key to characterize lake NEE.

Since nutrients stimulate primary production and DOC sustains ecosystem respiration, unsurprisingly lake biotic characteristics played a dominant role in modulating diurnal cycles of CO_2 flux magnitudes (Fig. 4.4). Here, we found that most lakes coherently showed NEE decrease (CO_2 uptake or reduced emission) during the day, with the highest uptake was in a productive reservoir with emergent macrophytes (Fig. 4.4). Nighttime NEE increased due to bacterial CO_2 production. Despite significant CO_2 flux reduction due to photosynthesis in majority of waterbodies, all waterbodies remained net heterotrophic (Fig. 4.4) suggesting that respiration

exceeded primary productivity, even in productive waterbodies with significant coverage of emergent macrophytes. Although recent studies argue that net autotrophic lakes also evade CO_2 to atmosphere [*McDonald et al.*, 2013; *Bogard and del Giorgio*, 2016], eddy covariance measured CO_2 above lake surface, and hence, reflected net excess of ER over GPP [*Aubinet et al.*, 2012].

Only shallow Lake Villjason with submerged macrophytes was a net sink of carbon during the summer months (Fig. 4.5). Also, Zarnekow Reservoir with emergent macrophytes showed the highest diurnal CO_2 drawdown. Several EC studies hypothesized small CO_2 sinks to presence of macrophytes [*Anderson et al.*, 1999; *Xiao et al.*, 2014; *Lohila et al.*, 2015; *Franz et al.*, 2016] although only [*Franz et al.*, 2016] addressed this issue only. These effects might have significant effects of CO_2 exchange in on-shore towers, which footprints cover mostly littoral zones.

In contrast to all waterbodies, flushing Estmain Reservoir showed daytime increases and nighttime increases, although those increases were low across entire growing season (Fig. 4.4). We hypothesize these increases might be due to water level fluctuation and stirring CO_2 -rich sediments (near on island tower) and/or temperature-mediated respiration increases. However, additional observations are needed to verify our hypotheses.

A few lakes had muted diurnal amplitudes during fall, primarily in seasonally stratified lakes, Valkea-Kotinen and Mendota (Fig. 4.4). We attribute them to fall turnover bringing CO_2-rich waters from hypolimnion by convective mixing, typically occurring in late September/early October [*Vesala et al.*, 2006]. We saw an earlier “fall mixis footprint”, which was likely due to upwellings of hypolimnetic waters to epilimnion due to wind shear forcing on thermocline [*Ojala et al.*, 2011]. We still observed diurnal cycles in October, probably due to delivery of nutrients and accelerated algal blooms, though the amplitude was generally smaller than in spring and summer.

The CO_2-rich upwellings imply lake morphometric characteristics can additionally modulate CO_2 flux responses to meteorological drivers (Fig. 4.4-4.5). Two deep lakes, for example, did not show diurnal CO_2 uptake in September (Fig. 4.4), and CO_2 flux increased in this month (Fig. 4.6), which was likely attributed to fall mixis. During convective mixing, CO_2-rich and nutrient-rich waters were brought to surface enhancing CO_2 efflux [*Riera et al.*, 1999]. Shallow lakes also had more cooling events relative to deeper lakes over the open water season coinciding with CO_2 fluxes (Fig. 4.7), and significantly contributing to annual CO_2 efflux [*Liu et al.*, 2016]. Space-for-time studies indicate that lake-specific characteristics like lake area, catchment:lake area ratio, mean depth explain nutrient and humic concentration differences between lakes [*Webster et al.*, 2008], and which in turn, may affect thermocline depth [*Fee et al.*, 1996] and sensitivity to hydrological inflows [*Weyhenmeyer et al.*, 2015]. An interplay of physical and biotic interactions certainly created extremely dynamic ecosystem CO_2 patterns in lentic systems.

Temperature is the strongest driver of lake seasonal NEE variation

We noted that gradual increase of NEE until end of August coinciding with warming of surface water temperature (Fig. 4.4-4.5) and temperature-mediated increases of pCO_2 and CO_2 flux. Because thermodynamic forcing on ΔpCO_2 is also affected by biology, mixing, and transport [*Wanninkhof et al.*, 2009], the temperature effect can be overridden by other effects. In contrast, regular oscillations at 20-30-day frequencies observed (Fig. 4.5) might be due to trophic cascades, when declines in phytoplankton biomass followed zooplankton biomass increases [*Sommer et al.*, 2011] likely affected the GPP:ER ratio and CO_2 exchange at water-air interface. Moreover, frequent phytoplankton biomass fluctuations might be due to upwellings of CO_2 -rich and nutrient-rich water to epilimnion induced by wind-induced internal waves [*Evans et al.*, 2008]. Though

these findings require additional observations and models, our findings are consistent with regular temperature and pCO_2 signals oscillations observed in deep and shallow lakes [*Atilla et al.*, 2011; *Pannard et al.*, 2011; *Heiskanen et al.*, 2014].

Few consistent drivers in other timescales

High scatter and inability to detect strong relationship of un-binned NEE with environmental drivers, indicate significant multi-temporal multi-driver relationships of NEE that require a modeling approach. However, a few consistent relationships stand out. Binned wind speed explained 0 to 96% of binned NEE variability with average of 36% (Fig. S4.1), and indicate variable but consistent positive dependencies of wind and CO_2. The wind speed and CO_2 flux relationship may change with degree of thermal stratification [*Heiskanen et al.*, 2014], warming or cooling seasons [*Read et al.*, 2012] and diurnal timescales. Interestingly, the relationship to friction velocity (U*) showed lower coherence despite being a dominant physical control of CO_2 exchange at air-water interface because of its relationship to near-surface turbulence [*Wanninkhof et al.*, 2009]. The EC technique can suffer from advective flows in periods of low u_*, making comparison in those periods less reliable. In low wind conditions, waterside convection can contribute to fluxes, furthering masking wind speed relationships [*MacIntyre et al.*, 2010; *Mammarella et al.*, 2015; *Podgrajsek et al.*, 2015].

We also found sub-daily NEE variation dominated by diurnal cycle of solar radiation and temperature. We observed large differences in summer daytime and nighttime CO_2 fluxes across lakes (Table 4.2) and across months (Fig. 4.4), suggesting potential for ΔT to control NEE at diurnal cycle. Because of high thermal capacity of water and small T_w diurnal fluctuations, T_{air} mainly contributed to temperature difference between water and air, and hence daytime warming and nighttime cooling. However, this temperature effect on CO_2 flux might be overridden by lake

metabolism and lead to spurious relationships with temperature [*Alin and Johnson*, 2007], and perhaps nonlinearities. Photosynthetic CO_2 uptake dominated diurnal cycles in majority of lakes (Fig. 4.4), leading to strong NEE and PAR (a proxy of lake productivity) coherence, particularly in waterbodies with macrophytes (Fig. 4.7).

Lastly, the diurnal signals of latent heat (LE) and NEE showed high coherence (Fig. 4.7) in many waterbodies. In Zarnekow reservoir with substantial contribution of emergent macrophytes to tower footprints, stomatal conductance control of photosynthesis in response to fluctuations of vapor pressure deficit may be the primary factor that links the two [*Stoy et al.*, 2005]. LE is also an indicator of water-side buoyancy flux [*Imberger*, 1985], influencing gas transfer velocity. Therefore, it is possible LE and NEE to show coherence during lake convective mixing periods in boreal lakes [*Eugster et al.*, 2003; *Heiskanen et al.*, 2014; *Podgrajsek et al.*, 2015] or low wind, high insolation conditions in tropical reservoirs [*Polsenaere et al.*, 2013]. Large pulses of CO_2 also occur during synoptic events, when heat is released from waterbodies and thermocline tilting induced intrusion of CO_2 -rich waters from hypolimnion [*Liu et al.*, 2016].

Potential long lagged impact on NEE

Seasonal timescale of NEE correspond to annual solar cycle, biological processes and spring/fall mixis events [*Hanson et al.*, 2006; *Sturtevant et al.*, 2015], which strongly vary by climatic region and latitude. Unlike in shorter time scales, Tair became unimportant variable in explaining CO_2 flux variability across all lakes (Fig. 4.7). During lake cooling, the rates of heat release stored in water column depends not only on autumn weather but also on lake volume. Therefore, large water bodies like Lake Superior have six-month time lag to start releasing heat [*Blanken et al.*, 2011]. The importance variables related to heat loss at seasonal scale, LE in lakes Eastmain and Mendota and ΔT in Zarnekow and Mendota, also seem to at least partly support this

hypothesis as Zarnekow is a shallow reservoir. Moreover, temperature control at seasonal and annual timescales over dissolved inorganic carbon in North temperate lakes is attributed to controls over mixis events and suppressing biotic processes during cold season [*Hanson et al.*, 2006].

Precipitation however had no explanatory power of CO_2 flux variability across all lakes (with precipitation data) and at any time scale, despite importance of rain on (+) gas transfer velocities [*Guérin et al.*, 2007; *Wanninkhof et al.*, 2009] and delivery of OC and IC from watershed [*Stets et al.*, 2009; *Weyhenmeyer et al.*, 2015]. One of the possible explanation is that raindrops interferes with sonic anemometer-thermometry measurements used in eddy towers, causing data gaps during rain events [*Aubinet et al.*, 2012]. Therefore, pulses of CO_2 during and after storms [*Ojala et al.*, 2011; *Vachon and del Giorgio*, 2014] might be missed in EC time series. Finally, lakes are considered to integrate precipitation effects of CO_2 flux through indirect effects like delivery of carbon and nutrients from catchments than from precipitation itself [*Williamson et al.*, 2008; *Tranvik et al.*, 2009]. Such effects are likely to unveil at longer temporal scales, from annual to decadal [*Hanson et al.*, 2006].

Implications for upscaling CO_2 *fluxes*

Assuming all waterbodies with surface area >0.10 km2 (total surface area, 2582600 km2, [*Lehner and Döll*, 2004]) emitted mean CO_2 flux (0.30 gC m^{-2} d^{-1}) over ice-free season, we estimated that carbon evasion from lakes and reservoirs in the Northern Hemisphere (which has significantly more lakes than the Southern Hemisphere) was 0.23±0.19 Pg C yr^{-1}, 0.09 Pg C yr^{-1} (40%) less than current global estimate (Fig. 4.8, *Raymond et al.*, [2013]). In our calculations, we included diurnal CO_2 flux cycle and ice-cover duration but excluded 418409 km^2 of lakes in 0.01-0.1 km^2 bin which are not reported in the global database and lakes south of the equator. If we instead assume year-round CO_2 emissions and scale up for an estimate of smaller waterbodies, do

we get a value comparable to Raymond's value of 0.33 Pg yr^{-1}. Previous CO_2 emission rates accounted for 0.14 PgG yr^{-1} [*Cole et al.*, 1994], 0.39 PgG yr^{-1} [*Cole et al.*, 2007], 0.32 PgG yr^{-1} [*Duarte et al.*, 2008], 0.44 PgG yr^{-1} [*Marotta et al.*, 2009], 0.53 PgG yr^{-1} [*Tranvik et al.*, 2009], 0.64 PgG yr^{-1} [*Aufdenkampe et al.*, 2011].

Although most recent global CO_2 efflux estimate [*Raymond et al.*, 2013] and our estimate are incomparable, our empirical CO_2 flux rates highlight large mismatch between empirical and CO_2 flux mostly modelled from carbonate equilibria (pH and alkalinity/dissolved inorganic carbon) and approximated gas transfer velocities. With more direct CO_2 observations from a wider range of ecosystem types, the CO_2 source strength from inland waters will likely be re-evaluated. Our global emission estimate from lakes >10 ha outgasses nearly 12% (1.7 PgC yr^{-1}) and 5% (4.3 PgC yr^{-1}) of net inland flux without and without anthropogenic fluxes [*Ciais et al.*, 2013], respectively.

Including temporal consideration in CO_2 flux estimation and upscaling may also affect the emission rates from freshwaters. We observed large variance over time within lakes of any trophic state (Fig. 4.2). Depending on the time of the season, humic lakes were classified as sink of CO_2 while highly productive lakes were classified as sources of carbon. Most upscaling studies rely on point-in-time measurements in fair-weather conditions during the day, potentially leading to biased flux estimates [*Alin and Johnson*, 2007; *Liu et al.*, 2016; *Wik et al.*, 2016]. Moreover, most studies exclude diel cycles of CO_2 which might underestimate global carbon balances by 42% [*Liu et al.*, 2016]. However, our global estimate was lower despite including understudied diurnal and seasonal cycles.

Study limitations

Eddy covariance suffers for a range of random and systematic error [*Aubinet et al.*, 2012]. Random error dominated half hourly averages of CO_2 flux, with error magnitudes ranging from 26% in humic lakes [*Mammarella et al.*, 2015] to 40% in eutrophic lake (data not shown) despite smaller CO_2 fluxes. High random error likely masked regression at short-time scales. Further, systematic errors due to gap filling was large and ranged from 0.12-0.73 μM m^{-2} s^{-1}(Table S4.1), which biases comparisons of flux magnitudes. Around 10% uncertainty of CO_2 flux attributed to gap filling in Lake Erie [*Shao et al.*, 2015].

Current observations of NEE over lake are mostly limited to an open water season therefore wavelet analysis and wavelet coherence analyzes were limited to up to 3 to 6 months for majority of lakes. Due to challenges of collecting winter data with eddy covariance technique, we unfortunately have year-round data for three ice-covered lakes. However, even in this case, measurements are limited. Some researchers have dealt with wintertime measurement challenges by placing flux towers on the lake shore. This introduced an additional problem with nighttime CO_2 advection from catchments and flux contamination [*Eugster et al.*, 2003]. Even towers located in the middle of lake can be affected by CO_2 advection [*Eugster et al.*, 2003; *Morin et al.*, 2014]. The contribution of advected air to annual CO_2 lake budgets is unknown but can be substantial.

Although eddy covariance technique is a mature technique for terrestrial systems [*Baldocchi et al.*, 1996; *Law et al.*, 2002], the use of this technique over inland waters is relatively new. Consequently, researchers studying limnetic systems still have not developed a standard protocol for making measurements and post-processing procedures using eddy flux towers. It is also plausible that many corrections developed for terrestrial systems might not be suitable for freshwater systems.

Additionally, more attention should be paid to ecosystem characteristics themselves as many sites lacked water temperature strings, and DO and pCO_2 measurements which significantly limited data interpretation. Given lakes have two boundary layers affecting the water-air interface (from above and from below), the knowledge on in-water biotic and abiotic drivers are essential toward improving mechanistic understanding of processes driving NEE in freshwater systems. In fact, lake prosses likely dominate atmospheric forcing in NEE variability [*Aubinet et al.*, 2012]. Therefore, eddy covariance measurements should also be accompanied with basic chemical (like pH, TP, DOC), ecological (plant community types and coverage) and morphometric (depth within footprint) measurements to inform site-characterization. Also, having in-water pCO_2 measurements are essential for deriving gas transfer velocities and improving k parameterizations, which is particularly important for limnologists upscaling point-in-time measurements.

Finally, like any synthesis project, we synthesized already existing data from *ad hoc* locations rather than carefully designed space-for-time substitution studies. Therefore, future eddy covariance studies should put more effort to include lake types and from regions that underrepresented represented in this data set to reduce uncertainty in flux estimation.

4.5 CONCLUSIONS

To better evaluate the role of lakes and reservoirs in global carbon balances at multiple time scales, we conduct first synthesis of continuous, direct CO_2 flux estimates over 19 globally distributed lakes and reservoirs. Our results indicate that despite consistent midday photosynthetically-driven CO_2 drawdown at diurnal time scale, most lakes were net heterotrophic and source of CO_2 to atmosphere. Seasonally integrated CO_2 fluxes, unlike terrestrial ecosystems, were insufficiently explained by climatic patterns of annual temperature and precipitation means. Instead, waterbody productivity, color, and management were the key indicators of CO_2 flux sign and magnitude.

Despite of all ecosystem differences and high seasonal variability, CO_2 flux showed consistent 20-30-day oscillatory patterns across all lakes. While temperature, solar radiation, and wind speed best predicted ecosystem level CO_2 flux responses, waterbody characteristic such as lake nutrient-color contents, macrophyte communities, and morphometry significantly modulated CO_2 flux responses to climatic drivers. However, these responses were time scale dependent with importance of drivers shifting over time and often confounded with other factors. Our results imply significant multi-temporal multi-driver relationships with NEE that require a modeling approach to separate drivers' contribution towards CO_2 flux variability. Moreover, including diurnal and seasonal cycles and ice phenology resulted in 40% lower up-scaled CO_2 fluxes than global CO_2 efflux determined from indirect, point-in-time measurements. According to our global efflux estimates, lakes and reservoirs outgassed nearly 12% of net inland flux. We expect that with more empirical, continuous data and from more diverse aquatic ecosystems, the global CO_2 emissions from lakes and reservoirs and their contribution to global carbon balances will require re-evaluation.

ACKNOWLEDGEMENTS

We thank all project participants for kindly sharing data and time for. Special thanks go to Jonathan Thom for maintaining Lake Mendota flux tower in Madison, WI. This research was supported by funding from the National Science Foundation LTER Program for North Temperature Lakes LTER (NSF DEB-1440297, NTL LTER).

4.6 TABLES

Table 4.1 Site List and their climatic and limnological characteristics

Site No.	Site Name	Lake Description	Latitude [decimal °]	Longitude [decimal °]	Climatic Zone[1]
25	L. Toolik	Unproductive, medium DOC, deep	68.37	-149.36	Cool continental
6	L. Långa Harrsjön	Unproductive, medium DOC, deep	68.21	19.02	Cool continental
7	L. Villasjön	Shallow, humic, submerged vegetation	68.21	19.03	Cool continental
1	L. Pallasjärvi	Clearwater, oligotrophic, shallower parts of a deep lake	68.01	24.12	Cool continental
5	L. Merasjarvi	Medium DOC, low productivity, deep	67.31	21.59	Cool continental
13	L. Daring	n/a	64.51	-111.36	Cool continental
16	L. Valkea-Kotinen	Humic, productive, deep	61.14	25.03	Cool continental
15	L. Kuivajärvi	Humic, unproductive, deep	60.47	23.51	Cool continental
12	L. Tamnaren	Shallow, productive, submerged vegetation	60.08	17.16	Temperate continental
23	R. Zarnekow	Eutrophic, shallow, emergent vegetation, high DOC (formerly peatland)	53.52	12.53	Temperate continental
14	R. Estmain	Flushing reservoir, humic	52.07	-75.55	Cool continental
4	R. Maneswaard	n/a	51.56	5.37	Temperate Oceanic
3	R. Ilzendoorn	n/a	51.54	5.31	Temperate Oceanic
2	L. Douglas	Mesotrophic, low DOC, deep	45.34	-84.41	Humid continental
19	L. Mendota	Eurtrophic, deep, moderate DOC	43.04	-89.24	Humid continental
18	L. Erie	Eutrophic, shallow basin,	41.47	-83.11	Humid continental
17	R. Ross Barnett	Deep, productivity	32.26	-90.01	Humid subtropical climate
9	L. Taihu	Eutrophic, shallow	31.16	120.15	Humid subtropical climate
8	Nam Theun 2	Deep, high DOC	17.59	104.57	Tropical moist

[1] According Koppen climate classification

[2] Annual values derived from monthly averages for year 2010 and do not always match year of measurements

Table 4.2 Comparison of summer NEE sums for a period between 199 - 234 day of year, daily totals, daytime and nighttime fluxes

Site No.	Site Name	NEE EC Sums [gC m^{-2} 36 day^{-1}]	NEE Daily Total [mgC m^{-2} d^{-1}] Mean ±1SD	NEE Daytime flux [mgC m^{-2} hr^{-1}] Mean ±1SD	NEE Nighttime flux [mgC m^{-2} hr^{-1}] Mean ±1SD
25	L. Toolik	7.5	209±54	7.0±9.3	11.1±10.4
7	L. Villasjön	-6.3	$^{-1}$74±92	$^{-1}$2.1±8.8	-0.5±9.7
1	L. Pallasjärvi	8.8	245±78	6.7±5.8	15.2±6.7
5	L. Merasjarvi	9.3	257±70	8.6±5.4	13.7±5.7
13	L. Daring	1.0	27.2±38	-4.0±5.4	8.3±6.9
16	L. Valkea-Kotinen	21.3 (2003)	591±113	23.5±5.5	26.3±5.6
		24.4 (2004)	679±278	24.2±16.8	34.0±10.8
		14.0 (2005)	390±226	12.6±11.0	21.3±12.7
		8.6 (2006)	238±357	9.3±16.2	10.7±15.7
		21.9 (2007)	609±64	22.8±3.9	29.0±7.2
15	L. Kuivajärvi	26.4 (2011)	734±123	30.8±8.4	30.3±6.1
		20.3 (2012)	567±218	23.3±9.8	29.0±14.0
12	L. Tamnaren	6.2 (2011)	174±83	4.9±5.4	10.5±6.3
		12.6 (2012)	350±96	9.7±6.8	22.1±8.2
23	R. Zarnekow	12.1 (2013)	337±356	3.2±20.0	29.2±24.3
		14.4 (2015)	400±140	2.4±20.8	36.7±19.1
14	R. Estmain	14.7 (2008)	409±225	16.9±10.6	17.1±13.1
		19.6 (2009)	545±198	18.1±10.5	25.5±11.3
		20.1 (2011)	557±88	24.8±6.4	20.8±7.9
		13.6 (2012)	378±108	14.5±6.1	15.5±7.4
4	R. Maneswaard	27.8	772±209	34.8±13.0	28.4±16.9
3	R. Ilzendoorn	15.8	439±150	15.6±17.0	22.0±11.8
2	L. Douglas	14.1 (2013)	393±166	12.4±14.1	22.0±12.4
		8.8 (2014)	245±146	9.9±13.3	10.6±15.6
19	L. Mendota	4.9 (2012)	274±136	4.6±13.5	21.0±15.0
		5.0 (2014)	108±128	$^{-2}$.8±12.0	17.9±15.5
		7.8 (2015)	245±145	5.3±12.9	14.2±14.8
18	L. Erie	1.7 (2012)	46±130	-0.2±3.3	-0.4±3.3
		-0.18 (2013)	-5.1±185	0.1±5.2	0.0±5.0
9	L. Taihu	11.9 (2012)	332±217	17.6±9.3	8.5±17.5

4.7 FIGURES

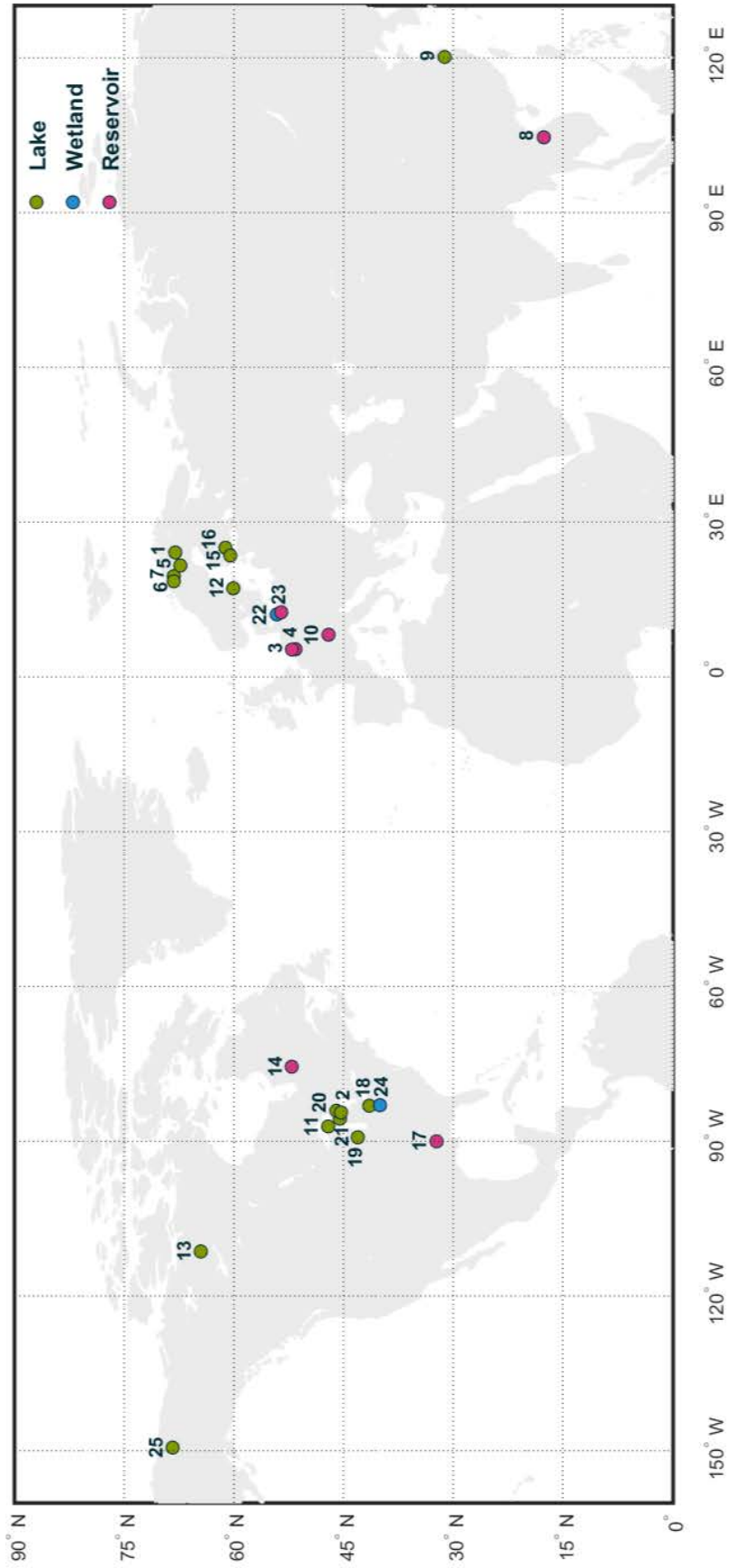

Figure 4.1 Site distribution with eddy fluxes (net ecosystem exchange, methane, sensible heat, latent heat) available in data set

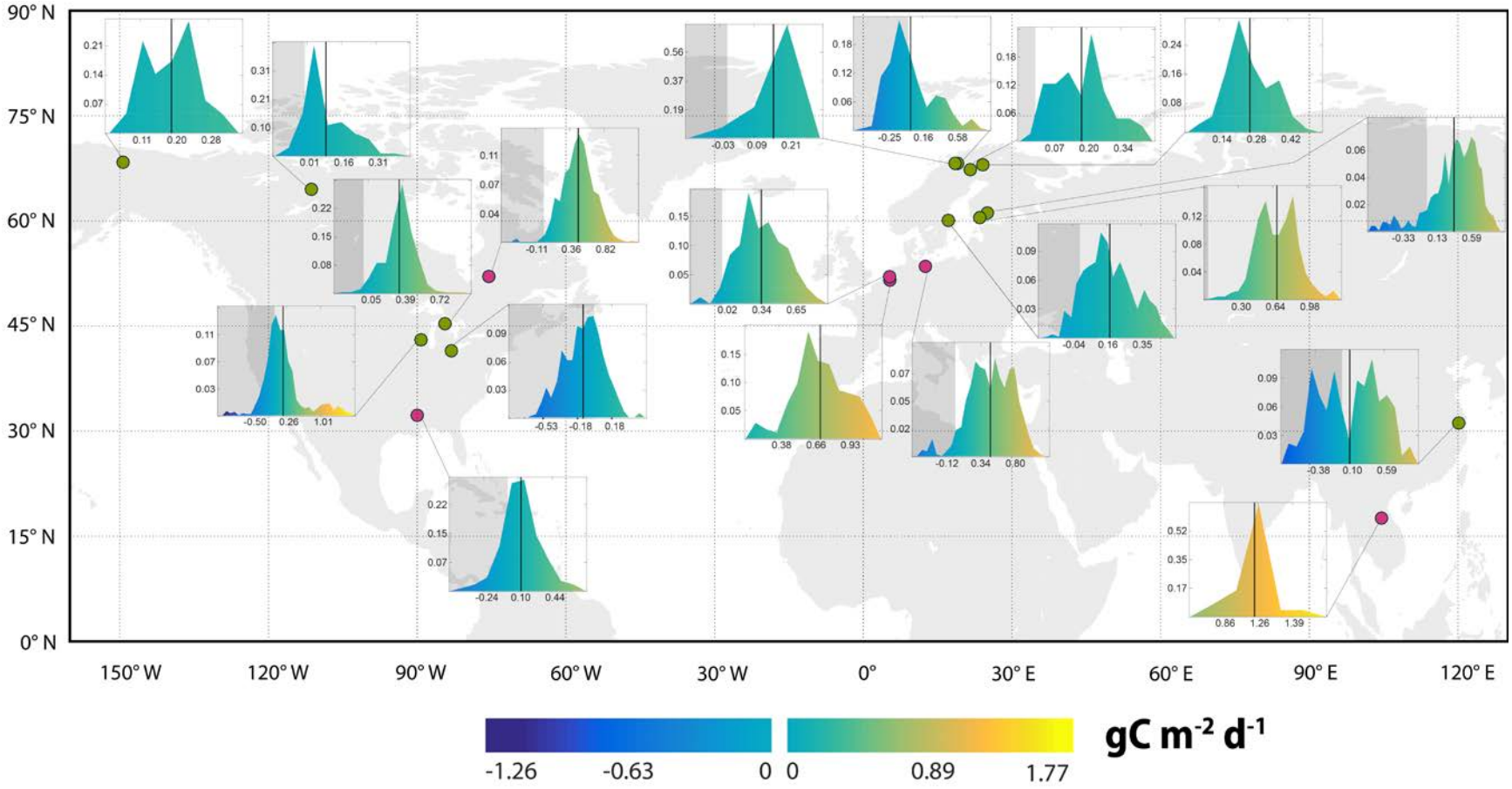

Figure 4.2 Distribution of 13 lakes (green) and 6 reservoirs (magenta) with normalized histograms of daily net ecosystem exchange over ice-free season for each site (A) indicates that majority of ecosystems emitted CO_2 to atmosphere. Vertical solid lines and shaded areas indicate mean daily CO_2 and observations below equilibrium with atmosphere, respectively.

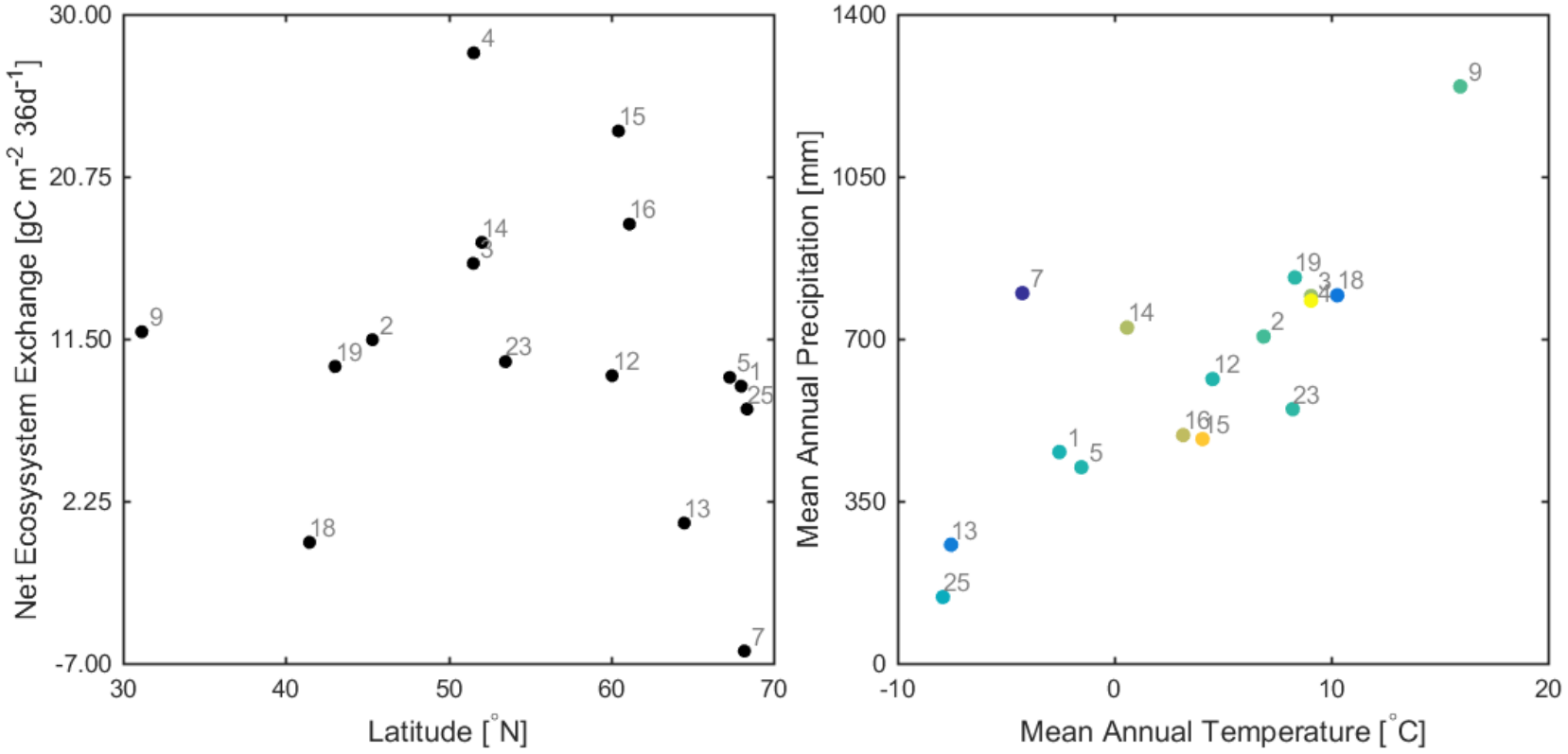

Figure 4.3 The comparison of net ecosystem exchanges (NEE) of sites across latitude over a period of 199-234 day of year (A) and color-coded NEE along precipitation and air temperature gradients (B) indicating poor predictions of CO_2 emissions from latitude and associated climatic drivers. Negative signs indicate that carbon is absorbed by the water body while positive signs indicate release of carbon to atmosphere. Labels indicate site numbers. Multi-year data from sites were averaged. Mean annual temperature and mean annual precipitation data refer to standardized data set for 2010. Compared values are in table 2.

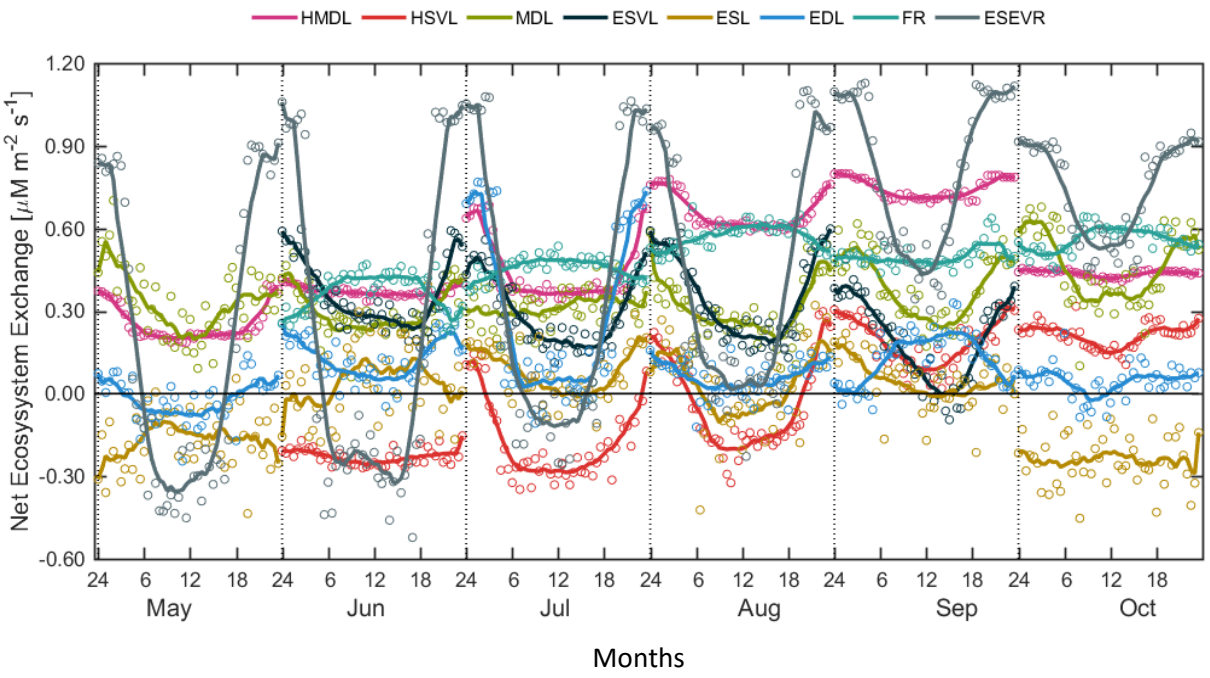

Figure 4.4 Mean diurnal course of net ecosystem exchange in eight representative for dataset water bodies during an open water season. Line represents 6-hour moving average. Site labels indicate: HMDL – humic meromictic deep lake (L. Valkea-Kotinen); HSVL – humic shallow with submerged vegetation lake (L. Villasjön); MDL – mesotrophic deep lake (L. Douglas); ESVL – eutrophic shallow lake with submerged vegetation (L. Tamnaren); ESL – eutrophic shallow lake (L. Erie, shallow western basin); EDL – eutrophic deep lake (L. Mendota); FR – flushing reservoir (R. Estmain); ESEVR – eutrophic shallow reservoir with emergent vegetation (R. Zarnekow)

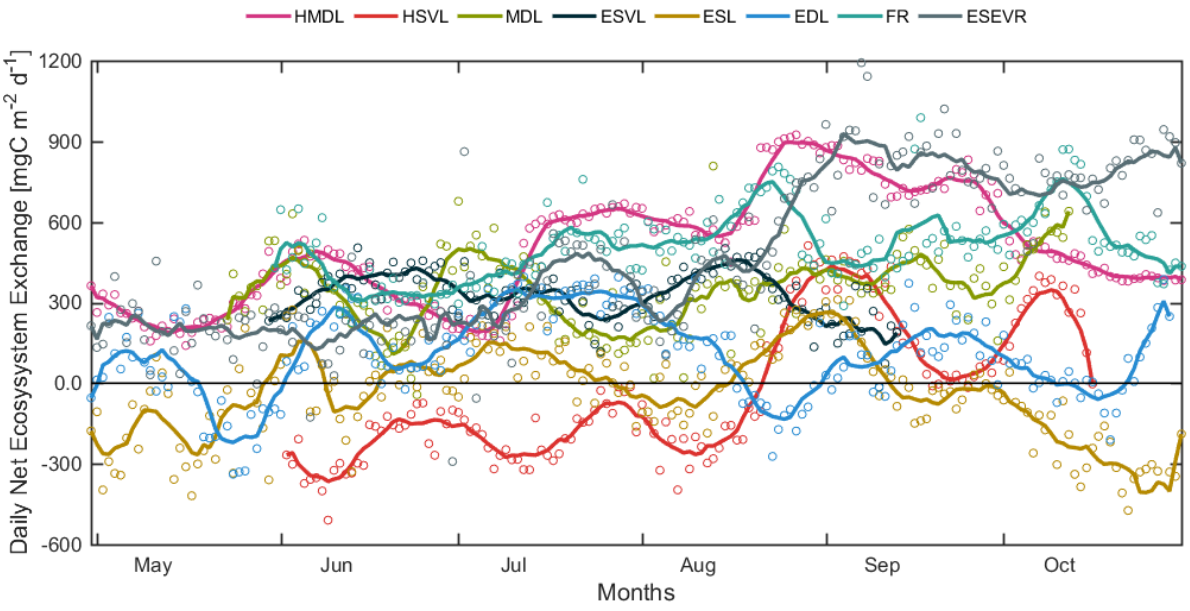

Figure 4.5 Seasonal patterns of net ecosystem exchange in eight water bodies presented in fig. 4.4. Line represent 10-day moving average. Site labels indicate: HMDL – humic meromictic deep lake (L. Valkea-Kotinen); HSVL – humic shallow with submerged vegetation lake (L. Villasjön); MDL – mesotrophic deep lake (L. Douglas); ESVL – eutrophic shallow lake with submerged vegetation (L. Tamnaren); ESL – eutrophic shallow lake (L. Erie, shallow western basin); EDL – eutrophic deep lake (L. Mendota); FR – flushing reservoir (R. Estmain); ESEVR – eutrophic shallow reservoir with emergent vegetation (R. Zarnekow)

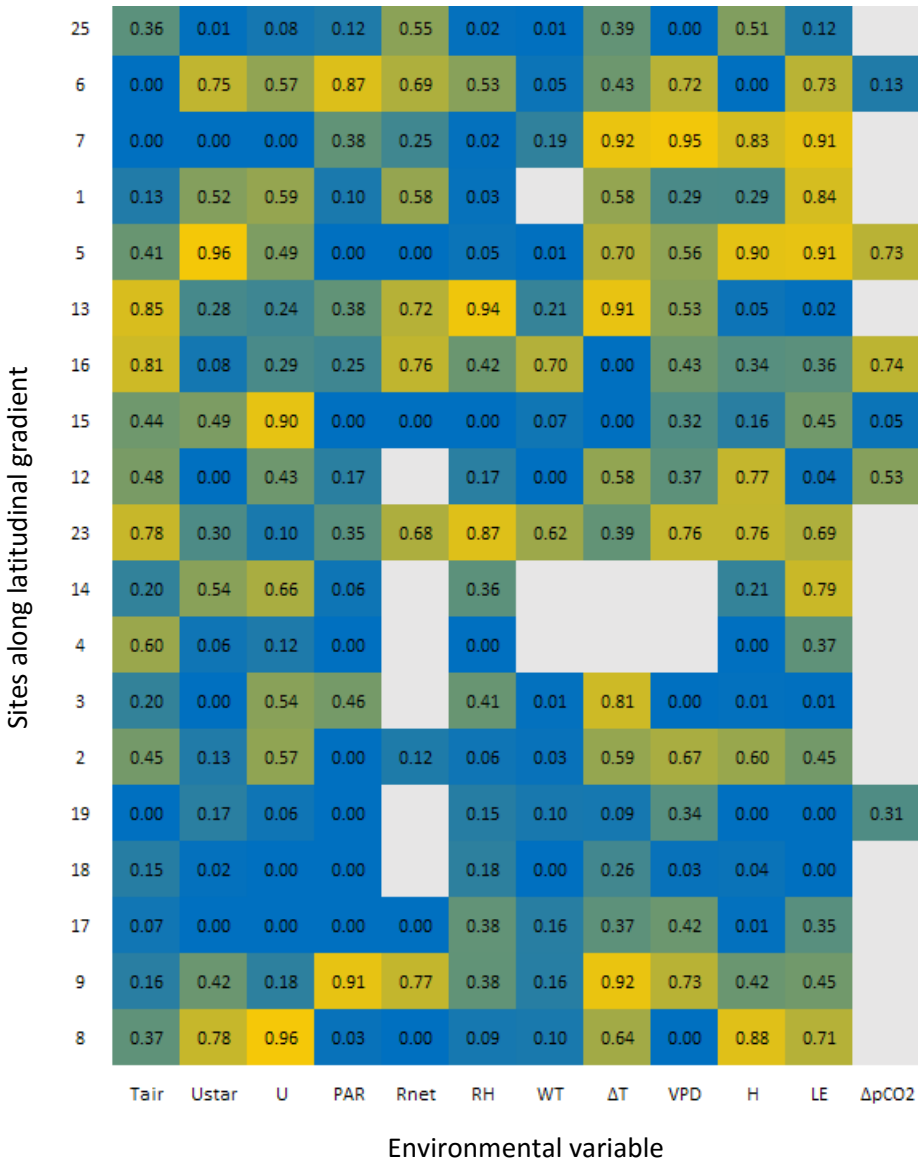

Figure 4.6 Coefficients of determination (r^2) of NEE with binned environmental drivers for each site. Sites were ordered according to latitude, from Artic (top) to subtropical (bottom) climatic zones. Site identification numbers are in Table 1. Gradient of colors from blue (no correlation) to yellow (perfect correlation) indicates increasing r^2 values from 0-1.

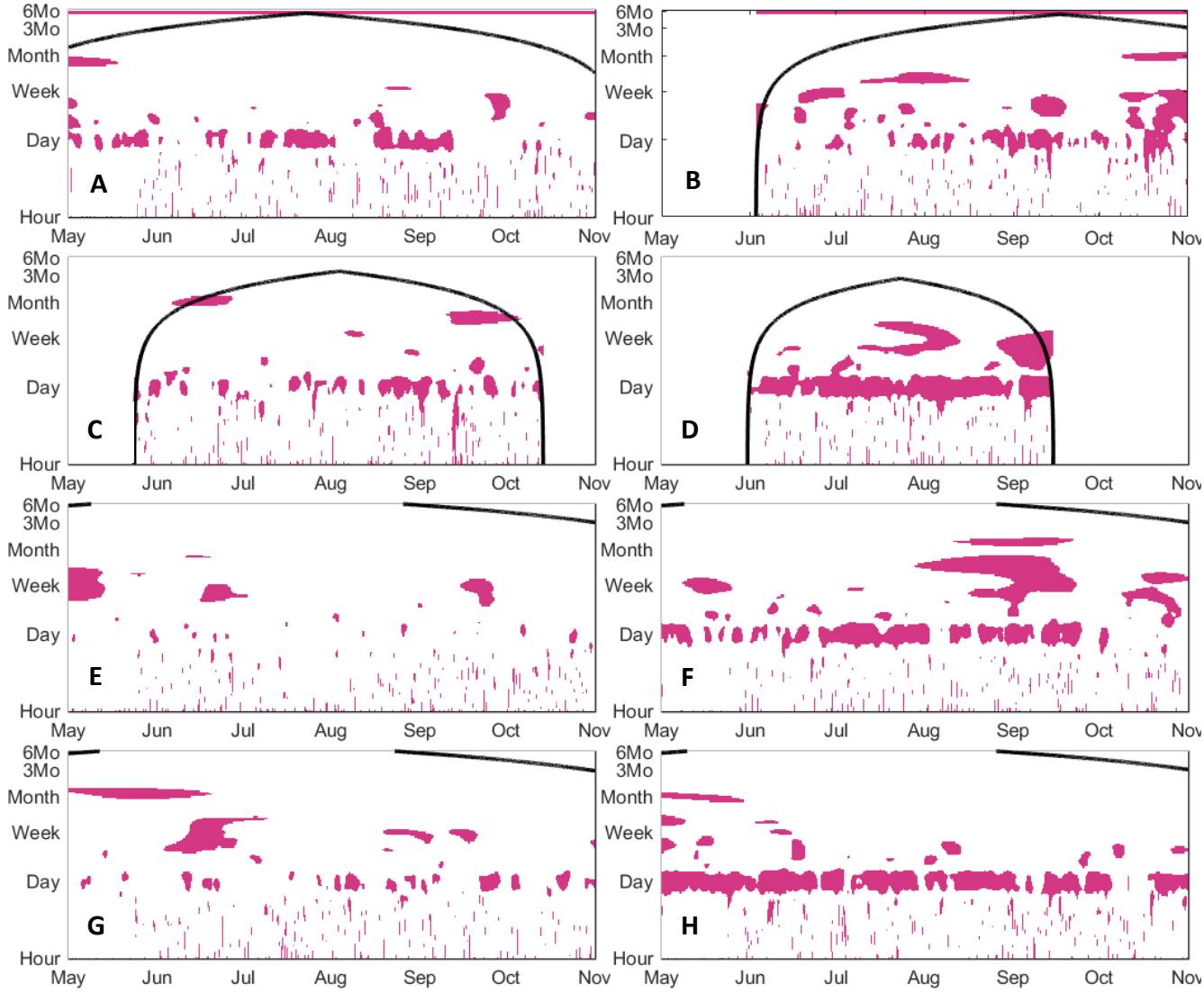

Figure 4.7 Multi-temporal wavelet coherence of Tair and ecosystem NEE during an open water season. Region outside of cone of influence indicates insignificant relationship. Site labels indicate: (A) humic meromictic deep lake (L. Valkea-Kotinen); (B) humic shallow with submerged vegetation lake (L. Villasjön); (C) mesotrophic deep lake (L. Douglas); (D) eutrophic shallow lake with submerged vegetation (L. Tamnaren); (E) eutrophic shallow lake (L. Erie, shallow western basin); (F) eutrophic deep lake (L. Mendota); (G) flushing reservoir (R. Estmain); (H) eutrophic shallow reservoir with emergent vegetation (R. Zarnekow)

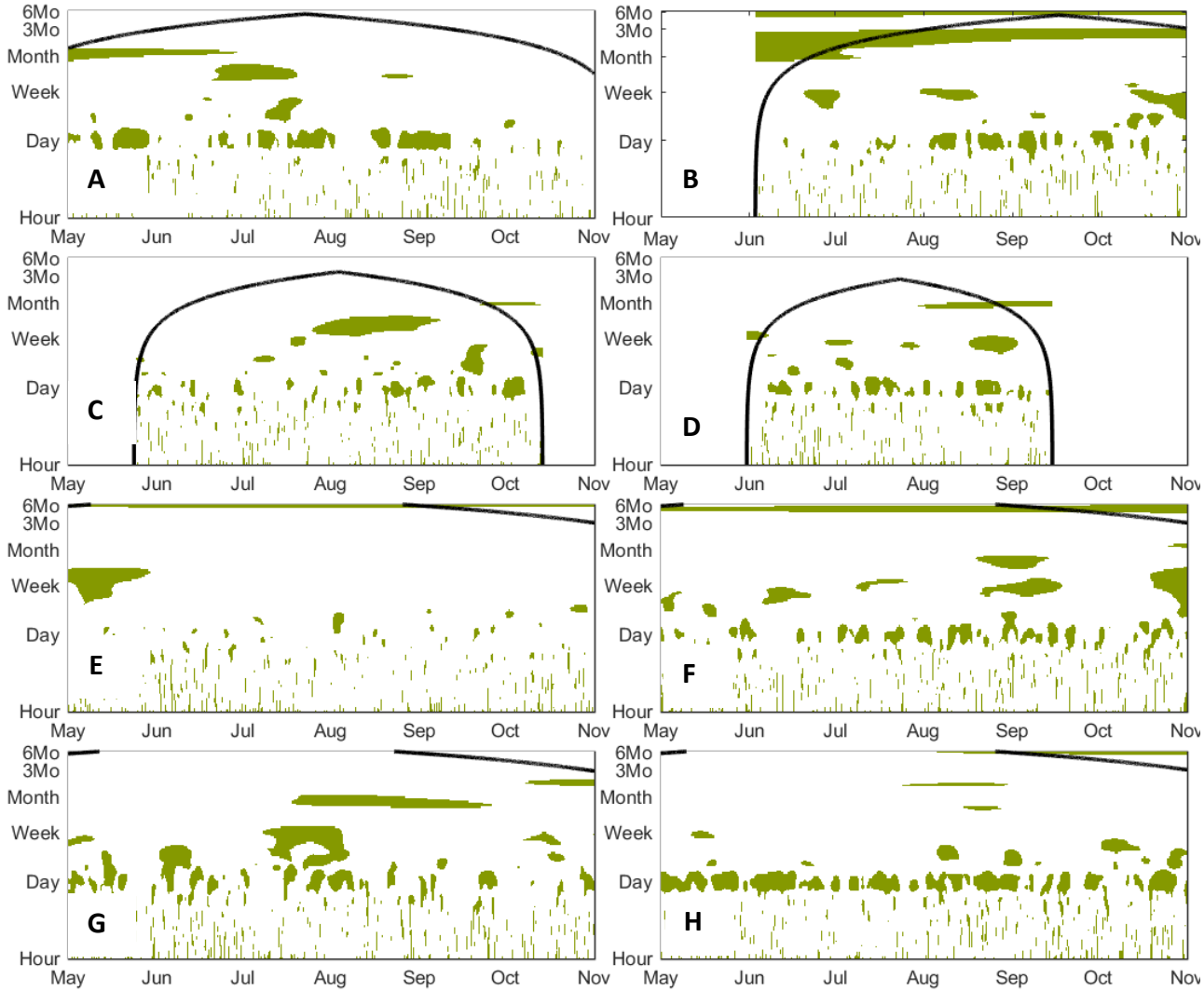

Figure 4.7 continued. Multi-temporal wavelet coherence of friction velocity and ecosystem NEE during an open water season. Region outside of coin of influence indicates insignificant relationship. Site labels indicate: (A) humic meromictic deep lake (L. Valkea-Kotinen); (B) humic shallow with submerged vegetation lake (L. Villasjön); (C) mesotrophic deep lake (L. Douglas); (D) eutrophic shallow lake with submerged vegetation (L. Tamnaren); (E) eutrophic shallow lake (L. Erie, shallow western basin); (F) eutrophic deep lake (L. Mendota); (G) flushing reservoir (R. Estmain); (H) eutrophic shallow reservoir with emergent vegetation (R. Zarnekow)

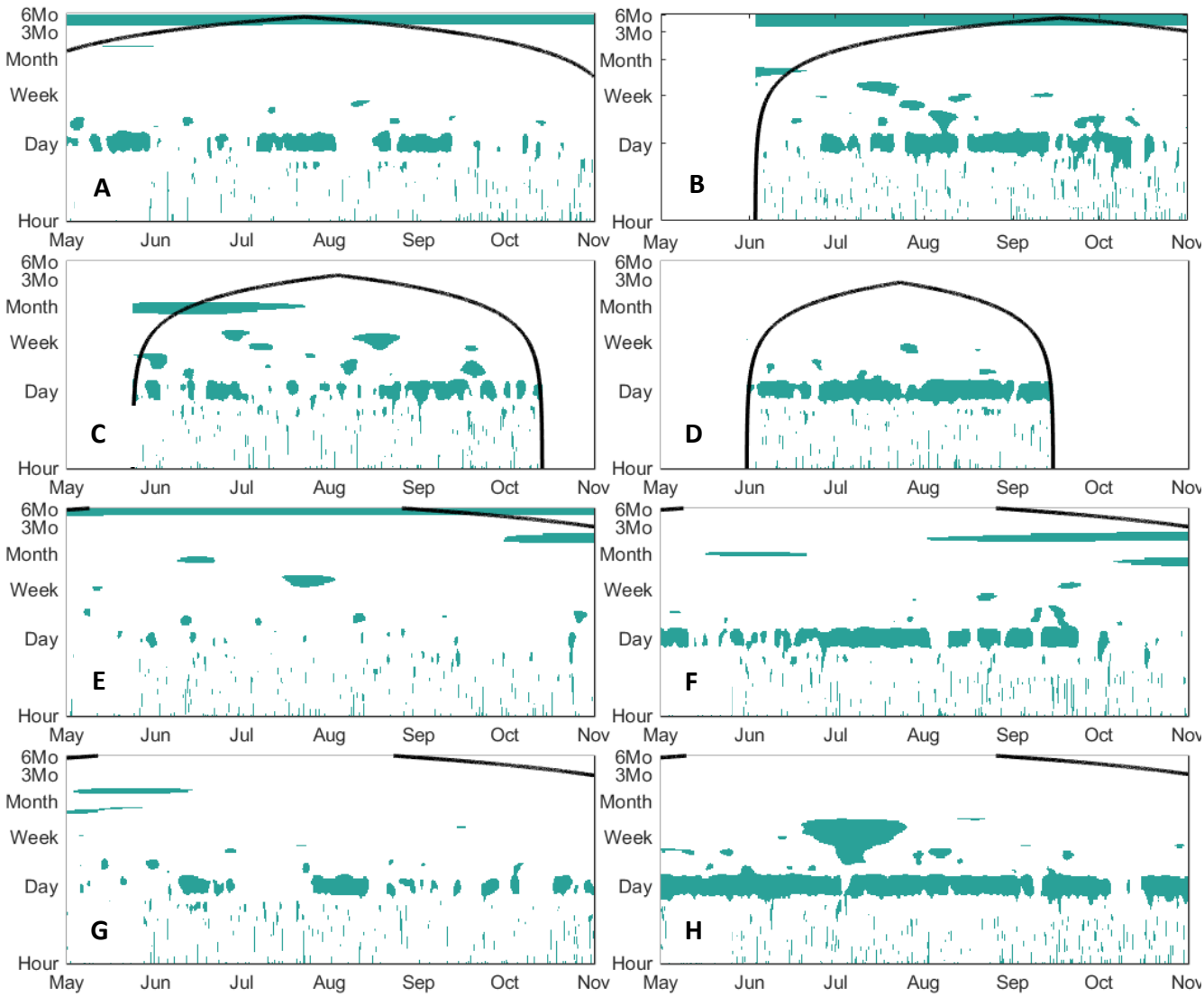

Figure 4.7 continued. Multi-temporal wavelet coherence of photosynthetically active radiation and ecosystem NEE during an open water season. Region outside of coin of influence indicates insignificant relationship. Site labels indicate: (A) humic meromictic deep lake (L. Valkea-Kotinen); (B) humic shallow with submerged vegetation lake (L. Villasjön); (C) mesotrophic deep lake (L. Douglas); (D) eutrophic shallow lake with submerged vegetation (L. Tamnaren); (E) eutrophic shallow lake (L. Erie, shallow western basin); (F) eutrophic deep lake (L. Mendota); (G) flushing reservoir (R. Estmain); (H) eutrophic shallow reservoir with emergent vegetation (R. Zarnekow)

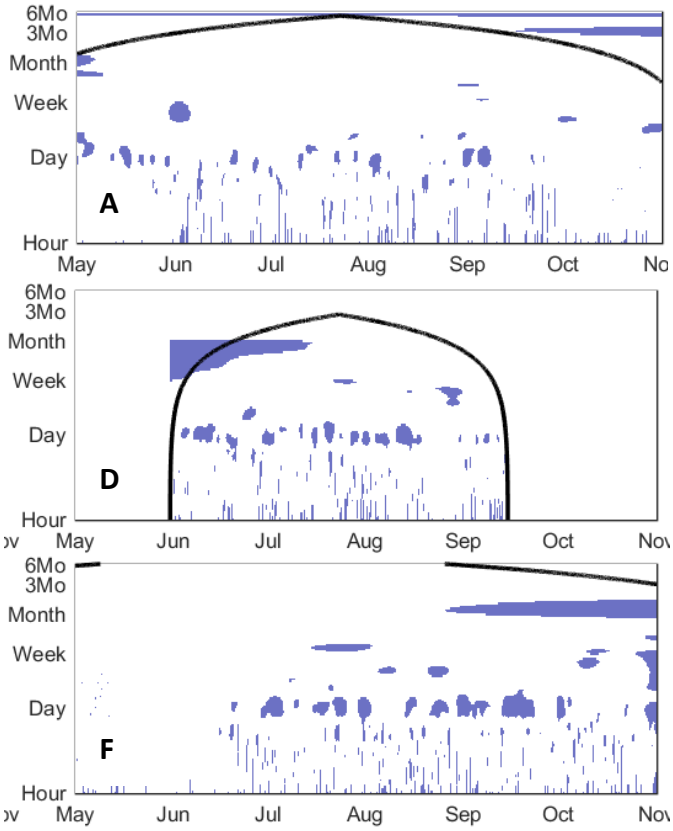

Figure 4.7 continued. Multi-temporal wavelet coherence of ΔpCO_2 and ecosystem NEE during an open water season. Region outside of coin of influence indicates insignificant relationship. Site labels indicate: (A) humic meromictic deep lake (L. Valkea-Kotinen); (D) eutrophic shallow lake with submerged vegetation (L. Tamnaren); (F) eutrophic deep lake (L. Mendota).

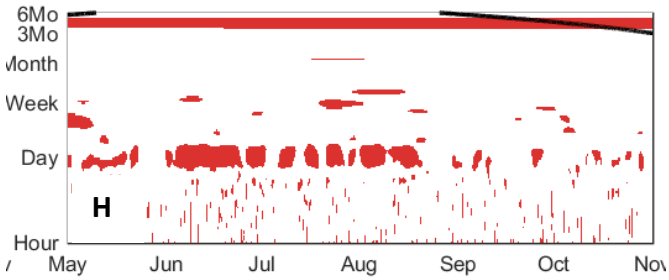

Figure 4.7 continued. Multi-temporal wavelet coherence of water level and ecosystem NEE during an open water season. Region outside of coin of influence indicates insignificant relationship. Site label indicate: (H) eutrophic shallow reservoir with emergent vegetation (R. Zarnekow)

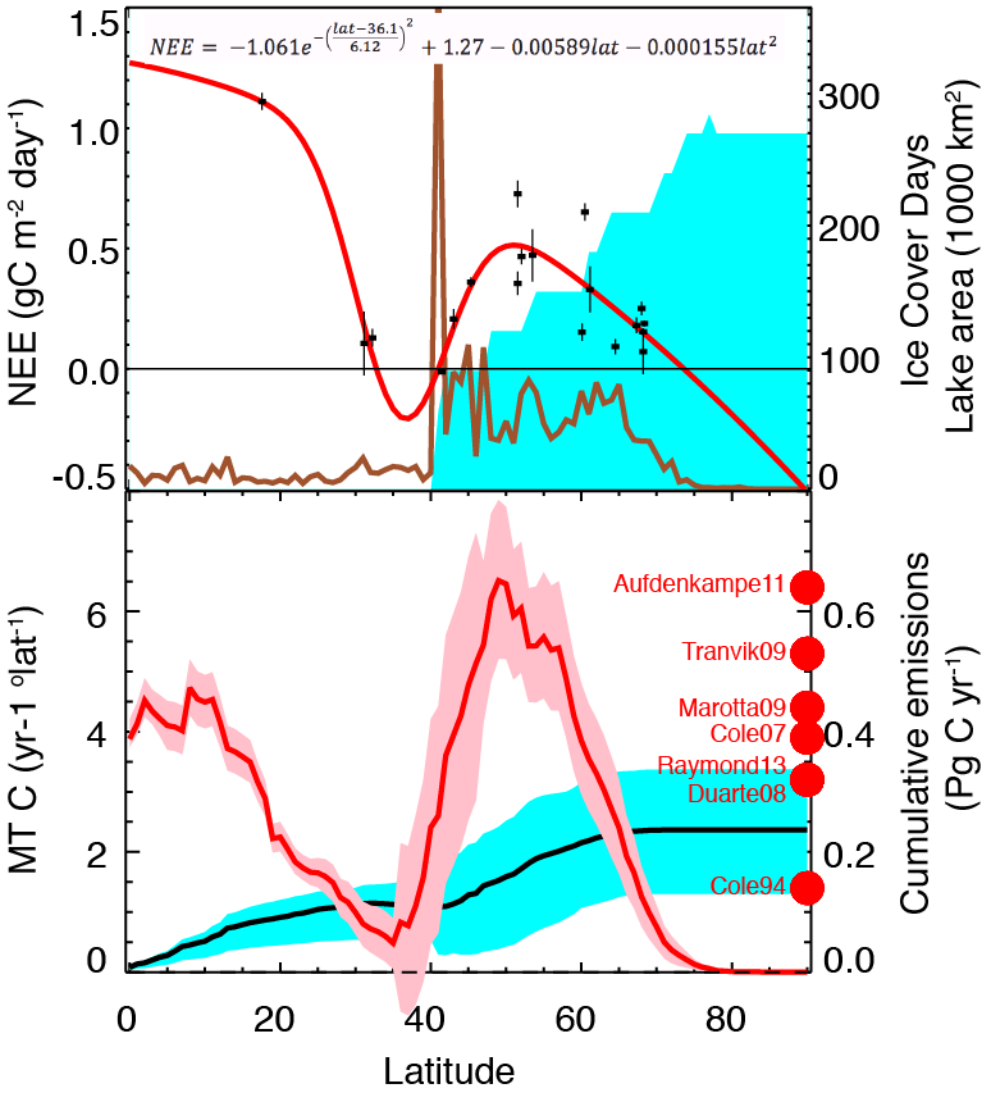

Figure 4.8. Global model of CO_2 emission along latitude (red line), ice-covered days (cyan), and lake surface area (brown, upper panel); Latitudinal contribution of CO_2 efflux (red, bottom panel) and cumulative emissions by latitude (black, bottom panel) with propagation of uncertainty. Red dots indicate previous C estimates.

Table S4.1. Site list with seasonal data coverage and percentage of valid and gap filled fluxes, and uncertainty estimates attributed to gap-filling using artificial neural network. Nighttime fluxes were assigned when shortwave radiation was <10 W m^{-2}.

Site Number	Site Name	Water Body Type	Year	Start Day	End Day	NEE missing observations		Uncertainty	
						Day [%]	Night [%]	R^2 [unitless]	RMSE [µM m^{-2} s^{-2}]
1	Pallasjärvi	Lake	2013	199	293	71	77	0.29	0.21
2	Douglas	Lake	2013	158	261	45	64	0.18	0.45
2	Douglas	Lake	2014	144	286	52	63		
3	IJzendoorn	Reservoir	2012	108	282	80	86	0.14	0.68
4	Maneswaard	Reservoir	2010	140	306	88	88	0.12	0.65
5	Merasjarvi	Lake	2005	167	285	06	08	0.43	0.15
6	Stordalen LH	Lake	2009	171	186	64	80	0.41	0.12
7	Stordalen VL	Lake	2012	154	366	90	89	0.61	0.31
7	Stordalen VL	Lake	2013	001	196	82	88		
8	NamTheun2	Reservoir	2008	136	136	na	na	0.32	0.25
8	NamTheun2	Reservoir	2009	141	149	60	63		
8	NamTheun2	Reservoir	2010	070	081	79	77		
8	NamTheun2	Reservoir	2011	071	074	44	26		
9	Taihu	Lake	2012	136	365	91	97	0.46	0.45
9	Taihu	Lake	2013	001	087	92	98		
12	Tamnaren	Lake	2010	257	306	23	29	0.38	0.23
12	Tamnaren	Lake	2011	070	360	75	77		
12	Tamnaren	Lake	2012	151	257	47	49		
13	Daring	Lake	2006	141	236	86	94	0.48	0.16
14	Eastmain	Reservoir	2008	1	365	87	90	0.51	0.27
14	Eastmain	Reservoir	2009	3	363	88	89		
14	Eastmain	Reservoir	2011	4	362	86	90		

14	Eastmain	Reservoir	2012	2	261	88	88		
15	Kuivajärvi	Lake	2010	226	285	57	62	0.46	0.29
15	Kuivajärvi	Lake	2011	152	304	70	73		
15	Kuivajärvi	Lake	2012	164	332	73	71		
16	Valkea-Kotinen	Lake	2003	117	325	89	91	0.71	0.19
16	Valkea-Kotinen	Lake	2004	109	344	93	95		
16	Valkea-Kotinen	Lake	2005	097	323	94	95		
16	Valkea-Kotinen	Lake	2006	112	365	96	97		
16	Valkea-Kotinen	Lake	2007	093	314	95	96		
16	Valkea-Kotinen	Lake	2008	147	355	n/a	n/a		
16	Valkea-Kotinen	Lake	2009	108	181	n/a	n/a		
17	Ross Barnett	Reservoir	2007	236	348	25	29	0.28	0.40
18	Erie	Lake	2012	002	366	09	11	na[1]	Na
18	Erie	Lake	2013	001	365	12	13		
19	Mendota	Lake	2012	031	366	90	96	0.25	0.73
19	Mendota	Lake	2013	001	365	91	95		
19	Mendota	Lake	2014	001	365	90	96		
19	Mendota	Lake	2015	001	303	89	96		
23	Zarnekow	Reservoir	2013	134	365	70	73	0.50	0.49
23	Zarnekow	Reservoir	2014	1	365	68	69		
23	Zarnekow	Reservoir	2015	1	365	67	70		
25	Toolik	Lake	2012	173	234	17	41	0.47	0.22

[1] NEE gap filled using LUT (Reichstein et al., 2005) adopted to gap-fill eddy fluxes, no uncertainty estimates are available

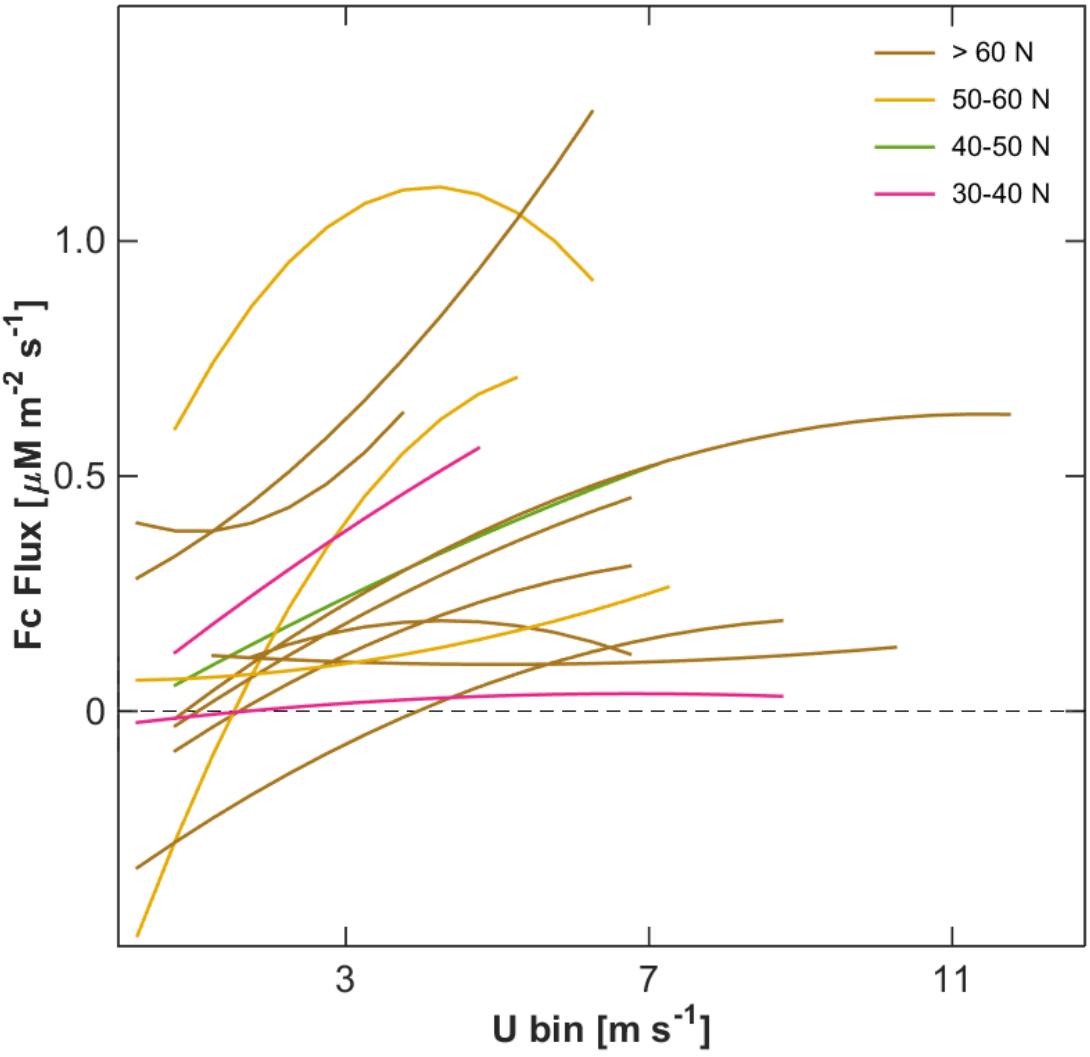

Figure S4.1 Relationship between net ecosystem exchanges of CO_2 with binned wind speed for each site. Colors indicate different sites located along latitudinal 10-degree intervals.

CHAPTER 5

CONCLUSIONS

5.1. *Why temporal variability matters?*

The overarching goal of this dissertation is to address the lack of temporal consideration in air-lake exchanges of CO_2 at time scales ranging from hours to decades. Knowing of the CO_2 fluxes is critical for balancing lake carbon budgets [*Hanson et al.*, 2004; *Bennington et al.*, 2012; *Weyhenmeyer et al.*, 2015] and assessing lake ecosystems roles in the regional and global carbon balances [*Cole et al.*, 2007]. However, current regional and global CO_2 efflux estimates from lakes and reservoirs reflect a statistic view, where fluxes are mainly inferred from point-in-time measurements [*Tranvik et al.*, 2009; *Ciais et al.*, 2013; *Raymond et al.*, 2013]. Consequently, temporal CO_2 flux variability and governing processes remain understudied and predicting future responses of flux to environmental changes is significantly hindered [*Phillips et al.*, 2015; *Hasler et al.*, 2016]. Moreover, understanding processes governing short-term CO_2 flux variability is essential to understanding processes influencing gas exchanges at longer temporal timescales. Including temporal resolution also allows us to establish if the CO_2 flux variability is within the natural ranges of variation or has significantly changed over time [*Magnuson*, 1990]. Uncertainty in CO_2 flux estimation contributes to already uncertain future CO_2 efflux predictions from lakes and reservoirs.

To address knowledge gaps related to uncertainty of CO_2 estimates, limited availability of direct, multi-site and multi-temporal CO_2 observations, and incomplete understanding of factors governing temporal variability in CO_2 flux from lakes and reservoirs, I combined the

analysis of CO_2 fluxes and their drivers at the short time scale (hourly-seasonal) using eddy covariance observations together with longer time scale drivers (seasonal-decadal) using synthesis of long-term lake chemistry observations and application of the traditional boundary layer techniques.

5.2 Key findings for estimating CO_2 in lakes and reservoirs

Chapter 2 evaluated uncertainties attributed to pCO_2 estimation using carbonate equilibria. The results show that systematic errors dominate random errors in pCO_2 calculations, and given all sources of error, the historical observations of carbon system parameters are unlikely to provide robust estimates of mean or temporal trends in pCO_2. These findings are troubling, as carbonate equilibria to date are the most commonly used method of estimating CO_2 flux from freshwater systems and assessing the role of aquatic ecosystems in regional and global carbon balances. We argue that direct measurements are the appropriate way to constrain CO_2 evasion estimates from heterogenous freshwater systems.

Chapter 3 explored ice feedbacks on interannual pCO_2 variability in seven lakes in northern Wisconsin. We find that although declining ice cover significantly increases epilimnetic and hypolimnetic water temperature, these increases do not correspond to temperature-mediated pCO_2 increases. Ice duration and length of thermal stratification prove to be poor indicators of springtime and fall pCO_2 because of biogeochemically dynamic waters below ice (winter) and thermocline (summer). We also demonstrate that even extreme warming events remain undetected when pCO_2 is estimated from pH-based carbonate equilibria. Our results imply an interplay of biotic and abiotic factors affecting pCO_2 variability and therefore should be considered together. Moreover, we are rather unlikely to detect pCO_2 variability and change in

response to climate warming. These results add additional sources of uncertainty to reported in Chapter 2 to already overall high uncertainty CO_2 fluxes.

Chapter 4 attempts to rectify the issue of lack of continuous, direct CO_2 measurements in freshwater systems by synthesizing published and unpublished eddy covariance flux observations from 19 globally distributed lakes and reservoirs. Advances in eddy covariance technique improves our temporal sampling capability of freshwater ecosystems. In contrast to terrestrial ecosystems, we find higher variability of temporal patterns of CO_2 flux and a lack of relationship with latitudinal gradients of annual means of precipitation and temperature. Lake CO_2 fluxes show consistent dependencies with temperature, solar radiation, and wind speed, however ecosystem level CO_2 responses are regulated by lake littoral and pelagic productivity, color, and presence/absence of thermal stratification. All representative lakes showed surprisingly coherent CO_2 flux oscillations in sub-monthly time scales. When we up-scaled CO_2 flux, despite including diurnal cycle, high springtime/fall CO_2 emissions, and uncertainty of flux towers, we find that current global CO_2 fluxes derived from carbonate equilibria are in comparison overestimated by 40%. Therefore, the lake and reservoir CO_2 contribution to global balance balances will require continual refinement as more high temporal and low uncertainty observations are added to the database.

Chapters 2-4 focused on key aspects of our question on drivers and uncertainties in temporal variability in lake CO_2 cycle, with a focus on lake-atmosphere exchanges. The work together showed the role of systematic and random errors (Chapter 2), theoretical assumptions combined with methodological limitations (Chapter 3), and sampling uncertainty and high temporal variability (Chapter 4), all of which highlight the overall limited understanding of controls over CO_2 exchanges in freshwater systems. It was striking how existing indirect

(carbonate) and direct (eddy fluxes) are prone to diverse sources of errors, and how often these are ignored in flux estimation. Comparing eddy fluxes from waterbodies representing different trophic states, morphometric, and climatic conditions showed that NEE coherently responded to some environmental drivers, despite all ecosystem differences. Probably most surprising finding was overall high contribution of in-lake processes to CO_2 flux dynamics at air-water interfaces compared to forcings affecting in fluxes from atmosphere.

5.3 Implications for understanding the roles of lakes in regional and global carbon cycles

Overall, major contributions of this research were:

1. Conducting a comprehensive analysis of empirical error propagation through three carbonate equilibria and in four chemically heterogenous lake groups. To my knowledge, this is the first random error analysis for freshwaters. The results highlight these sources of error are non-negligible and should be considered in data analysis and results interpretation in the case of estimating pCO_2 from carbonate equilibria.
2. Error analysis coupled with model simulations highlighted overall high uncertainty of long-term pCO_2 trends, low sensitivity pCO_2 to even extreme warming events, and inability to separate temperature from other biogeochemical effects on pCO_2 calculated from carbonate equilibria. All these results imply significantly reduced applicability of using water chemistry data for estimating pCO_2 in freshwaters, despite a wide availability of such data.
3. Highlighting the limited direct and indirect ice effects on understudied interannual variability of pCO_2 in lakes, and the unclear CO_2 flux responses to disappearing ice cover.

4. Expanding eddy flux analysis beyond short-term, single-site analysis over freshwater waterbodies. The NEE comparisons highlight cross-site similarities and dissimilarities of NEE in terms of flux sign and magnitudes and flux sensitivities to environmental drives. Underrepresented ecosystems types are highlighted, potentially providing guidance on selecting tower locations.
5. Providing an open source data product containing 25 eddy flux towers with meteorological and in-lake data for limnologist and micrometeorologists studying various aspects of air-water NEE.

5.4 Future work

My dissertation research showed high uncertainty attributed to CO_2 estimation from carbonate equilibria. Therefore, I would focus future research on direct CO_2 observations and further exploration of eddy flux dataset. The proposed future research themes are highlighted below.

Like any correlative statistical approaches, the wavelet coherence approach did not identify which physical and biological processes drive exchanges of CO_2 at the air-water interface. While I first examined the variables with potential relevance for CO_2 flux in lakes, I found that most micrometeorological variables exhibited high coherence with NEE because of strong diurnal and seasonal cycles attributed to influx of solar radiation. I would remove solar cycles from timescales ranging from diurnal to seasonal and re-run wavelet coherence on anomalies of environmental variables and CO_2 flux to distinguish environmental drivers governing NEE variability from spuriously correlating variables. I would also include the time-lag analysis as lagged responses to drivers in aquatic systems are likely as indicated in Chapter 4.

The wavelet-based analysis mentioned above does not consider multiple drivers affecting CO_2 fluxes. I would couple the wavelet analysis with an information theory approach described by [*Sturtevant et al.*, 2015] to quantify drivers' contribution to CO_2 flux variability at multiple time scales. To my knowledge, such approach has never been applied to freshwater systems.

In Chapter 4, I show consistent seasonal patterns of net ecosystem exchanges across all lakes with regular oscillations over the entire open water season. I hypothesized that these oscillations were related to trophic cascades and/or internal waves affecting metabolic balances and CO_2 fluxes. To test these hypotheses, I would use high resolution lake temperature profiles to calculate stratification indices and waterside shear/convection, and in-water dissolved oxygen and carbon dioxide data to calculate metabolic balances (and differences between these two methods). I would also attempt to partition NEE into its components, gross primary production and ecosystem respiration to gain insight regarding biological controls over temporal NEE variability. Several sites in eddy flux dataset contain such information.

Finally, as I showed in Charter 3 and 4, the modeling approach is necessary to improve our mechanistic understanding of processes governing CO_2 flux variability. General lake and community land models rarely include biogeochemical modules for inorganic carbon cycle and were not tested on small lakes. I would use eddy fluxes to evaluate either of these models and verify mechanistic processes underlying and/or how lakes ecosystems affect and are affected by climate.

REFERENCES

Åberg, J., and M. B. Wallin (2014), Evaluating a fast headspace method for measuring DIC and subsequent calculation of pCO_2 in freshwater systems, *Inl. Waters*, *4*, 157–166, doi:10.5268/IW-4.2.694.

Åberg, J., M. Jansson, and A. Jonsson (2010), Importance of water temperature and thermal stratification dynamics for temporal variation of surface water CO_2 in a boreal lake, *J. Geophys. Res.*, *115*(G2), G02024, doi:10.1029/2009JG001085.

Abril, G. et al. (2015), Technical note: Large overestimation of pCO_2 calculated from pH and alkalinity in acidic, organic-rich freshwaters, *Biogeosciences*, *12*(1), 67–78, doi:10.5194/bg-12-67-2015.

Algesten, G., S. Sobek, A. K. Bergstroom, A. Jonsson, L. J. Tranvik, and M. Jansson (2005), Contribution of sediment respiration to summer CO_2 emission from low productive boreal and subarctic lakes, *Microb. Ecol.*, *50*(4), 529–535, doi:10.1007/s00248-005-5007-x.

Alin, S. R., and T. C. Johnson (2007), Carbon cycling in large lakes of the world: A synthesis of production, burial, and lake-atmosphere exchange estimates, *Global Biogeochem. Cycles*, *21*(3), n/a-n/a, doi:10.1029/2006GB002881.

Allan, J. D. et al. (2015), Using cultural ecosystem services to inform restoration priorities in the Laurentian Great Lakes, *Front. Ecol. Environ.*, *13*(8), 418–424, doi:10.1890/140328.

Anderson, D. E., R. G. Striegl, D. I. Stannard, C. M. Michmerhuizen, T. A. McConnaughey, and J. W. LaBaugh (1999), Estimating lake-atmosphere CO_2 exchange, *Limnol. Oceanogr.*, *44*(4), 988–1001.

Andrews, A. E. et al. (2014), CO_2, CO, and CH_4 measurements from tall towers in the NOAA earth system research laboratory's global greenhouse gas reference network: Instrumentation, uncertainty analysis, and recommendations for future high-accuracy greenhouse gas monitoring efforts, *Atmos. Meas. Tech.*, *7*(2), 647–687, doi:10.5194/amt-7-647-2014.

Atilla, N., G. A. McKinley, V. Bennington, M. Baehr, N. Urban, M. DeGrandpre, A. R. Desai, and C. Wu (2011), Observed variability of Lake Superior pCO_2, *Limnol. Oceanogr.*, *56*(3), 775–786, doi:10.4319/lo.2011.56.3.0775.

Attermeyer, K., S. Flury, R. Jayakumar, P. Fiener, K. Steger, V. Arya, F. Wilken, R. van Geldern, and K. Premke (2016), Invasive floating macrophytes reduce greenhouse gas emissions from

a small tropical lake, *Sci. Rep.*, *6*(August 2015), 20424, doi:10.1038/srep20424.

Attig, J. W. (1985), *Pleistocene geology of Vilas County.*, Wisconsin Geological and Natural History Survey, Information Circular 50, Madison, WI.

Aubinet, M. (2008), Eddy Covariance CO_2 flux measurement in nocturnal conditions: an an analysis of the problem, *Ecol. Appl.*, *18*(6), 1368–1378, doi:10.1890/06-1336.1.

Aubinet, M., T. Vesala, and D. Papale (2012), *Eddy Covariance: A Practical Guide toMeasurement and Data Analysis*, Springer.

Aufdenkampe, A. K., E. Mayorga, P. A. Raymond, J. M. Melack, S. C. Doney, S. R. Alin, R. E. Aalto, and K. Yoo (2011), Riverine coupling of biogeochemical cycles between land, oceans, and atmosphere, *Front. Ecol. Environ.*, *9*(1), 53–60, doi:10.1890/100014.

Austin, J. A., and S. M. Colman (2007), Lake Superior summer water temperatures are increasing more rapidly than regional temperatures: A positive ice-albedo feedback, *Geophys. Res. Lett.*, *34*(6), 1–5, doi:10.1029/2006GL029021.

Baehr, M. M., and M. D. DeGrandpre (2002), Under-ice CO_2 and O_2 variability in a freshwater lake, *Biogeochemistry*, *61*(1), 95–133, doi:10.1023/A:1020265315833.

Baehr, M. M., and M. D. DeGrandpre (2004), In situ pCO_2 and O_2 measurements in a lake during turnover and stratification: Observations and modeling, *Limnol. Oceanogr.*, *49*(2), 330–340, doi:10.4319/lo.2004.49.2.0330.

Baldocchi, D. (2014), Measuring fluxes of trace gases and energy between ecosystems and the atmosphere - the state and future of the eddy covariance method, *Glob. Chang. Biol.*, *20*(12), 3600–3609, doi:10.1111/gcb.12649.

Baldocchi, D., D. Baldocchi, R. Valentini, R. Valentini, S. Running, S. Running, W. Oechel, W. Oechel, R. Dahlman, and R. Dahlman (1996), Strategies for measuring and modelling carbon dioxide and water vapour fluxes over terrestrial ecosystems, *Glob. Chang. Biol.*, *2*(June 1995), 159–68, doi:10.1111/j.1365-2486.1996.tb00069.x.

Balmer, M. B., and J. a Downing (2011), Carbon dioxide concentrations in eutrophic lakes : undersaturation implies atmospheric uptake, *Inl. Waters*, (1), 125–132, doi:10.5268/IW-1.2.366.

Barros, N., J. J. Cole, L. J. Tranvik, Y. T. Prairie, D. Bastviken, V. L. M. Huszar, P. del Giorgio, and F. Roland (2011), Carbon emission from hydroelectric reservoirs linked to reservoir age and latitude, *Nat. Geosci.*, *4*(9), 593–596, doi:10.1038/ngeo1211.

Battin, T. J., S. Luyssaert, L. a. Kaplan, A. K. Aufdenkampe, A. Richter, and L. J. Tranvik (2009), The boundless carbon cycle, *Nat. Geosci.*, *2*(9), 598–600, doi:10.1038/ngeo618.

Bennett, E. M., G. D. Peterson, and L. J. Gordon (2009), Understanding relationships among multiple ecosystem services, *Ecol. Lett.*, *12*(12), 1394–1404, doi:10.1111/j.1461-0248.2009.01387.x.

Bennington, V., G. A. McKinley, N. R. Urban, and C. P. McDonald (2012), Can spatial heterogeneity explain the perceived imbalance in Lake Superior's carbon budget? A model study, *J. Geophys. Res. Biogeosciences*, *117*(3), 1–20, doi:10.1029/2011JG001895.

Benson, B. J., J. J. Magnuson, O. P. Jensen, V. M. Card, G. Hodgkins, J. Korhonen, D. M. Livingstone, K. M. Stewart, G. A. Weyhenmeyer, and N. G. Granin (2012), Extreme events, trends, and variability in Northern Hemisphere lake-ice phenology (1855-2005), *Clim. Change*, *112*(2), 299–323, doi:10.1007/s10584-011-0212-8.

Bevington, P., and D. K. Robinson (2002), *Data Reduction and Error Analysis for the Physical Sciences*, 3rd ed., McGraw-Hill Education, New York, NY.

Blanken, P. D., C. Spence, N. Hedstrom, and J. D. Lenters (2011), Evaporation from Lake Superior: 1. Physical controls and processes, *J. Great Lakes Res.*, *37*(4), 707–716, doi:10.1016/j.jglr.2011.08.009.

Blenckner, T. (2005), A conceptual model of climate-related effects on lake ecosystems, *Hydrobiologia*, *533*(1–3), 1–14, doi:10.1007/s10750-004-1463-4.

Bogard, M. J., and P. A. del Giorgio (2016), The role of metabolism in modulating CO_2 fluxes in boreal lakes, *Global Biogeochem. Cycles*, doi:10.1002/2016GB005463.

Brezonik, P. L., and W. A. Arnold (2011), *Water Chemistry An Introduction to the Chemistry of Natural and Engineered Aquatic Systems*.

Buffam, I., M. G. Turner, A. R. Desai, P. C. Hanson, J. A. Rusak, N. R. Lottig, E. H. Stanley, and S. R. Carpenter (2010), Integrating aquatic and terrestrial components to construct a complete carbon budget for a north temperate lake district, *Glob. Chang. Biol.*, *17*(2), 1193–1211, doi:10.1111/j.1365-2486.2010.02313.x.

Butman, D., and P. a. Raymond (2011), Significant efflux of carbon dioxide from streams and rivers in the United States, *Nat. Geosci.*, *4*(12), 839–842, doi:10.1038/ngeo1294.

Carpenter, S. R. et al. (2007), Understanding Regional Change: A Comparison of Two Lake Districts, *Bioscience*, *57*(4), 323–335, doi:10.1641/B570407.

Carpenter, S. S. R., E. H. Stanley, and M. J. Vander Zanden (2011), State of the World's Freshwater Ecosystems: Physical, Chemical, and Biological Changes, *Annu. Rev. Environ. Resour.*, *36*(1), 75–99, doi:10.1146/annurev-environ-021810-094524.

Cazelles, B., M. Chavez, D. Berteaux, F. Manard, J. O. Vik, S. Jenouvrier, and N. C. Stenseth (2008), Wavelet analysis of ecological time series, *Oecologia*, *156*(2), 287–304, doi:10.1007/s00442-008-0993-2.

Chernick, M. R., and R. A. LaBudde (2011), *An Introduction to Bootstrap Methods with Applications to R.*

Christensen, M. R., M. D. Graham, R. D. Vinebrooke, D. L. Findlay, M. J. Paterson, and M. A. Turner (2006), Multiple anthropogenic stressors cause ecological surprises in boreal lakes, *Glob. Chang. Biol.*, *12*(12), 2316–2322, doi:10.1111/j.1365-2486.2006.01257.x.

Ciais, P. et al. (2013), Carbon and Other Biogeochemical Cycles, *Clim. Chang. 2013 - Phys. Sci. Basis*, 465–570, doi:10.1017/CBO9781107415324.015.

Clayton, L., and J. W. Attig (1997), *Pleistocene Geology of Dane County , Wisconsin*, Wisconsin Geological and Natural History Survey, Bulletin 95, Madison, WI.

Cole, J. J., and N. F. Caraco (1998), Atmospheric exchange of carbon dioxide in a low-wind oligotrophic lake measured by the addition of SF6, *Limnol. Oceanogr.*, *43*(4), 647–656, doi:10.4319/lo.1998.43.4.0647.

Cole, J. J., N. F. Caraco, G. W. Kling, and T. K. Kratz (1994), Carbon dioxide supersaturation in the surface waters of lakes., *Science*, *265*(5178), 1568–1570, doi:10.1126/science.265.5178.1568.

Cole, J. J. et al. (2007), Plumbing the global carbon cycle: Integrating inland waters into the terrestrial carbon budget, *Ecosystems*, *10*(1), 171–184, doi:10.1007/s10021-006-9013-8.

Cole, J. J., D. L. Bade, D. Bastviken, M. L. Pace, and M. Van de Bogert (2010), Multiple approaches to estimating air-water gas exchange in small lakes, *Limnol. Oceanogr. Methods*, *8*, 285–293, doi:10.4319/lom.2010.8.285.

Coloso, J. J., J. J. Cole, and M. L. Pace (2011), Difficulty in Discerning Drivers of Lake Ecosystem Metabolism with High-Frequency Data, *Ecosystems*, *14*(6), 935–948, doi:10.1007/s10021-011-9455-5.

Cueva, A., M. Bahn, M. Litvak, J. Pumpanen, and R. Vargas (2015), A multisite analysis of temporal random errors in soil CO_2 efflux, *J. Geophys. Res. Biogeosciences*, n/a-n/a,

doi:10.1002/2014JG002690.

Demars, B. O. L., G. M. Gíslason, J. S. Ólafsson, J. R. Manson, N. Friberg, J. M. Hood, J. J. D. Thompson, and T. E. Freitag (2016), Impact of warming on CO_2 emissions from streams countered by aquatic photosynthesis, *Nat. Geosci.*, *9*(September), doi:10.1038/ngeo2807.

Demarty, M., J. Bastien, and a. Tremblay (2010), Annual follow-up of carbon dioxide and methane diffusive emissions from two boreal reservoirs and nearby lakes in Québec, Canada, *Biogeosciences Discuss.*, *7*, 5429–5461, doi:10.5194/bgd-7-5429-2010.

Demarty, M., J. Bastien, and A. Tremblay (2011), Annual follow-up of gross diffusive carbon dioxide and methane emissions from a boreal reservoir and two nearby lakes in Quebec, Canada, *Biogeosciences*, *8*(1), 41–53, doi:10.5194/bg-8-41-2011.

Denfeld, B. A., P. Kortelainen, M. Rantakari, S. Sobek, and G. A. Weyhenmeyer (2015), Regional Variability and Drivers of Below Ice CO_2 in Boreal and Subarctic Lakes, *Ecosystems*, (August), doi:10.1007/s10021-015-9944-z.

Dickson, A.G., Sabine, C.L., Christian, J. R. (2007), *Guide to best practices for ocean CO_2 measurements*, PICES Special Publication 3.

Dickson, A. A. G., and C. Goyet (1994), Handbook of methods for the analysis of the various parameters of the carbon dioxide system in sea water, , *1994*(September), 22, doi:ORNL/CDIAC-74.

Dickson, A. G., and J. P. Riley (1978), The effect of analytical error on the evaluation of the components of the aquatic carbon-dioxide system, *Mar. Chem.*, *6*(1), 77–85, doi:10.1016/0304-4203(78)90008-7.

Downing, J. a., Y. T. Prairie, J. J. Cole, C. M. Duarte, L. J. Tranvik, R. G. Striegl, W. H. McDowell, P. Kortelainen, N. F. Caraco, and J. M. Melack (2006), The global abundance and size distribution of lakes, ponds, and impoundments, *Limnol. Oceanogr.*, *51*(5), 2388–2397, doi:10.4319/lo.2006.51.5.2388.

Duarte, C. M., Y. T. Prairie, C. Montes, J. J. Cole, R. Striegl, J. Melack, and J. A. Downing (2008), CO_2 emissions from saline lakes: A global estimate of a surprisingly large flux, *J. Geophys. Res. Biogeosciences*, *113*(4), 1–7, doi:10.1029/2007JG000637.

Dubois, K., R. Carignan, and J. Veizer (2009), Can pelagic net heterotrophy account for carbon fluxes from eastern Canadian lakes?, *Appl. Geochemistry*, *24*(5), 988–998, doi:10.1016/j.apgeochem.2009.03.001.

Ducharme-Riel, V., D. Vachon, P. A. Del Giorgio, and Y. T. Prairie (2015), The Relative Contribution of Winter Under-Ice and Summer Hypolimnetic CO_2 Accumulation to the Annual CO_2 Emissions from Northern Lakes, *Ecosystems*, *2*, 547–559, doi:10.1007/s10021-015-9846-0.

Eugster, W., G. Kling, T. Jonas, J. P. McFadden, A. Wuest, S. MacIntyre, and F. S. Chapin (2003), CO_2 exchange between air and water in an Arctic Alaskan and midlatitude Swiss lake: Importance of convective mixing, *J. Geophys. Res.*, *108*(D12), 20, doi:4362 10.1029/2002jd002653.

Evans, C. D., P. J. Chapman, J. M. Clark, D. T. Monteith, and M. S. Cresser (2006), Alternative explanations for rising dissolved organic carbon export from organic soils, *Glob. Chang. Biol.*, *12*(11), 2044–2053, doi:10.1111/j.1365-2486.2006.01241.x.

Evans, M. A., S. MacIntyre, and G. W. Kling (2008), Internal wave effects on photosynthesis: Experiments, theory, and modeling, *Limnol. Oceanogr.*, *53*(1), 339–353, doi:10.4319/lo.2008.53.1.0339.

Fee, E. J., R. E. Hecky, S. E. M. Kasian, and D. R. Cruikshank (1996), Physical and chemical responses of lakes and streams, *Limnol. Oceanogr.*, *41*(5), 912–920, doi:10.4319/lo.1996.41.5.0912.

Finlay, K., R. J. Vogt, M. J. Bogard, B. Wissel, B. M. Tutolo, G. L. Simpson, and P. R. Leavitt (2015), Decrease in CO_2 efflux from northern hardwater lakes with increasing atmospheric warming., *Nature*, *519*(7542), 215–8, doi:10.1038/nature14172.

Franz, D., F. Koebsch, E. Larmanou, J. Augustin, and T. Sachs (2016), High net CO_2 and CH_4 release at a eutrophic shallow lake on a formerly drained fen, , 3051–3070, doi:10.5194/bg-13-3051-2016.

French, C. R., J. J. Carr, E. M. Dougherty, L. A. . K. Eidson, J. C. Reynolds, and M. D. DeGrandpre (2002), Spectrophotometric pH measurements of freshwater, *Anal. Chim. Acta*, *453*(1), 13–20, doi:10.1016/S0003-2670(01)01509-4.

Gaeta, J. W., J. S. Read, J. F. Kitchell, and S. R. Carpenter (2012), Eradication via destratification: Whole-lake mixing to selectively remove rainbow smelt, a cold-water invasive species, *Ecol. Appl.*, *22*(3), 817–827, doi:10.1890/11-1227.1.

Galfalk, M., D. Bastviken, S. Fredriksson, and L. Arneborg (2013), Determination of the piston velocity for water-air interfaces using flux chambers, acoustic Doppler velocimetry, and IR

imaging of the water surface, *J. Geophys. Res. Biogeosciences*, *118*(2), 770–782, doi:10.1002/jgrg.20064.

Gelbrecht, J., M. Fait, M. Dittrich, and C. Steinberg (1998), Use of GC and equilibrium calculations of CO_2 saturation index to indicate whether freshwater bodies in north-eastern Germany are net sources or sinks for atmospheric CO_2, *Fresenius. J. Anal. Chem.*, *361*(1), 47–53, doi:10.1007/s002160050832.

del Giorgio, P. a., J. J. Cole, and A. Cimbleris (1997), Respiration rates in bacteria exceed phytoplankton production in unproductive aquatic systems, *Nature*, *385*(6612), 148–151, doi:10.1038/385148a0.

Grinsted, A., J. C. Moore, and S. Jevrejeva (2004), Application of the cross wavelet transform and wavelet coherence to geophysical time series, *Nonlinear Process. Geophys.*, *11*(5/6), 561–566, doi:10.5194/npg-11-561-2004.

Guérin, F., G. Abril, D. Serça, C. Delon, S. Richard, R. Delmas, A. Tremblay, and L. Varfalvy (2007), Gas transfer velocities of CO_2 and CH_4 in a tropical reservoir and its river downstream, *J. Mar. Syst.*, *66*(1–4), 161–172, doi:10.1016/j.jmarsys.2006.03.019.

Hanson, P. C., D. L. Bade, S. R. Carpenter, and T. K. Kratz (2003), Lake metabolism: Relationships with dissolved organic carbon and phosphorus, *Limnol. Oceanogr.*, *48*(3), 1112–1119, doi:10.4319/lo.2003.48.3.1112.

Hanson, P. C., A. I. Pollard, D. L. Bade, K. Predick, S. R. Carpenter, and J. A. Foley (2004), A model of carbon evasion and sedimentation in temperate lakes, *Glob. Chang. Biol.*, *10*(8), 1285–1298, doi:10.1111/j.1365-2486.2004.00805.x.

Hanson, P. C., S. R. Carpenter, D. E. Armstrong, E. H. Stanley, and T. K. Kratz (2006), Lake Dissolved Inorganic Carbon and Dissolved Oxygen: Changing Drivers From Days To Decades, *Ecol. Monogr.*, *76*(3), 343–363, doi:10.1890/0012-9615(2006)076[0343:LDICAD]2.0.CO;2.

Hasler, C. T., D. Butman, J. D. Jeffrey, and C. D. Suski (2016), Freshwater biota and rising pCO_2, *Ecol. Lett.*, *19*(1), 98–108, doi:10.1111/ele.12549.

Heiskanen, J. J., I. Mammarella, S. Haapanala, J. Pumpanen, T. Vesala, S. Macintyre, and A. Ojala (2014), Effects of cooling and internal wave motions on gas transfer coefficients in a boreal lake, *Tellus, Ser. B Chem. Phys. Meteorol.*, *66*(1), 1–16, doi:10.3402/tellusb.v66.22827.

Herczeg, A. L., and R. H. Hesslein (1984), Determination of hydrogen ion concentration in

softwater lakes using carbon dioxide equilibria, *Geochim. Cosmochim. Acta*, *48*(4), 837–845, doi:10.1016/0016-7037(84)90105-4.

van Heuven, S., Pierrot, D., Rae, J.W.B., Lewis, E., Wallace, D. V. R. (2011), Program Developed for CO_2 System Calculations. ORNL/CDIAC-105b. Carbon Dioxide Information Analysis Center, Oak Ridge National Laboratory, U.S. Department of Energy, Oak Ridge, Tennessee., , doi:10.3334/CDIAC/otg.CO2SYS_MATLAB_v1.1.

Holgerson, M. A. (2015), Drivers of carbon dioxide and methane supersaturation in small, temporary ponds, *Biogeochemistry*, *124*(1–3), 305–318, doi:10.1007/s10533-015-0099-y.

Holgerson, M. A., and P. A. Raymond (2016), Large contribution to inland water CO_2 and CH_4 emissions from very small ponds, *Nat. Geosci.*, *9*(3), 222–226, doi:10.1038/ngeo2654.

Hollinger, D. Y., and A. D. Richardson (2005), Uncertainty in eddy covariance measurements and its application to physiological models., *Tree Physiol.*, *25*(7), 873–85.

Hunt, C. W., J. E. Salisbury, and D. Vandemark (2011), Contribution of non-carbonate anions to total alkalinity and overestimation of pCO_2 in New England and New Brunswick rivers, *Biogeosciences*, *8*(10), 3069–3076, doi:10.5194/bg-8-3069-2011.

Huotari, J., A. Ojala, E. Peltomaa, J. Pumpanen, P. Hari, and T. Vesala (2009), Temporal variations in surface water CO_2 concentration in a boreal humic lake based on high-frequency measurements, *Boreal Environ. Res.*, *14*(SUPPL. A), 48–60.

Huotari, J., A. Ojala, E. Peltomaa, A. Nordbo, S. Launiainen, J. Pumpanen, T. Rasilo, P. Hari, and T. Vesala (2011), Long-term direct CO_2 flux measurements over a boreal lake: Five years of eddy covariance data, *Geophys. Res. Lett.*, *38*(18), n/a-n/a, doi:10.1029/2011GL048753.

Imberger, J. (1985), The diurnal mixed layer, *Limnol. Oceanogr.*, *30*(4), 737–770, doi:10.4319/lo.1985.30.4.0737.

ISO (2010), ISO 21748:2010(en): Guidance for the use of repeatability, reproducibility and trueness estimates in measurement uncertainty estimation, *ISO, Geneva*.

Johnson, M. S., M. F. Billett, K. J. Dinsmore, M. Wallin, K. E. Dyson, and R. S. Jassal (2010), Direct and continuous measurement of dissolved carbon dioxide in freshwater aquatic systems-method and applications, *Ecohydrology*, n/a-n/a, doi:10.1002/eco.95.

Jones, J. B. (2003), Long-term decline in carbon dioxide supersaturation in rivers across the contiguous United States, *Geophys. Res. Lett.*, *30*(10), 0–3, doi:10.1029/2003GL017056.

Jonsson, A., J. Åberg, A. Lindroth, and M. Jansson (2008), Gas transfer rate and CO_2 flux between

an unproductive lake and the atmosphere in northern Sweden, *J. Geophys. Res.*, *113*(G4), G04006, doi:10.1029/2008JG000688.

Karlsson, J., R. Giesler, J. Persson, and E. Lundin (2013), High emission of carbon dioxide and methane during ice thaw in high latitude lakes, *Geophys. Res. Lett.*, *40*(6), 1123–1127, doi:10.1002/grl.50152.

Katul, G. G., D. Li, H. Liu, and S. Assouline (2016), Deviations from unity of the ratio of the turbulent Schmidt to Prandtl numbers in stratified atmospheric flows over water surfaces, *Phys. Rev. Fluids*, *1*(3), 34401, doi:10.1103/PhysRevFluids.1.034401.

Key, R. M., A. Kozyr, C. L. Sabine, K. Lee, R. Wanninkhof, J. L. Bullister, R. A. Feely, F. J. Millero, C. Mordy, and T. H. Peng (2004), A global ocean carbon climatology: Results from Global Data Analysis Project (GLODAP), *Global Biogeochem. Cycles*, *18*(4), n/a-n/a, doi:10.1029/2004GB002247.

Khatiwala, S. et al. (2013), Global ocean storage of anthropogenic carbon, *Biogeosciences*, *10*(4), 2169–2191, doi:10.5194/bg-10-2169-2013.

Kljun, N., P. Calanca, M. W. Rotach, and H. P. Schmid (2015), A simple two-dimensional parameterisation for Flux Footprint Prediction (FFP), *Geosci. Model Dev.*, *8*(11), 3695–3713, doi:10.5194/gmd-8-3695-2015.

Kosten, S., F. Roland, D. M. L. Da Motta Marques, E. H. Van Nes, N. Mazzeo, L. D. S. L. Sternberg, M. Scheffer, and J. J. Cole (2010), Climate-dependent CO_2 emissions from lakes, *Global Biogeochem. Cycles*, *24*(2), 1–7, doi:10.1029/2009GB003618.

Kosten, S., B. O. L. Demars, and B. Moss (2014), Distinguishing autotrophic and heterotrophic respiration based on diel oxygen change curves: Revisiting Dr. Faustus, *Freshw. Biol.*, *59*(3), 649–651, doi:10.1111/fwb.12288.

Kraemer, B. M. et al. (2016), Global patterns in aquatic ecosystem responses to warming based on activation energies, *Glob. Chang. Biol.*, 1–10, doi:10.1111/gcb.13459.

Kratz, T., K. E. Webster, C. Bowser, J. Maguson, B. Benson, and J. J. Magnuson (1997), The influence of landscape position on lakes in northern Wisconsin, *Freshw. Biol.*, *37*(1), 209–217, doi:10.1046/j.1365-2427.1997.00149.x.

Kucharik, C. J., S. P. Serbin, S. Vavrus, E. J. Hopkins, and M. M. Motew (2010), Patterns of Climate Change Across Wisconsin From 1950 to 2006, *Phys. Geogr.*, *31*(1), 1–28, doi:10.2747/0272-3646.31.1.1.

Law, B. E. et al. (2002), Environmental controls over carbon dioxide and water vapor exchange of terrestrial vegetation, *Agric. For. Meteorol.*, *113*, 97–120, doi:10.1016/S0168-1923(02)00104-1.

Lawson, Z. J., M. J. Vander Zanden, C. A. Smith, E. Heald, T. R. Hrabik, S. R. Carpenter, and J. Rosenfeld (2015), Experimental mixing of a north-temperate lake: testing the thermal limits of a cold-water invasive fish, *Can. J. Fish. Aquat. Sci.*, *72*(6), 926–937, doi:10.1139/cjfas-2014-0346.

Lee, X. (1998), On micrometeorological observations of surface-air exchange over tall vegetation, *Agric. For. Meteorol.*, *91*(1), 39–49, doi:10.1016/S0168-1923(98)00071-9.

Lee, X. (2014), The Taihu Eddy Flux Network: an observational program on energy, water and greenhouse gas fluxes of a large freshwater lake, , (April), 1–33, doi:10.1175/BAMS-D-13-00136.1.

Lehner, B., and P. Döll (2004), Development and validation of a global database of lakes, reservoirs and wetlands, *J. Hydrol.*, *296*(1–4), 1–22, doi:10.1016/j.jhydrol.2004.03.028.

Lehner, B. et al. (2011), High-resolution mapping of the world's reservoirs and dams for sustainable river-flow management, *Front. Ecol. Environ.*, *9*(9), 494–502, doi:10.1890/100125.

Liu, H., Q. Zhang, G. G. Katul, J. J. Cole, F. S. Chapin, S. Macintyre, F. S. C. Iii, and S. Macintyre (2016), Large CO_2 effluxes at night and during synoptic weather events significantly contribute to CO_2 emissions from a reservoir, *Environ. Res. Lett.*, *11*(6), 64001, doi:10.1088/1748-9326/11/6/064001.

Lohila, A., J. Tuovinen, J. Hatakka, and M. Aurela (2015), Carbon dioxide and energy fluxes over a northern boreal lake, *Boreal Environ. Res.*, *6095*(August), 474–488.

López Bellido, J., T. Tulonen, P. Kankaala, and A. Ojala (2009), CO_2 and CH_4 fluxes during spring and autumn mixing periods in a boreal lake (Pääjärvi, southern Finland), *J. Geophys. Res. Biogeosciences*, *114*(4), 1–12, doi:10.1029/2009JG000923.

St. Louis, V. L., C. A. KELLY, É. DUCHEMIN, J. W. M. RUDD, and D. M. ROSENBERG (2000), Reservoir Surfaces as Sources of Greenhouse Gases to the Atmosphere: A Global Estimate, *Bioscience*, *50*(9), 766, doi:10.1641/0006-3568(2000)050[0766:RSASOG]2.0.CO;2.

Lozovik, P. A. (2005), Contribution of Organic Acid Anions to the Alkalinity of Natural Humic

Water, *J. Anal. Chem.*, *60*(11), 1000–1004, doi:10.1007/s10809-005-0226-3.

Lueker, T. J., A. G. Dickson, and C. D. Keeling (2000), Ocean pCO_2 calculated from dissolved inorganic carbon, alkalinity, and equations for K_1 and K_2: Validation based on laboratory measurements of CO_2 in gas and seawater at equilibrium, *Mar. Chem.*, *70*, 105–119, doi:10.1016/S0304-4203(00)00022-0.

Lynch, J. K., C. M. Beatty, M. P. Seidel, L. J. Jungst, and M. D. DeGrandpre (2010), Controls of riverine CO_2 over an annual cycle determined using direct, high temporal resolution pCO_2 measurements, *J. Geophys. Res.*, *115*(G3), G03016, doi:10.1029/2009JG001132.

Maberly, S. C., P. a. Barker, A. W. Stott, D. Ville, and M. Mitzi (2013), Catchment productivity controls CO_2 emissions from lakes, *Nat. Clim. Chang.*, *3*(4), 391–394, doi:10.1038/nclimate1748.

MacIntyre, S., A. Jonsson, M. Jansson, J. Aberg, D. E. Turney, and S. D. Miller (2010), Buoyancy flux, turbulence, and the gas transfer coefficient in a stratified lake, *Geophys. Res. Lett.*, *37*(24), 2–6, doi:10.1029/2010GL044164.

Magnuson, J. (1990), Long-term ecological research and the invisible present, *Bioscience*, *40*(7), 495–501.

Magnuson, J. J. (2000), Historical Trends in Lake and River Ice Cover in the Northern Hemisphere, *Science (80-.).*, *289*(5485), 1743–1746, doi:10.1126/science.289.5485.1743.

Mammarella, I. et al. (2015), Carbon dioxide and energy fluxes over a small boreal lake in Southern Finland, *J. Geophys. Res. Biogeosciences*, *120*, 1296–1314, doi:10.1002/2014JG002873.Received.

Marotta, H., C. M. Duarte, S. Sobek, and A. Enrich-Prast (2009), Large CO_2 disequilibria in tropical lakes, *Global Biogeochem. Cycles*, *23*(4), 12–15, doi:10.1029/2008GB003434.

Marotta, H., L. Pinho, and C. Gudasz (2014), Greenhouse gas production in low-latitude lake sediments responds strongly to warming, *Nat. Clim. Chang.*, *4*(May), 11–14, doi:10.1038/NCLIMATE2222.

McCallister, S. L., and P. a. del Giorgio (2012), Evidence for the respiration of ancient terrestrial organic C in northern temperate lakes and streams, *Proc. Natl. Acad. Sci.*, *109*(42), 16963–16968, doi:10.1073/pnas.1207305109.

McDonald, C. P., E. G. Stets, R. G. Striegl, and D. Butman (2013), Inorganic carbon loading as a primary driver of dissolved carbon dioxide concentrations in the lakes and reservoirs of the

contiguous United States, *Global Biogeochem. Cycles*, *27*(2), 285–295, doi:10.1002/gbc.20032.

Meehl, G. A., C. Tebaldi, G. Walton, D. Easterling, and L. McDaniel (2009), Relative increase of record high maximum temperatures compared to record low minimum temperatures in the U.S., *Geophys. Res. Lett.*, *36*(23), 1–5, doi:10.1029/2009GL040736.

Millero, F. J. (1979), The thermodynamics of the carbonate system in seawater, *Geochim. Cosmochim. Acta*, *43*(10), 1651–1661, doi:10.1016/0016-7037(79)90184-4.

Millero, F. J. (2007), The marine inorganic carbon cycle, *Chem. Rev.*, *107*(2), 308–41, doi:10.1021/cr0503557.

Millero, F. J., D. Pierrot, K. Lee, R. Wanninkhof, R. Feely, C. L. Sabine, R. M. Key, and T. Takahashi (2002), Dissociation constants for carbonic acid determined from field measurements, *Deep Sea Res. Part I Oceanogr. Res. Pap.*, *49*(10), 1705–1723, doi:10.1016/S0967-0637(02)00093-6.

Monteith, D. T. et al. (2007), Dissolved organic carbon trends resulting from changes in atmospheric deposition chemistry., *Nature*, *450*(7169), 537–540, doi:10.1038/nature06316.

Morin, T. H., G. Bohrer, R. P. D. M. Frasson, L. Naor-Azreli, S. Mesi, K. C. Stefanik, K. V. R. Schaefer, and K. V. R. Schaefer (2014), Environmental drivers of methane fluxes from an urban temperate wetland park, *J. Geophys. Res. G Biogeosciences*, *119*(11), 2188–2208, doi:10.1002/2014JG002750.

O'Reilly, C. M., R. J. Rowley, P. Schneider, J. D. Lenters, P. B. Mcintyre, and B. M. Kraemer (2015), Rapid and highly variable warming of lake surface waters around the globe, *Geophys. Res. Lett.*, 1–9, doi:10.1002/2015GL066235.Received.

Ojala, A., J. L. Bellido, T. Tulonen, P. Kankaala, and J. Huotari (2011), Carbon gas fluxes from a brown-water and a clear-water lake in the boreal zone during a summer with extreme rain events, *Limnol. Oceanogr.*, *56*(1), 61–76, doi:10.4319/lo.2011.56.1.0061.

Pannard, a., B. E. Beisner, D. F. Bird, J. Braun, D. Planas, and M. Bormans (2011), Recurrent internal waves in a small lake: Potential ecological consequences for metalimnetic phytoplankton populations, *Limnol. Oceanogr. Fluids Environ.*, *1*, 91–109, doi:10.1215/21573698-1303296.

Papale, D., and R. Valentini (2003), A new assessment of European forests carbon exchanges by eddy fluxes and artificial neural network spatialization, *Glob. Chang. Biol.*, *9*(4), 525–535,

doi:10.1046/j.1365-2486.2003.00609.x.

Parkhurst, B. D. L., and C. a J. Appelo (1999), *User's Guide To PHREEQC (version 2) — a Computer Program for Speciation, and Inverse Geochemical Calculations*, Water-Resources Investigations Report 99-4259.

Perga, M. E., S. C. Maberly, J. P. Jenny, B. Alric, C. Pignol, and E. Naffrechoux (2016), A century of human-driven changes in the carbon dioxide concentration of lakes, *Global Biogeochem. Cycles*, *30*(2), 93–104, doi:10.1002/2015GB005286.

Phillips, J. C., G. A. McKinley, V. Bennington, H. A. Bootsma, D. J. Pilcher, R. W. Sterner, and N. R. Urban (2015), The potential for CO_2-induced acidification in freshwater: A Great Lakes case study, *Oceanography*, *28*(2), 136–145, doi:10.5670/oceanog.2015.37.

Podgrajsek, E., E. Sahlée, D. Bastviken, J. Holst, a. Lindroth, L. Tranvik, and a. Rutgersson (2014a), Comparison of floating chamber and eddy covariance measurements of lake greenhouse gas fluxes, *Biogeosciences*, *11*(11), 4225–4233, doi:10.5194/bg-11-4225-2014.

Podgrajsek, E., E. Sahlée, and a. Rutgersson (2014b), Diurnal cycle of lake methane flux, *J. Geophys. Res. Biogeosciences*, *119*(3), 236–248, doi:10.1002/2013JG002327.

Podgrajsek, E., E. Sahlée, and A. Rutgersson (2015), Diel cycle of lake-air CO_2 flux from a shallow lake and the impact of waterside convection on the transfer velocity, *J. Geophys. Res. Biogeosciences*, *120*(1), 29–38, doi:10.1002/2014JG002781.

Polsenaere, P., J. Deborde, G. Detandt, L. O. Vidal, M. a P. Pérez, V. Marieu, and G. Abril (2013), Thermal enhancement of gas transfer velocity of CO_2 in an Amazon floodplain lake revealed by eddy covariance measurements, *Geophys. Res. Lett.*, *40*(9), 1734–1740, doi:10.1002/grl.50291.

Posch, T., O. Köster, M. M. Salcher, and J. Pernthaler (2012), Harmful filamentous cyanobacteria favoured by reduced water turnover with lake warming, *Nat. Clim. Chang.*, *2*(11), 809–813, doi:10.1038/nclimate1581.

Rantakari, M., and P. Kortelainen (2005), Interannual variation and climatic regulation of the CO_2 emission from large boreal lakes, *Glob. Chang. Biol.*, *11*(8), 1368–1380, doi:10.1111/j.1365-2486.2005.00982.x.

Raymond, P. et al. (2013), Global carbon dioxide emissions from inland waters, *Nature*, *503*(7476), 355–359, doi:10.1038/nature12760.

Raymond, P. a, and J. J. Cole (2003), Increase in the export of alkalinity from North America's

largest river., *Science*, *301*(5629), 88–91, doi:10.1126/science.1083788.

Read, J. S., D. P. Hamilton, I. D. Jones, K. Muraoka, L. A. Winslow, R. Kroiss, C. H. Wu, and E. Gaiser (2011), Derivation of lake mixing and stratification indices from high-resolution lake buoy data, *Environ. Model. Softw.*, *26*(11), 1325–1336, doi:10.1016/j.envsoft.2011.05.006.

Read, J. S. et al. (2012), Lake-size dependency of wind shear and convection as controls on gas exchange, *Geophys. Res. Lett.*, *39*(9), 1–5, doi:10.1029/2012GL051886.

Reichstein, M. et al. (2005), On the separation of net ecosystem exchange into assimilation and ecosystem respiration: Review and improved algorithm, *Glob. Chang. Biol.*, *11*(9), 1424–1439, doi:10.1111/j.1365-2486.2005.001002.x.

Richardson, A. D., and D. Y. Hollinger (2005), Statistical modeling of ecosystem respiration using eddy covariance data: Maximum likelihood parameter estimation, and Monte Carlo simulation of model and parameter uncertainty, applied to three simple models, *Agric. For. Meteorol.*, *131*(3–4), 191–208, doi:10.1016/j.agrformet.2005.05.008.

Riera, J. L., J. E. Schindler, and T. K. Kratz (1999), Seasonal dynamics of carbon dioxide and methane in two clear-water lakes and two bog lakes in northern Wisconsin, U.S.A., *Can J Fish Aquat Sci*, *274*, 1–10, doi:10.1139/f98-182.

Risbey, J. S., S. Lewandowsky, C. Langlais, D. P. Monselesan, T. J. O. Kane, and N. Oreskes (2014), Well-estimated global surface warming in climate projections selected for ENSO phase, *Nat. Clim. Chang.*, *4*(July), 1–7, doi:10.1038/NCLIMATE2310.

Roehm, C. L., Y. T. Prairie, and P. A. Del Giorgio (2009), The pCO_2 dynamics in lakes in the boreal region of northern Quebec, Canada, *Global Biogeochem. Cycles*, *23*(3), 1–9, doi:10.1029/2008GB003297.

Roland, F., L. O. Vidal, F. S. Pacheco, N. O. Barros, A. Assireu, J. P. H. B. Ometto, A. C. P. Cimbleris, and J. J. Cole (2010), Variability of carbon dioxide flux from tropical (Cerrado) hydroelectric reservoirs, *Aquat. Sci.*, *72*(3), 283–293, doi:10.1007/s00027-010-0140-0.

Rouse, W. R., C. M. Oswald, J. Binyamin, P. D. Blanken, W. M. Schertzer, and C. Spence (2003), Interannual and Seasonal Variability of the Surface Energy Balance and Temperature of Central Great Slave Lake, *J. Hydrometeorol.*, *4*, 720–730, doi:10.1175/1525-7541(2003)004<0720:IASVOT>2.0.CO;2.

Sabine, C. L. et al. (2004), The Oceanic Sink for Anthropogenic CO_2, *Science (80-.).*, *305*(5682), 367–371, doi:10.1126/science.1097403.

Schneider, P., and S. J. Hook (2010), Space observations of inland water bodies show rapid surface warming since 1985, *Geophys. Res. Lett.*, *37*(22), 1–5, doi:10.1029/2010GL045059.

Shao, C., J. Chen, C. a. Stepien, H. Chu, Z. Ouyang, T. B. Bridgeman, K. P. Czajkowski, R. H. Becker, and R. John (2015), Diurnal to annual changes in latent, sensible heat and CO_2 fluxes over a Laurentian Great Lake: A case study in western Lake Erie, *J. Geophys. Res. Biogeosciences*, n/a-n/a, doi:10.1002/2015JG003025.

Skoog, D. A., D. M. West, F. J. Holler, and S. R. Crouch (2014), *Fundamentals of Analytical Chemistry*, 9th ed., Brooks/Cole, Belmont, CA.

Smith, V. (2003), Eutrophication of freshwater and coastal marine ecosystems a global problem, *Environ. Sci. Pollut. Res.*, *10*(2), 126–139, doi:10.1065/espr2002.12.142.

Sobek, S., L. J. Tranvik, and J. J. Cole (2005), Temperature independence of carbon dioxide supersaturation in global lakes, *Global Biogeochem. Cycles*, *19*(2), 1–10, doi:10.1029/2004GB002264.

Solomon, C. T. et al. (2013), Ecosystem respiration: Drivers of daily variability and background respiration in lakes around the globe, *Limnol. Oceanogr.*, *58*(3), 849–866, doi:10.4319/lo.2013.58.3.0849.

Sommer, U. et al. (2011), Beyond the Plankton Ecology Group (PEG) Model: Mechanisms Driving Plankton Succession, *Annu. Rev. Ecol. Evol. Syst.*, *43*(1), 120913143848009, doi:10.1146/annurev-ecolsys-110411-160251.

Staehr, P. a., J. P. a. Christensen, R. Batt, and J. Read (2012), Ecosystem metabolism in a stratified lake, *Limnol. Oceanogr.*, *57*(5), 1317–1330, doi:10.4319/lo.2012.57.5.1317.

Stets, E. G., R. G. Striegl, G. R. Aiken, D. O. Rosenberry, and T. C. Winter (2009), Hydrologic support of carbon dioxide flux revealed by whole-lake carbon budgets, *J. Geophys. Res. Biogeosciences*, *114*(1), 1–14, doi:10.1029/2008JG000783.

Stoy, P. C., G. G. Katul, M. B. S. Siqueira, J.-Y. Juang, H. R. McCarthy, H.-S. Kim, a C. Oishi, and R. Oren (2005), Variability in net ecosystem exchange from hourly to inter-annual time scales at adjacent pine and hardwood forests: a wavelet analysis., *Tree Physiol.*, *25*(7), 887–902, doi:10.1093/treephys/25.7.887.

Striegl, R. G., P. Kortelainen, J. P. Chanton, K. P. Wickland, G. C. Bugna, and M. Rantakari (2001), Carbon dioxide partial pressure and 13C content of north temperate and boreal lakes at spring ice melt, *Limnol. Oceanogr.*, *46*(4), 941–945, doi:10.4319/lo.2001.46.4.0941.

Sturtevant, C., B. L. Ruddell, S. H. Knox, J. Verfaillie, J. H. Matthes, P. Y. Oikawa, and D. Baldocchi (2015), Identifying scale-emergent, nonlinear, asynchronous processes of wetland methane exchange, , doi:10.1002/2015JG003054.

Takahashi, T., S. Sutherland, C. Sweeney, A. Poisson, and N. M. \it et. al (2002), Global Sea-Air CO_2 Flux Based on Climatological Surface Ocean pCO_2 and Seasonal Biological and Temperature Effects, *Deep. Res. Pt. II*, *49*, 1601.

Takahashi, T. et al. (2009), Climatological mean and decadal change in surface ocean pCO_2, and net sea–air CO_2 flux over the global oceans, *Deep Sea Res. Part II Top. Stud. Oceanogr.*, *56*(8–10), 554–577, doi:10.1016/j.dsr2.2008.12.009.

Teodoru, C. R., Y. T. Prairie, and P. A. del Giorgio (2011), Spatial Heterogeneity of Surface CO_2 Fluxes in a Newly Created Eastmain-1 Reservoir in Northern Quebec, Canada, *Ecosystems*, *14*(1), 28–46, doi:10.1007/s10021-010-9393-7.

Torgersen, T., and B. Branco (2007), Carbon and oxygen dynamics of shallow aquatic systems: Process vectors and bacterial productivity, *J. Geophys. Res. Biogeosciences*, *112*(3), 1–16, doi:10.1029/2007JG000401.

Tranvik, L. J., J. a. Downing, J. B. Cotner, S. a. Loiselle, R. G. Striegl, T. J. Ballatore, P. Dillon, K. Finlay, K. Fortino, and L. B. Knoll (2009), Lakes and reservoirs as regulators of carbon cycling and climate, *Limnol. Oceanogr.*, *54*(6_part_2), 2298–2314, doi:10.4319/lo.2009.54.6_part_2.2298.

Vachon, D., and P. A. del Giorgio (2014), Whole-Lake CO_2 Dynamics in Response to Storm Events in Two Morphologically Different Lakes, *Ecosystems*, 1338–1353, doi:10.1007/s10021-014-9799-8.

Vachon, D., and Y. T. Prairie (2013), The ecosystem size and shape dependence of gas transfer velocity versus wind speed relationships in lakes, *Can. J. Fish. Aquat. Sci.*, *70*(August), 1757–1764, doi:10.1139/cfjas-2013-0241.

Vesala, T., J. Huotari, Rannik, T. Suni, S. Smolander, A. Sogachev, S. Launiainen, and A. Ojala (2006), Eddy covariance measurements of carbon exchange and latent and sensible heat fluxes over a boreal lake for a full open-water period, *J. Geophys. Res. Atmos.*, *111*(11), 1–12, doi:10.1029/2005JD006365.

Villarini, G., J. A. Smith, and G. A. Vecchi (2013), Changing frequency of heavy rainfall over the central United States, *J. Clim.*, *26*(1), 351–357, doi:10.1175/JCLI-D-12-00043.1.

Wallin, M. B., S. Löfgren, M. Erlandsson, and K. Bishop (2014), Representative regional sampling of carbon dioxide and methane concentrations in hemiboreal headwater streams reveal underestimates in less systematic approaches, *Global Biogeochem. Cycles*, *28*(4), 465–479, doi:10.1002/2013GB004715.

Wang, Z. A., D. J. Bienvenu, P. J. Mann, K. A. Hoering, J. R. Poulsen, R. G. M. Spencer, and R. M. Holmes (2013), Inorganic carbon speciation and fluxes in the Congo River, *Geophys. Res. Lett.*, *40*(3), 511–516, doi:10.1002/grl.50160.

Wanninkhof, R. (1992), Relationship Between Wind Speed and Gas Exchange, *J. Geophys. Res.*, *97*(92), 7373–7382, doi:10.1029/92JC00188.

Wanninkhof, R., and M. Knox (1996), Chemical enhancement of CO_2 exchange in natural waters, *Limnol. Oceanogr.*, *41*(4), 689–697, doi:10.4319/lo.1996.41.4.0689.

Wanninkhof, R., W. E. Asher, D. T. Ho, C. Sweeney, and W. R. McGillis (2009), Advances in quantifying air-sea gas exchange and environmental forcing., *Ann. Rev. Mar. Sci.*, *1*, 213–244, doi:10.1146/annurev.marine.010908.163742.

Webster, K. E., P. A. Soranno, S. B. Baines, T. K. Kratz, C. J. Bowser, P. J. Dillon, P. Campbell, E. J. Fee, and R. E. Hecky (2000), Structuring features of lake districts: Landscape controls on lake chemical responses to drought, *Freshw. Biol.*, *43*(3), 499–515, doi:10.1046/j.1365-2427.2000.00571.x.

Webster, K. E., P. a. Soranno, K. S. Cheruvelil, M. T. Bremigan, J. a. Downing, P. D. Vaux, T. R. Asplund, L. C. Bacon, and J. Connor (2008), An empirical evaluation of the nutrient-color paradigm for lakes, *Limnol. Oceanogr.*, *53*(3), 1137–1148, doi:10.4319/lo.2008.53.3.1137.

Weiss, R. F. (1974), Carbon dioxide in water and seawater: the solubility of a non-ideal gas, *Mar. Chem.*, *2*(3), 203–215, doi:10.1016/0304-4203(74)90015-2.

Weyhenmeyer, G. A., D. M. Livingstone, M. Meili, O. Jensen, B. Benson, and J. J. Magnuson (2011), Large geographical differences in the sensitivity of ice-covered lakes and rivers in the Northern Hemisphere to temperature changes, *Glob. Chang. Biol.*, *17*(1), 268–275, doi:10.1111/j.1365-2486.2010.02249.x.

Weyhenmeyer, G. A., S. Kosten, M. B. Wallin, L. J. Tranvik, E. Jeppesen, and F. Roland (2015), Significant fraction of CO_2 emissions from boreal lakes derived from hydrologic inorganic carbon inputs, *Nat. Geosci.*, *8*(November), 933–936, doi:10.1038/NGEO2582.

Wik, M., B. F. Thornton, D. Bastviken, J. Uhlbäck, and P. M. Crill (2016), Biased sampling of

methane release from northern lakes: A problem for extrapolation, *Geophys. Res. Lett.*, doi:10.1002/2015GL066501.

Wilcox, B. P. (2010), Ecohydrology Bearing - Invited Commentary Transformation ecosystem change and ecohydrology: ushering in a new era for watershed management, *Ecohydrology*, *130*(February), 126–130, doi:10.1002/eco.

Wilkinson, K. J., H. G. Jones, P. G. C. Campbell, and M. Lachance (1992), Estimating organic acid contributions to surface water acidity in Quebec (Canada), *Water, Air, Soil Pollut.*, *61*(1–2), 57–74, doi:10.1007/BF00478366.

Williamson, C. E., D. P. Morris, M. L. Pace, and O. G. Olson (1999), Dissolved organic carbon and nutrients as regulators of lake ecosystems: Resurrection of a more integrated paradigm, *Limnol. Oceanogr.*, *44*(3_part_2), 795–803, doi:10.4319/lo.1999.44.3_part_2.0795.

Williamson, C. E., W. Dodds, T. K. Kratz, and M. A. Palmer (2008), Lakes and streams as sentinels of environmental change in terrestrial and atmospheric processes, *Front. Ecol. Environ.*, *6*(5), 247–254, doi:10.1890/070140.

Winder, M., and D. E. Schindler (2004), Climatic effects on the phenology of lake processes, *Glob. Chang. Biol.*, *10*(11), 1844–1856, doi:10.1111/j.1365-2486.2004.00849.x.

Winslow, L. A., J. S. Read, G. J. A. Hansen, and P. C. Hanson (2014), in Deepwater Temperatures, , 355–361, doi:10.1002/2014GL062325.Received.

Xiao, W. et al. (2014), A flux-gradient system for simultaneous measurement of the CH_4, CO_2, and H_2O fluxes at a lake-air interface., *Environ. Sci. Technol.*, *48*(24), 14490–8, doi:10.1021/es5033713.

Yanai, R. D., J. J. Battles, A. D. Richardson, C. A. Blodgett, D. M. Wood, and E. B. Rastetter (2010), Estimating Uncertainty in Ecosystem Budget Calculations, *Ecosystems*, *13*(2), 239–248, doi:10.1007/s10021-010-9315-8.

Yvon-Durocher, G., A. P. Allen, J. M. Montoya, M. Trimmer, and G. Woodward (2010), The temperature dependence of the carbon cycle in aquatic ecosystems, *Adv. Ecol. Res.*, *43*(C), 267–313, doi:10.1016/B978-0-12-385005-8.00007-1.

Yvon-Durocher, G. et al. (2012), Reconciling the temperature dependence of respiration across timescales and ecosystem types, *Nature*, *487*(7408), 472–476, doi:10.1038/nature11205.